



Digital controllable load electric motor test bench

CF Greyling

Mini-dissertation submitted for the degree Bachelor of
Engineering in Electromechanical Engineering at the North-
West University

Supervisors: Prof A Grobler, Mr W Kaiser, Mr A van der
Walt

Student number: 25924974

ABSTRACT

Electric motors should operate at its most efficient to deliver its best performance. To establish a factual basis for efficiency, measurements must be taken and recorded. The collected data and subsequent calculations provide the basis for improvement of the test bench. The solution proposed for this problem was to add a digital controllable load to the test bench. This will also enable the construction of an efficiency map of the electric motor. This can be used to test the NWU solar car to improve its performance.

A conceptual solution for a digital controllable load test bench is provided, as well as a detailed design. Implementation, testing and evaluation of the design is presented.

The structured design process was followed during this project. The current test bench with its existing hardware was identified and evaluated, the controllers suitable for use were identified, the modifications identified as required to merge the digital controller to the existing hardware, the hardware was manufactured, the software code written to control the load and the design implemented. Finally, the tests were run, the results recorded and an efficiency map was drawn.

The mechanical aspect of the solution fulfils its requirements satisfactory. The pressure setpoint digital control functions well and allows the user to digitally control the electric test bench and draw an efficiency map. The PID control does not function as required due to response delays and control increments that are not small enough. The PID control is not needed to create an efficiency map, as running the system at a range of loads controlled by the digital control will provide the necessary data points to draw the efficiency map. It was concluded that the use of the digital controllable load electrical test bench is practical and beneficial, which benefit will increase after implementation of the recommendations in this report.

DECLARATION

Declaration by student

I **CF Greyling** declare herewith that the mini-dissertation entitled, **Digital controllable load electric motor test bench** which I herewith submit to the North-West University as partial completion of the requirements set for the **Bachelor of Engineering in Electromechanical Engineering** degree, is my own work, has been text edited and has not already been submitted to any other university.

I understand and accept that copies that are submitted for examination are the property of the University. Signature of student  University-number **25924974**.

TABLE OF CONTENTS

Chapter 1. Introduction	1
1.1 Introduction.....	1
1.2 Background.....	1
1.3 Problem Statement.....	2
1.4 Project Scope	3
1.5 Project Objectives.....	4
1.5.1 Primary objective	4
1.5.2 Secondary objectives.....	4
1.5.3 Deliverables.....	4
1.6 Technical Requirements	4
1.6.1 Requirements	4
1.6.2 Limitations and Exclusions.....	5
1.7 Conclusion.....	5
Chapter 2. Literature Study	6
2.1 Introduction.....	6
2.2 HBM	6
2.3 DC Motor	6
2.4 Vented Disc Brake	7
2.4.1 Uniform wear	8
2.4.2 Uniform Pressure	9
2.4.3 Frictional coefficient	9
2.5 Control loops.....	10
2.6 Microcontroller	11
2.6.1 ESP32 WROOM	11
2.6.2 Arduino Uno®	11
2.7 Hydraulic system	11
2.8 Stepper motor	11

2.9	Sun XMD-01	11
2.10	RS422 serial data standard.....	12
2.11	Operational amplifier.....	12
2.12	Conclusion	12
	Chapter 3. Design.....	13
3.1	Introduction.....	13
3.2	Load concept designs	14
3.2.1	Design 1: Hydraulic controlled calliper disc brake with VSD.....	14
3.2.2	Design 2: Disc brake and DC motor combinations	14
3.2.3	Design 3: Hydraulic pump as load controlled by electric valve	15
3.2.4	Design 4: Airflow controlled fan in combination with magnets	15
3.2.5	Design 5: Stepper motor-controlled Disc brake.....	15
3.2.6	Design 6: Hydraulic system with lever pressure reducer	15
3.2.7	Design 7: Reduce piston calliper diameter	16
3.2.8	Load concept design trade-off.....	16
3.3	Spring concept design	17
3.4	Controller concept design	17
3.4.1	Controller V1.0: ESP32 WROOM.....	17
3.4.2	Controller V2.0: Arduino Uno®.....	17
3.4.3	Controller trade off	17
3.5	Data measurement system connection to controller concept design	18
3.5.1	Data measurement V1.0 0-5V.....	18
3.5.2	Data measurement V2.0 RS422 to Arduino adapter	18
3.5.3	Data measurement V4.0 T40B torque transducer -10V to +10V	18
3.6	Motor Coupling concept design.....	19
3.6.1	Design 1: Motor connected external to the test bench securing	19
3.6.2	Design 2: Solar car motor connection	19
3.7	Combined Concept Design	19
3.7.1	Design 1	19

3.7.2	Design 2	20
3.8	Detailed design	20
3.9	Disc brake detailed design.....	20
3.9.1	Pressure calculations.....	20
3.9.2	Heat transfer calculations.....	22
3.9.3	Piston spring return.....	22
3.10	Hydraulic system detailed design.....	23
3.10.1	Reduce calliper size of brake's piston	25
3.10.2	Reduce brake pad size	26
3.10.3	Reduce pump size	27
3.10.4	Pressure relieving(reduction) valve	27
3.11	Controller detailed design	28
3.11.1	Controller design V1.0 ESP 32 WROOM	28
3.11.2	Controller design V2.0 Arduino Uno®	28
3.12	XMD-01 valve control detailed design	28
3.13	Voltage Signal control detailed design	28
3.14	Torque Transducer Signal Measurement Detailed Design	29
3.14.1	Torque Transducer Signal Measurement V1.0.....	29
3.14.2	Torque Transducer Signal Measurement V2.0.....	29
3.14.3	Torque Transducer Signal Measurement V3.0.....	30
3.15	Control loop design.....	31
3.16	Motor coupling detailed design.....	33
3.16.1	Test bench couple.....	33
3.16.2	Motor spacers	33
3.17	Integrated system detailed design.....	33
3.17.1	Combined electronic system V1.0.....	33
3.17.2	Combined electronic system V2.0.....	34
3.17.3	Combined electronic system V2.1.....	34
3.18	Combined electronic system V2.2.....	34

3.19 Conclusion	34
Chapter 4. Implementation.....	35
4.1 Introduction.....	35
4.2 Disc brake piston and sleeve	35
4.3 Spring return	35
4.4 Hydraulic system	36
4.5 Controller	37
4.5.1 ESP 32 WROOM	37
4.5.2 Arduino Uno®	37
4.6 Grundfos motor replacement	38
4.7 Software User interface	39
4.8 Control loop	41
4.9 Conclusion	41
Chapter 5. Testing and evaluation	43
5.1 Introduction.....	43
5.2 Predesign tests	43
5.2.1 Disc brake predesign experiment 1: Frictional coefficient of brake pads	43
5.2.2 Disc brake predesign experiment 2: Disc brake pressure required.....	44
5.2.3 Disc brake predesign experiment 3: Disc brake calliper	45
5.2.4 Hydraulic predesign experiment 1: Basic operation.....	45
5.2.5 Hydraulic predesign experiment 2: Pressure output to the hydraulic system.....	46
5.2.6 Hydraulic predesign experiment 3: DMDA Configuration test.....	46
5.3 Subsystem tests	47
5.3.1 XMD-01 operational test	47
5.3.2 MCP41100 digital potentiometer test	47
5.3.3 G070A torque adapter RS422 output voltage test.....	48
5.3.4 G070A torque adapter RS422 output frequency test.....	49
5.3.5 T40B torque transducer voltage output test	49
5.3.6 Operational amplifier test	50

5.3.7	Disc brake system test.....	51
5.3.8	Spring return system.....	51
5.4	Integrated system test.....	52
5.5	Electric motor test	53
5.6	Conclusion.....	56
	Chapter 6. Conclusion and Recommendations	58
6.1	Introduction.....	58
6.2	Project Overview.....	58
6.3	Recommendations.....	58
6.4	ECSA ELOs.....	59
	BIBLIOGRAPHY	62
	APPENDIX A.1: SCHEMATICS AND FLOWCHARTS FROM OTHER SOURCES	65
	APPENDIX A.2: SCHEMATICS AND FLOWCHARTS	73
	APPENDIX B.1: FABRICATION DATA	90
	APPENDIX B.2: SOFTWARE	92
	APPENDIX B.3: TEST REPORTS	93

LIST OF TABLES

Table 3-1: Load design trade-off	16
Table 3-2: Microcontroller trade off study	17
Table 3-3: Disc brake pressure calculations results	22
Table 3-4: Heat transfer calculations parameters and results.....	22
Table 3-5: Parameters of brake pad.....	26
Table 3-6: Brake pad area reduction calculation results	27
Table 3-7: Pin assignment MCP41100 [22]	29
Table 3-8: Connection between G070A and Shield.....	30
Table 3-9: Op amp circuit IC pin assignment.....	31
Table 3-10: Voltage output after op amp	31
Table 3-11: Operating range improvements	32
Table 5-1: Disc brake measured parameters	44
Table 5-2: MCP41100 test results.....	48
Table 5-3: Piston and sleeve operation results.....	51
Table 5-4: Spring return system test results	52
Table 6-1: XMD-01 voltage relation to pressure data	94
Table 6-2: Relation between voltage and torque at plug 3 of the T40B	95
Table 6-3: Op amp test results	95
Table 6-4: Combined system measurements	99

LIST OF FIGURES

Figure 1-1: Existing Hardware Breakdown Structure	2
Figure 3-1: High-level functional units	13
Figure 3-2: System breakdown structure.....	14
Figure 3-3: Combined concept design 2.....	20
Figure 3-4: Disc brake angle calculations.....	21
Figure 4-1: Disc brake calliper.....	35
Figure 4-2: Spring return system implemented.....	36
Figure 4-3: XMD-01 App interface.....	36
Figure 4-4: MCP41100 LED test circuit	37
Figure 4-5: Photo of MGE90SB2 Grundfos motor	38
Figure 4-6: Photo of spacer implemented.....	39
Figure 4-7: IDE serial monitor user interface	40
Figure 4-8: Example data output	40
Figure 4-9: Photo of combined circuit implemented on a breadboard.....	41
Figure 5-1: test breakdown structure.....	43
Figure 5-2: disc and brake pad frictional coefficient.....	44
Figure 5-3: Pressure to XMD-01 voltage relation.....	47
Figure 5-4: Relationship between torque and voltage of the T40B linearization	50
Figure 5-5: op amp test results.....	51
Figure 5-6: Input voltage average filter	53
Figure 5-7: Mechanical vs Input power measured with HBM system.....	55
Figure 5-8: Torque and speed in relation to the applied pressure.....	55
Figure 5-9: Grundfos motor efficiency map	56
Figure 6-1: Axiom hydraulic schematic [1].....	65
Figure 6-2: DMDAMNN directional valve [23].....	66
Figure 6-3: RBAPMBN [23]	66
Figure 6-4: SCCALAN [23]	66
Figure 6-5: Contact-pressure distribution on the face of the cone after the wear-in period [8]	67
Figure 6-6: Geometry of the contact area of an annular-pad segment of a calliper brake [11]	67
Figure 6-7: Summing amplifier [20]	67
Figure 6-8 Square wave signals A/B and reference signal (0-index) [21]	68
Figure 6-9 ESP 32 pin connections [24]	68
Figure 6-10: Arduino Uno® pinout [25].....	69

Figure 6-11: XMD-01 data sheet schematic [23]	69
Figure 6-12: Normalized resistance to End Terminal resistance vs code [22].....	70
Figure 6-13: Potentiometer resistance are as function of code [22].....	70
Figure 6-14: Torque sensor connector pin assignment [26].....	71
Figure 6-15: RS485 Shield [27].....	71
Figure 6-16: T40B Plug 3 assignment [28]	72
Figure 6-17: Concept design VSD controlled hydraulic Disc brake system.....	73
Figure 6-18: Disc brake and DC motor concept schematic.....	73
Figure 6-19: Airflow controlled fan concept design	74
Figure 6-20: stepper motor-controlled disc brake	74
Figure 6-21: lever pressure reduction.....	75
Figure 6-22: Concept design for piston and sleeve	75
Figure 6-23: Basic flow chart of the control system	75
Figure 6-24: Input and output of the ESP 32	76
Figure 6-25: Flowchart Arduino Uno®.....	76
Figure 6-26: Solar car motor connection concept design 2.....	77
Figure 6-27: Combined concept design 1	77
Figure 6-28: Spring return system Solidworks assembly	78
Figure 6-29: Hydraulic system flow diagram DMDA valve A powered	78
Figure 6-30: Hydraulic system flow diagram DMDA valve B powered	79
Figure 6-31: ESP 32 connections.....	79
Figure 6-32: Control loop flowchart	80
Figure 6-33: operating ranges	80
Figure 6-34: combined digital circuitry	81
Figure 6-35: process of electrical circuit flow of XMD-01	81
Figure 6-36: Combined electronic system V2.1	81
Figure 6-37: Combined electronic system V2.2	82
Figure 6-38: motor mounting	82
Figure 6-39: Torque flange adapter revision 1	83
Figure 6-40: Motor coupling diagram.....	84
Figure 6-41: Spring assembly drawing	85
Figure 6-42: piston shield drawing.....	86
Figure 6-43: Torque Transducer Signal Measurement V1.0 simulation circuit	87
Figure 6-44: Summing amplifier circuit with voltage regulators.....	87
Figure 6-45: RC 66Hz filter	88
Figure 6-46: MCP41100 voltage divider	88
Figure 6-47:Arduino Uno® circuit	89

Figure 6-48: Piston calliper	90
Figure 6-49: Piston and sleeve assembly drawing	91
Figure 6-50: Torque adapter RS422 output signal.....	93
Figure 6-51: Expected frequency output.....	93
Figure 6-52: Serial plotter 1000 000 Baud rate no load test	94
Figure 6-53: 2000 000 Baud rate serial monitor output.....	94
Figure 6-54: Operational amplifier test circuit	95
Figure 6-55: Noise input to Arduino ADC Pin	96
Figure 6-56: TiePie measurement of T40B output voltage, IM off and Grundfos motor off ..	97
Figure 6-57: TiePie measurement of T40B output voltage, Grundfos motor switched on	97
Figure 6-58: TiePie measurement of T40B voltage output, induction motor controlled by VSD	98
Figure 6-59: TiePie measurement of T40B output voltage, induction motor powered by variac	98
Figure 6-60: Filtered output to the Arduino vs unfiltered output	99

Chapter 1. Introduction

1.1 Introduction

The aim of this project is to design and create an improved system to test electric motors under different loads, to determine at what speed and torque the motor operates most efficiently. This will be done by digitally controlling different loads to the motor under test and measuring the basic parameters: current, voltage, input power, mechanical power, speed and torque. An efficiency map of the motor under test's operation will be drawn up.

The motivation for this project is to identify the most efficient state of electric motors. This may then be applied to the NWU solar car. The NWU technical team identified the electric motor of the solar car as an aspect that could be improved.

This project will provide for the testing of electrical motors under selected testing conditions. This will enable the operation of electric motors at their highest efficiency. The secondary motivation is to test the Solar Car electrical motor by way of a controllable load. The testing will enable the NWU to understand under which conditions the Solar Car performs most efficiently.

1.2 Background

Electric motors are widely used throughout the industry to measure performance. The NWU uses electric motors for their solar racing cars. In order to improve the solar car's performance, one should identify the state when the performance of its electrical motor and drive is at its optimum efficiency. One will obtain the most reliable measurements with tests during a hardware simulation of the route of the solar car.

Previous projects have been done in order to test electric motors with a controllable load. The previous electric motor test bench iteration, was designed and built by Mr M Zaaiman in 2018.

The test bench consists of four units, namely the hydraulic system, VSD control, disc brake and the HBM measuring system, as reflected in the hardware breakdown structure shown in Figure 1-1 below. The system was designed to control the load applied by a Citi Golf disc brake with a SUN hydraulic valve system. According to the Axiom design, as per Appendix B.2, the pressure of the SUN hydraulic valve system should have been controlled by a XMD-01 controller. However, the hydraulic valve system operates between 10-100 Bar [1], resulting in such high pressure that testing of the electric motor was impossible. Therefore, past tests were conducted by bypassing the valves and controlling the pressure on the disc brake, by changing the power supply to the oil pump with VSD control of the induction motor.



Figure 1-1: Existing Hardware Breakdown Structure

1.3 Problem Statement

The NWU requires the Solar Car electrical motor to undergo testing under simulated scenarios for an extended period. One can reach this goal by improving the existing electrical motor test bench to fulfil the NWU's needs.

The testing in this project will be done on the Grundfos MGE90SB2 electric motor with a built-in drive.

The current electrical motor test bench load consists of a vented disc brake and a hydraulic control block. This combination presents two problems. The hydraulic system's operation is unsatisfactory as the valves are only controllable between 10 and 100 Bar and therefore needs modification in order to implement the intended system successfully.

Tests on the vented disc brake were not done for extreme cases such as the continuous application of up to 8 hours; therefore, it must still be determined whether the disc brake will be able to perform correctly or if a cooling system or a new design will be required.

The test bench is designed in order that the NWU's Mitsuba solar car motor with a separate drive can undergo testing with the controllable load designed in this project. Both the driver operation and the motor should be tested with the test bench, as the respective efficiency curves may prove not to be the same. Plotting the efficiency curve for the motor and the drive on the same graph will allow an analysis of the optimal efficiency operation area for the combination of the motor and the drive.

1.4 Project Scope

The scope of this project is to design a system to digitally control a load of a 1.5kW electrical motor test bench in order to test an electrical motor (NWU solar car electrical motor/ or similar) via a hardware simulation. The electrical motor test bench to be improved in this project consists of a disc brake that is controlled by a hydraulic system. In order to improve the electrical motor test bench as desired, the following aspects are to be determined: the hydraulic system, the disc brake, the controller and the data analysis.

Firstly, the hydraulic control block must be analysed to determine its precise function and any limitations. From this, any problem with the hydraulic control block must be identified and repaired. If it is impossible to repair the hydraulic control block, a new method of operating the disc brake must be devised.

Secondly, the expected operation of the disc brake must be calculated and then tested. This is to determine whether the disc brake will be able to withstand the heat of operation under extreme conditions, such as, at high speed and/or for prolonged periods. If the calculations and testing indicate that the disc brake is unable to operate under the extreme conditions, one should find a solution.

The third aspect is the controller for the electrical motor test bench load. The controller will be used to control the load as desired by the user, automatic or manual. The automatic control requires a setting to control the load for a set period under a set load specified by the user. If possible, with the HBM system a second functionality of a feedback loop should be included in the automatic control. By implementing a feedback loop, the controller will be able to control the load on its own once the user has loaded the necessary data to the controller for the test. Therefore, the controller will enable the user to test the electric motor for extended periods and with micro reactions as the control will be automated. The controller will then log the data that will be used to analyse the electrical motor performance.

Finally, the data analysis consists of the following: the data required to set the test bench up for testing under the desired scenario and the data collected throughout the testing. The first step is to design a system of data input that will be the most beneficial for the project. Next, the user will need complete data logging in order to analyse the electrical motor operation.

1.5 Project Objectives

1.5.1 Primary objective

The primary objective of the project is to digitally control the load on a 1.5kW electric motor.

1.5.2 Secondary objectives

The secondary objectives are as follow:

- i. Improve the disc brake hydraulic control system to operate with the existing hydraulic control block
- ii. Create an efficiency map of the electric motor
- iii. Determine whether the disc brake will overheat under extreme speeds and/or long test periods
- iv. Use a controller to control the system
- v. Use HBM torque transducer output to control load with a feedback loop
- vi. Display the necessary information to the user
- vii. Test the electrical motor for several hours under different loads and speeds
- viii. Collect data for analysis

1.5.3 Deliverables

The deliverable for this project is a digitally controllable system for a load of a 1.5kW electrical motor test bench with a load capable of operating under extended periods and with high rotor speeds. The control system will function in such a way as to collect data on the operation of the electric motor under load for extended periods and different loads in order to draw an efficiency map for the electrical motor.

1.6 Technical Requirements

1.6.1 Requirements

1.6.1.1 Functional Requirements

- i. Must be able to apply a reasonable range of loads to the electrical motor under test
- ii. Must implement automatic control system with user defined load set-point

1.6.1.2 Non-functional Requirements

- i. The control system for the load of the electrical motor test bench must be user-friendly
- ii. Must provide reasonable basic user setup guide for system

1.6.1.3 Physical requirements

- i. The modification to the electric motor test bench should fit on the existing electrical motor test bench
- ii. Modifications must allow room to set up an alternative motor

1.6.1.4 Performance Requirements

- i. The load control system of the electrical motor test bench must be able to operate for approximately 4 hours
- ii. The load control system of the electrical motor test bench must be able to operate at high rotor speeds of the electrical motor
- iii. The load control system of the electrical motor test bench must be able to brake an electrical motor with the rating of between 1kW and 2kW.

1.6.1.5 Health and Safety Requirements

- i. Shielding for the rotor must be applied
- ii. Electric isolation must comply with standards

1.6.2 Limitations and Exclusions

The project has the following limitations:

- i. Existing electrical motor test bench functional parameters
- ii. HBM T40B torque flange
 - a. 20 000 r/min maximum rotation speed
 - b. 100 Nm maximum torque
 - c. RS422 output signal
- iii. Data writing rate limited to controller
- iv. Hydraulic system control range of 10-100Bar
- v. Volkswagen Citi Golf vented disc rotor diameter of 236 mm
- vi. Budget set for the project by the NWU

Exclusions of the project:

- i. Creation of a representation of the road the NWU solar car will drive
- ii. Building a new essential electrical motor test bench

1.7 Conclusion

The solution will enable the characterisation of electrical motors at low rotational speeds and digitally test the electrical motors for a controllable load pattern. The solution may be applied to the NWU Solar Car in order to test the Solar Car operation on the racing route by using the controllable load. Thus, the solution can be used to emulate a scenario under which electric motors undergo testing.

Chapter 2. Literature Study

2.1 Introduction

The following section documents the literature studied in order to research relevant aspects of the project. The vented disc brake operation and disc pad pressure requirements were investigated. Control theory was researched; specifically, different types of proportional control in order to determine the best type of control to be implemented in the system. Microcontrollers were investigated to determine which provides the required functionality for the project. To understand the operation of the hydraulic system implemented, research was done on hydraulic systems in general and the currently implemented system.

2.2 HBM

Genesis High-Speed Transient Recorder & Data Acquisition System (GEN3t transient/high-speed data acquisition system) from HBM is implemented to measure the parameters of the tests. The GEN3t is optimal for test bench applications as it is compact and suitable for high-speed data recording applications [2]. The GEN3t operates independently, which allows for passive testing [2]. The GEN3t has a protection class of IP20, therefore it will be robust enough to operate in the substantial current laboratory of the NWU [3]. The GEN3t operates with the Linux operating system as seen in the datasheet [3] that allows more freedom and control over the operation. The T40B torque transducer connects to a G070A torque adapter that connects to the GEN3t to provide the torque measurements of the torque and speed output. The G070A torque adapter can be connected to a control system through RS422.

2.3 DC Motor

A direct current (DC) motor consists out of a stationary part, the stator, rotating members called the armature, the armature windings and fixed poles mounted inside the stator. The DC motor operates by creating a uniform magnetic field from the poles mounted in the stator [4]. A DC current starts to flow through the armature windings by applying a DC voltage over the armature windings.

The disc brake implemented in the test bench is ideal for low-speed braking. However, at higher rotational speeds, a DC machine would function better to act as a load for the electrical motor undergoing testing. The DC machine should only be used at high speeds as it only provides a load directly proportional to the electrical motor speed. Therefore, its linear properties mean that the load it can provide is directly proportional to the speed. As the load is directly proportional to the speed, the DC motor will not be able to provide starting resistance. Therefore, the vented disc brake was implemented as the electrical motor test bench's load [1].

2.4 Vented Disc Brake

The disc brake used in this project is the Volkswagen Citi Golf, is manufactured from cast iron. The cast iron normally used for the disc brake is grey cast iron [5] (FG 25). The FG 25 is the Spanish index for the grey cast iron; the cast iron contains 1.5-4.3% carbon and 0.3-5% silicon as well as manganese, sulphur and phosphorus [6]. The high carbon content allows for heat dissipation because of the thermal conductivity [7]. The second reason for the use of cast iron is that it is cheaper than aluminium, which is used in race cars. Another benefit is its resistance to wear and that it is relatively hard [5]. The disc brake is designed for dry operation and may be vented to cool down the disc, unlike the multidisc cooled with oil application [8].

In this section, it is necessary to investigate the thermal dynamics of the disc brake. One needs to determine whether the disc brake will be able to operate as a load under the desired condition of the electric motor testing, or whether the disc will overheat and require a form of cooling. If the vented disc brake requires further cooling, a cooling method will be investigated. Overheating is the result of the temperature rise pattern in the disc brake: each time the disc brake does not reach its required cooldown period, its subsequent maximum temperature rise will be higher than the previous maximum temperature rise for the applied period [9].

The braking kinetic energy of the disc brake is converted to thermal energy using the first law of thermodynamics. The friction of the brake, the venting slots and external environmental factors impact the heat exchange rate for the vented disc brake, while the angular velocity of the rotor disc and the frictional coefficient of the brake pads form the input heat flux [5].

For purposes of calculation, radiation heat transfer is negligible as it is 5-10% of the heat transfer [10]. For these purposes, the following assumptions prevail: that the rotor disc material is isotropic and homogeneous and the brake pad pressure on the disc is uniformly distributed.

The pressure across the face of the disc is at a maximum at the inner radius of the disc as can be seen in Figure 6-5 in Appendix B. The general pressure on the disc can, therefore, be calculated with the following equation.

$$p = \frac{p_{max}d}{2r} \quad (1)$$

The braking temperature rise can be calculated with the following equation below as defined in Shigley [8],

$$\Delta T = \frac{E}{Cm} \quad (2)$$

Where ΔT is the temperature rise, and m the mass of the object touching the frictional surface and C represents the specific heat of the disc in $[J/kg \cdot ^\circ C]$.

The average heat dissipation rate is calculated with the following equation,

$$H_{av} = \frac{ES}{3600} \quad (3)$$

Where S is the stops per hour, and E is the kinetic energy of the rotating machine which is equal to the heat energy the brake must dissipate. The kinetic energy is calculated with the following equation,

$$E = \frac{I(\omega_o^2 - \omega_f^2)}{2} \quad (4)$$

Where ω is the speed in rad/s. The equation below is used to calculate the rate at which the disc can dissipate heat (H_{ess}),

$$H_{diss} = hA(T_d - T_a) \quad (5)$$

The following equation calculates the total heat transfer coefficient (h)

$$h = h_r + f_v h_c \quad (6)$$

Where h_r is the radiation heat transfer coefficient, f_v is the ventilation factor, and h_c is the convection heat transfer coefficient. The equation for the governing axial wear is as follows,

$$w = f_1 f_2 K P V t \quad (7)$$

The effective radius (r_e) is the equivalent radius which is,

$$r_e = \frac{T}{fF} = \frac{\int_{r_i}^{r_o} pr^2 dr}{\int_{r_i}^{r_o} pr dr} \quad (8)$$

Where F is the actuating force, and the frictional torque is T . The line of action force is locating coordinate \bar{r} around the x-axis, as shown in Figure 6-6 in Appendix A.1. Therefore, we calculate the locating coordinate as follow,

$$\bar{r} = \frac{M_x}{F} = \frac{(\cos\theta_1 - \cos\theta_2)}{\theta_2 - \theta_1} r_e \quad (9)$$

2.4.1 Uniform wear

For uniform wear PV is constant, once again as seen in Figure 6-6 in Appendix A.1 the locating coordinate \bar{r} of the force is calculated as follows [11],

$$\bar{r} = \frac{(\cos\theta_1 - \cos\theta_2) r_o + r_i}{\theta_2 - \theta_1} \quad (10)$$

The pressure (p) can be expressed in terms of the largest allowed pressure (p_a) as [11],

$$p = p_a \frac{r_i}{r} \quad (11)$$

Where the force F is expressed as [11],

$$F = (\theta_2 - \theta_1)p_a r_i(r_o - r_i) \quad (12)$$

Moreover, the frictional torque T is expressed as [11],

$$T = (\theta_2 - \theta_1)f p_a r_i \int_{r_i}^{r_o} r dr \quad (13)$$

2.4.2 Uniform Pressure

During uniform pressure it is approximated by a new brake, the locating coordinate is calculated as follows [11],

$$\bar{r} = \frac{2}{3} \frac{(\cos\theta_1 - \cos\theta_2)}{\theta_2 - \theta_1} \frac{r_o^3 - r_i^3}{r_o^2 - r_i^2} \quad (14)$$

For uniform pressure $p = p_a$ the actuating force F is calculated as follow,

$$F = (\theta_2 - \theta_1)p_a \int_{r_i}^{r_o} r dr \quad (15)$$

Also, the frictional torque T is determined as follow,

$$T = (\theta_2 - \theta_1)f p_a \int_{r_i}^{r_o} r^2 dr \quad (16)$$

2.4.3 Frictional coefficient

The frictional coefficient can be determined experimentally when the frictional coefficient of a material is unknown. The frictional coefficient between the disc and the brake pad can be calculated by tilting the disc and sliding the brake pad down the disc. The angle is measured as the angle when the brake pad just starts sliding down the disc.

The theory behind the method is as follow,

$$f_s = \mu_s N \quad (17)$$

For the system splitting into x and y components Newton's law is applied that the x component is as follow,

$$\sum F_x = ma_x = 0 \quad (18)$$

$$mg \sin(\theta) - f_s = 0$$

$$mg \sin(\theta) = \mu_s N$$

And the y component,

$$\sum F_y = ma_y \quad (19)$$

$$N - mg \cos(\theta) = 0$$

$$mg \cos(\theta) = N$$

The x component can be substituted into the y component,

$$mg \sin(\theta) = \mu_s mg \cos(\theta)$$

$$\frac{\sin(\theta)}{\cos(\theta)} = \mu_s$$

Therefore, the frictional coefficient is calculated as

$$\tan(\theta) = \mu_s \quad (20)$$

2.5 Control loops

Proportional controllers have limitations as it becomes unreliable when working with changing inputs [12]. Therefore, one of the following controllers should be in use, namely the proportional integral (PI) controller, proportional derivative (PD) controller or the proportional integral derivative (PID) controller.

Proportional plus integral (PI) controller

The proportional plus integral controller has the following transfer function as shown in Modern Control systems [13],

$$G_c(s) = K_p + \frac{K_I}{s} \quad (21)$$

Where K_p is the proportional control term and K_I is the integral control term. PI controllers are used in order to compensate for the lack of steady state accuracy in a system due to the lack of integration in the system [13].

Proportional plus derivative (PD) controller

The proportional plus integral control transfer function is defined as following in Modern Control Systems [13],

$$G_c(s) = K_p + K_D s \quad (22)$$

Where K_D is the derivative control term.

Proportional plus integral plus derivative (PID) controller

Proportional plus integral plus derivative control transfer function is defined as follow,

$$G_c(s) = K_p + K_D s + \frac{K_I}{s} \quad (23)$$

This is widely used in the industry for complex systems.

2.6 Microcontroller

The two primary controllers considered in this project were the ESP32 WROOM and the Arduino Uno®. They are both relatively similarly powerful with similar functionality.

2.6.1 ESP32 WROOM

ESP32 is a microprocessor with Wi-Fi and Bluetooth capabilities and ultra-low power consumption [14]. The ESP32 can be programmed in simple programming environments such as Arduino studio. The ESP32 IO pins operate at 3.3V. The ESP32 is a wearable device that will be able to perform sufficiently for the requirements of the project.

2.6.2 Arduino Uno®

Arduino Uno® is a small microcontroller based on the ATmega328P [15]. The Arduino Uno® has a wide range of applications and is compatible with a wide range of shields for interfacing with applications.

The main advantages of the Arduino Uno® are:

- i. Low cost
- ii. Simple programming environment
- iii. Open source software
- iv. 5V IO pins

2.7 Hydraulic system

A hydraulic system circulates an almost non-compressible liquid in order to drive actuators as precisely as possible. The hydraulic system controls position, speed or force depending on the requirement [16]. The hydraulic system implemented in this project uses force to control the disc brake with a calliper. The hydraulic system implemented is shown in Appendix A.1-Hydraulic system. An 80V 3kW induction motor drives the hydraulic system. The hydraulic system implemented is defined further in detailed design chapter of the report.

2.8 Stepper motor

A stepper motor is a brushless DC motor that divides a rotation into a number of equal steps. The stepper motor can be controlled without a feedback mechanism, as the partial rotation steps are used to control the motor [17]. Stepper motors cannot operate at high speeds but have a high holding torque [18]. This makes a stepper motor ideal for the control of the disc brake.

2.9 Sun XMD-01

The XMD-01 is a device to electrically control hydraulic systems. The XDM-01 controls the hydraulic system by controlling the valves with a current output. The user can control and

program the XMD-01 via Bluetooth. The app presents secure access to the XMD-01 and requires a password to gain access therefore making the device tamper proof.

The XMD-01 has only one input pin for the system its controlling, of either a 0-10V, 0-5V or 0-20mA, whereas the XMD-02 has two input pins. This input can be used to control the output of the XDM-01 to the valve being controlled.

2.10 RS422 serial data standard

RS422 can transfer data over 15m at 10Mbps [19]. Voltage between -2V to -6V represent a mark and +2V to +6V represent a space. -2V to +2V provides a noise margin. Communication modes are full and half duplex. Two RS485 adapters can be used in conjunction to represent one RS422 connection. RS485 data equals 1 for 1.5V to 5V where B is greater than A and data equals 0 for 1.5V to 5V where A is greater than B.

2.11 Operational amplifier

An operational amplifier can be used to convert bipolar to unipolar output. This can be done with a summing amplifier as depicted in Figure 6-7 below. Where the summing amplifier has the following transfer function [20].

$$V_{out} = \left(V_1 \frac{R2}{R1 + R2} + V_2 \frac{R1}{R1 + R2} \right) \left(1 + \frac{R4}{R3} \right) \quad (24)$$

2.12 Conclusion

The literature study provides clarity on all the aspects of the project. From Chapter 2 informed concept designs and decisions on design aspects can be made. However, the literature study was continuously updated throughout the project development as part of research in the engineering process. Chapter 3 provides the concept designs for the project units.

Chapter 3. Design

3.1 Introduction

This chapter provides the concept and detailed designs for the complex problem. Concept designs for the three functional units, namely the controller, load and motor connection are provided. The project consists out of 3 units, control, load and an electric motor under test shown in Figure 3-1.

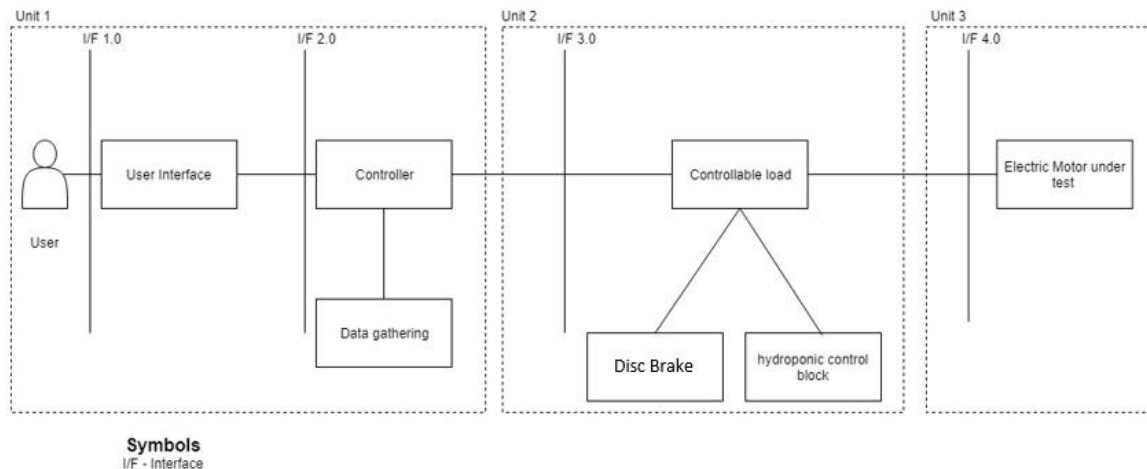


Figure 3-1: High-level functional units

Unit 1 is the control unit, consisting of the user, controller, personal computer and data. The user will provide input to the computer that will send it to the controller to control the load in order to test under the desired conditions. The controller will gather data from the torque transducer to transmit to the user. Unit 2 is the load applied to the electrical test motor. The initial test bench load consisted of a disc brake controlled by a hydraulic calliper system. Unit 3 is the electrical motor and drive under testing.

The final system breakdown structure can be seen in Figure 3-2 below. Several designs were changed and improved throughout the project life cycle therefore the system breakdown structure assists with the final representation of the project aspects.

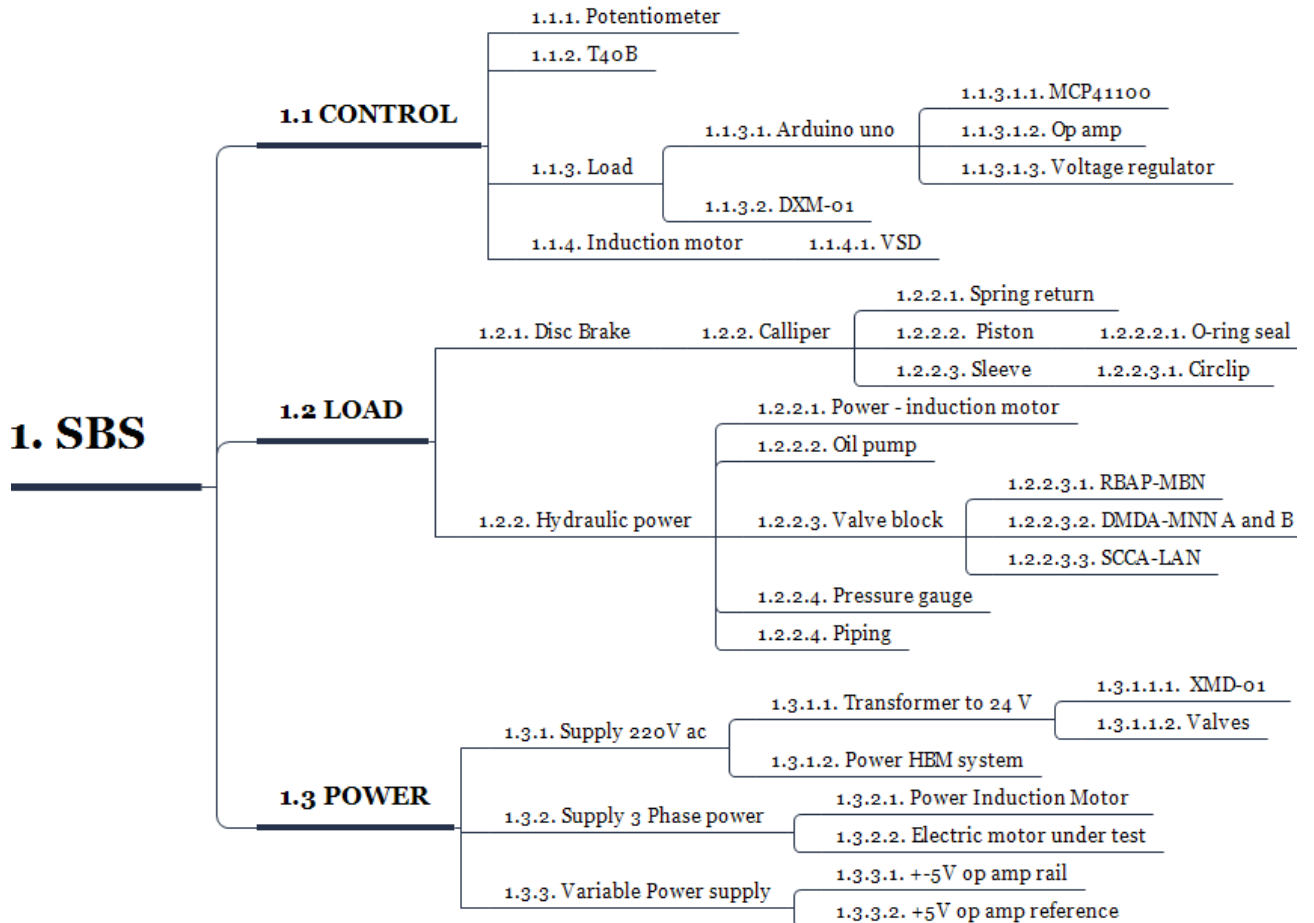


Figure 3-2: System breakdown structure

3.2 Load concept designs

3.2.1 Design 1: Hydraulic controlled calliper disc brake with VSD

The loading system consists out of a motor, hydraulic system and disc brake. The induction motor acts as a pump to power the hydraulic system. The induction motor is controlled using a variable speed drive to control the hydraulic system. The pressure needed to operate the disc brakes is provided by the hydraulic system as can be seen in Figure 6-17. VSD is not an effective way to operate the system as the hydraulic system was designed to operate at variable pressures by use of the valves. A system must be designed to control the hydraulic system electrically.

3.2.2 Design 2: Disc brake and DC motor combinations

The DC motor is set up to work in unison with the disc brake to provide a load for the electric motor under test as depicted in Figure 6-18. The disc brake is implemented as a small load at low speeds. Once the motor reaches sufficient speed, the DC motor is implemented to apply the bulk of the load. The DC motor speed is controlled using a low side switch, and the disc brake is controlled by the hydraulic system in the load design 1 above.

The electric motor under test is 1kW. Therefore, the DC motor in combination with the disc brake would be over specification for the required load on the motor.

3.2.3 Design 3: Hydraulic pump as load controlled by electric valve

The hydraulic pump is connected to the electrical motor with a shaft. The load on the motor produced by the hydraulic pump is controlled by a valve. The electrical valve will increase the load on the electrical motor as it is closed. The electrical valve is controllable by ESP32.

The temperature of the oil in the hydraulic pump can be measured using a waterproof temperature sensor. If testing concludes that the oil overheats during operation, the oil will be pumped through a radiator in order to be cooled.

As a large hydraulic pump and radiator are not required, used truck parts is a feasible and affordable option. It is possible to purchase the radiator and hydraulic pump from a scrap metal yard in order to reduce cost.

After a consultation, this design was disregarded, as the load on the electric motor would decrease as the electric valve is closed. Therefore, the design works in reverse, which does not allow for the starting resistance required.

3.2.4 Design 4: Airflow controlled fan in combination with magnets

The idea originates from Watt bikes, where the load is applied by reducing the airflow gaps of a fan that is being turned by peddling. By closing the airflow slots, the force required to turn the fan increases. However, in this case, the electrical motor will apply the torque to turn the fan. This is accompanied by magnets to apply extra load to the system. Both the magnets and the airflow control will be applied using a small electric motor applying torsional force to close or open the airflow as can be seen in Figure 6-19. The electric motor will be controlled by the ESP 32.

This design will not overheat or require substantial external power. The small electric motor to control the torque of the airflow restrictor is the only power consumer in the system. Discussion with supervisors revealed that the air-flow controlled fan would not provide enough starting resistance. Therefore, this design was not pursued further.

3.2.5 Design 5: Stepper motor-controlled Disc brake

A small stepper motor controls the existing disc brake operation by applying force to the braking cylinder. The stepper motor shaft connects to a worm gear controlling the master piston, as shown in Figure 6-20. The stepper motor increments are controlled by the ESP32 control unit.

3.2.6 Design 6: Hydraulic system with lever pressure reducer

In this design the basic elements are retained. The hydraulic valves control the pressure in the system and a disc brake is used to apply the load to the electric motor. To reduce the

pressure output of the hydraulic system, a lever will be connected between the hydraulic system and the disc brake calliper. The concept design can be seen Figure 6-21. In the design the lever is set in a ratio of 10:1 where the lever is 10 times longer at the hydraulic system side than at the output the disc brake. Therefore, the pressure will be reduced by a factor of 10.

3.2.7 Design 7: Reduce piston calliper diameter

The force output on the rotor disc is related to the surface area of the piston. Therefore, the force with which the brake clamps the disc, can be reduced by reducing the surface area where the hydraulic fluid applies pressure. However, if the surface area is reduced, the piston will no longer fit in the calliper. To solve this problem a sleeve is designed to fit between the calliper and the piston. The sleeve is then kept from being forced out by the hydraulic fluid, with a circlip in the groove of the disc brake calliper. The concept design for the new piston and sleeve is shown in Figure 6-22 above.

3.2.8 Load concept design trade-off

Though some alternative solutions were found that would be more energy efficient and operational cost efficient, the client required that the existing hydraulic system be implemented. There were two solutions utilizing the hydraulic systems and reducing the pressure load on the rotor disc. The first was to place a lever between the hydraulic system output and the input to the disc brake calliper, as described in subparagraph 3.2.6 above. The second solution is to reduce the piston pressure surface area to reduce the force applied to the rotor disc as shown in subparagraph 3.2.7. These two solutions are compared in Table 3-1 below.

Table 3-1: Load design trade-off

Criteria	Lever system	Piston area reduction
Cost	R 1000.00	R 500.00
Parts	3	2
Implementation	The radial movement will have to be designed for	Simple to implement
Oil leak probability	High	Low
Elegance of design	Awkward added bulk to design and more parts to get in the way of measurement	Simple internal solution to problem

From the trade-off in Table 3-1 above it is clear that the piston area reduction concept design is the best design solution for the project.

3.3 Spring concept design

In order to retract the disc brake calliper piston a spring return system must be designed.

Option 1

The first concept design is a shield shown in Figure 6-42, which can be placed over the brake pad and connect to a spring. This will pull back the brake pad and allow the disc to move freely. The issue with this design is that it will rub against the disc when the load is applied.

Option 2

The second concept design a compression spring system is connected to the brake pad and through the brake calliper body. The design can be seen in Figure 6-41.

3.4 Controller concept design

3.4.1 Controller V1.0: ESP32 WROOM

The basic flowchart of the control system is shown in Figure 6-23 in Appendix A.2. The inputs and outputs of the ESP 32 controller are shown in Figure 6-24 in Appendix A.2. The ESP 32 runs on a 5V power supply and the input and output pins of the ESP 32 controller is 0-3.3 V.

However, after new aspects of the design came to light namely that the output of the controller to the load must be between 0 – 5V and that the torque transducer communicates with a RS422 signal the trade-off study in subparagraph 3.4.3 was done.

3.4.2 Controller V2.0: Arduino Uno®

The Arduino Uno® was chosen to replace the ESP 32 in order to overcome the issues faced by the ESP 32 specified above. The Figure 6-25 shows the flow diagram of the Arduino Uno®.

3.4.3 Controller trade off

The primary choice is between using an ESP 32 and the Arduino Uno®. The ESP 32 is selected on the decision matrix shown below. In the matrix, the best score is 10, and the weakest score is zero.

Table 3-2: Microcontroller trade off study

Microcontroller	ESP 32 WROOM	Arduino Uno®	% Weight	ESP 32 WROOM score	Arduino Uno® Score
Price	R269.00	R699.00	10	10	5
Arduino IDE compatible	Yes	Yes	20	10	10
IO Pin operation	3.3V	5V	40	5	10
RS 422 Shield compatible	No, but can be connected with	Yes	30	5	10

	extra jumper cables				
Score		6.5		9.5	

From the decision matrix, it is clear that the best choice is the Arduino Uno® for the control of the system.

3.5 Data measurement system connection to controller concept design

3.5.1 Data measurement V1.0 0-5V

The T40B torque transducer produces a 0-5V output at 1024 pulses per revolution [21]. There are two output signals that are 90 degrees out of phase that can be seen in Figure 6-8 Appendix A.1. During clockwise rotation signal B is a phase ahead of A and anticlockwise signal A is a phase ahead of B.

3.5.2 Data measurement V2.0 RS422 to Arduino adapter

The torque output cannot be measured from the T40B torque transducer. The measurement must be done from the G070A torque adapter. The G070A torque adapter connects to the control system with RS422. The RS422 can be converted to UART communication with the controller.

3.5.3 Data measurement V4.0 T40B torque transducer -10V to +10V

The torque output can be measured directly at plug 3 of the T40B torque transducer. The output signal is a -10V to 10V voltage relative to the torque. Where 0V is zero load, -10V is minimum torque and +10V maximum torque. Therefore, depending on the rotation of the shaft, the torque will be represented as a 0 to 10V or 0 to -10V. As the motor's shaft will only be turning in one direction which produces a negative torque output, only the 0 to -10V output will be taken into account. The Arduino Uno® cannot measure a negative voltage as it would damage components on the board. Another concern is that the Arduino Uno® is only able to divide the voltage into 1024 increments. Therefore, if the control voltage range is too small within the total voltage range, the increments will be insufficient to be recorded.

Option 1

One option is to use a voltage divider to reduce the voltage from -10V to -5V. If one connects the -5V to the ground pin of the Arduino Uno®, the Arduino Uno® will not be damaged as the lowest voltage would be at zero. However, this would mean that the ground pin would move around as the -5V is the minimum but there will be no load at 0V, therefore all the other components in the system will be impacted.

Option 2

Another option is to design an operational amplifier circuit to invert the -10V to 0V output voltage from the T40B in order to produce a positive voltage output to the Arduino Uno®.

Option 3

If the torque direction can be changed with a setting, the voltage would be between 0 and 10V. The voltage can then be reduced to 0 to 5 V with a voltage divider. One can place a diode between the positive and the Arduino Uno® ADC pin to protect against negative voltage. This will not work if the operating voltage range is too low as the diode will only be measured above 1V.

Option 4

Option 4 is similar to option 2, on the precondition that the operational voltage range must first be determined during testing before the operational amplifier circuit is designed.

Design selected

Option 4 was selected for detailed design because the circuit would allow for reverse voltage protection, operate in the required range and will allow for the Arduino Uno's® 1024 division restriction.

3.6 Motor Coupling concept design

3.6.1 Design 1: Motor connected external to the test bench securing

The electrical motor is connected with the motor mounting flange to the test bench external to the current securing. The manufacturing is done by Mr Arno de Bruin of the NWU. The motor flange can be seen in Figure 6-38 in Appendix B. The torque flange adapter connects the motor shaft to the torque transducer, as shown in Figure 6-39 in Appendix B.

The torque flange adapter and motor connector will require modification as shown in Design 2as the solar car motor must be connected after the test bench stabilization.

3.6.2 Design 2: Solar car motor connection

The solar car motor must be connected to the interior of the test bench securing, as shown in Figure 6-26, as the motor does not have a shaft to connect to the torque transducer. The connection of the solar car motor to the test bench securing is shown in red. The solar car motor is connected to the torque transducer with the torque coupling shown in red. The coupling consists of two discs connected to a shaft that allows the coupling between the torque transducer and the solar car motor.

3.7 Combined Concept Design

3.7.1 Design 1

No solution was found for the hydraulic system pressure issue at that point; therefore, the stepper motor-controlled disc brake load was selected as the second choice. The ESP 32 was selected as the controller for the system. Design 2 of the motor connection concept design was selected, as shown in Figure 6-27 below.

The stepper motor operation is controlled by the ESP 32, as required by the feedback loop from the torque transducer. The data is sent to the PC, where it is logged for data analysis.

3.7.2 Design 2

A solution was found for the hydraulic system. Therefore, the stepper motor concept was discarded in favour of using the hydraulic system. The solution found for the hydraulic system was to reduce the piston diameter of the disc brake and returning the piston to its original position when pressure is reduced, with a spring return system. Furthermore, the ESP32 was abandoned in favour of an Arduino Uno®. Therefore, the new combined system consists out of the aspects depicted in Figure 3-3.

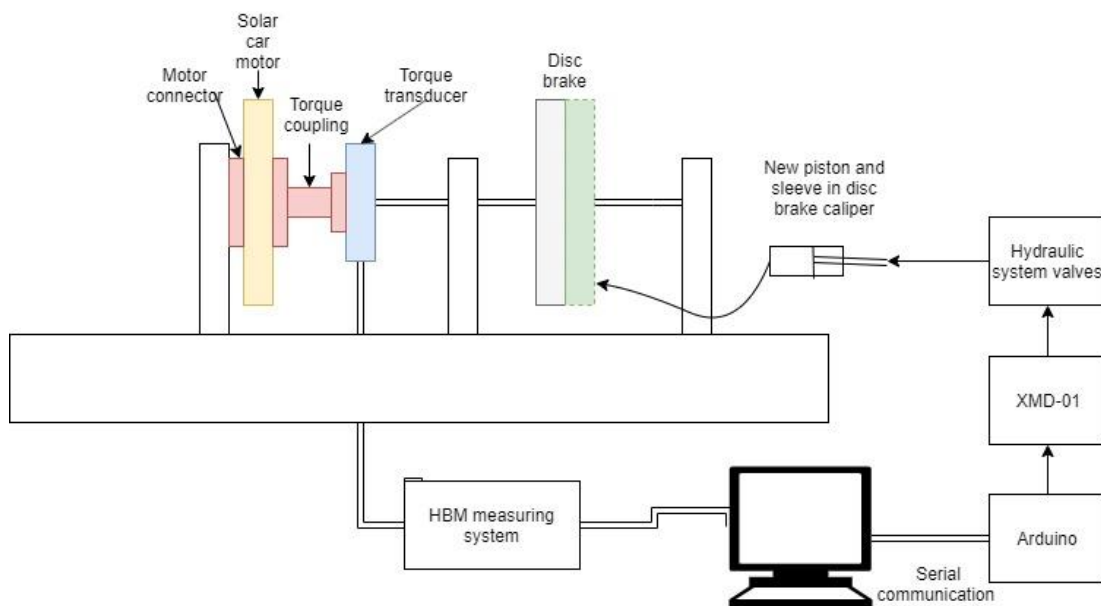


Figure 3-3: Combined concept design 2

3.8 Detailed design

The following provides the detailed design of all of the components of the project. A few different concept designs were considered; the most effective concept design was selected with the help of trade-off study matrixes, and detailed design will be based on the selected concept designs.

3.9 Disc brake detailed design

3.9.1 Pressure calculations

The disc brake is implemented to act as a load on the electrical motor. The disc brake is required to stop the motor at rated power and speed. The motor has a rated power of 1.5kW and rated speed of 1500rpm. Therefore, the shaft torque is calculated,

$$T_s = \frac{P_m}{\omega} \quad (25)$$

Where, T_s – shaft torque [Nm], P_m – motor rated power [W], ω – speed [Rad/s]

Therefore, the shaft torque is,

$$T_s = \frac{P_m}{\omega} = \frac{1500}{157,0796325}$$

The disc brake's operation is dependent on two major aspects namely the effect of friction and the effect of heat transfer. The following calculations were done to establish the required pressure of the system in order to determine the required pressure of the hydraulic system.

Using the uniform wear method, as discussed in the literature study, the pressure required is determined. The characteristics of the disc brake, determined through testing and evaluation, are documented in chapter 5.

From the parameters calculated in chapter 5 the following calculations are made. Firstly, the difference between θ_2 and θ_1 is calculated using the cosine rule,

$$a^2 = b^2 + c^2 - 2bc \cos(A) \quad (26)$$

Therefore, taking the following parameters in Figure 3-4 in Appendix B, into account the angle can be calculated as follow

$$0.099^2 = 0.1175^2 + 0.1175^2 - 2(0.1175)(0.1175) \cos(A)$$

$$A = 49.5^\circ$$

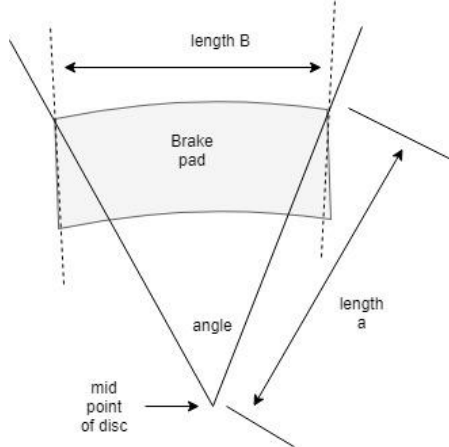


Figure 3-4: Disc brake angle calculations

Where the force F is expressed as,

$$F = (\theta_2 - \theta_1)p_a r_i (r_o - r_i)$$

Moreover, the frictional torque T is expressed as

$$T = (\theta_2 - \theta_1)f p_a r_i \int_{r_i}^{r_o} r dr$$

The EES calculations can be seen in the digital appendix. The results from the calculations are set out in Table 3-3.

Table 3-3: Disc brake pressure calculations results

Parameter	Value	Unit
Calliper pressure	11.928	kPa
Brake pad pressure	9.608	kPa
Brake pad force	29.98	N

3.9.2 Heat transfer calculations

The heat transfer calculations were done based on the theory set out in Shigley [11]. The temperature rise of a clutch brake assembly is approximated with,

$$\Delta T = \frac{E}{C_p m} \quad (27)$$

Where, ΔT – Temperature rise [k], C_p – Specific heat capacity [J/kgK], m – mass of the brake [kg].

E is calculated as follow,

$$E = \frac{I}{2} (\omega_o^2 - \omega_f^2) \quad (28)$$

And the maximum temperature is calculated with,

$$T_{max} = T_\infty + \frac{\Delta T}{1 - \exp(-\beta t_1)} \quad (29)$$

The calculations are available in the EES program in the digital appendix. From these calculations the following results were determined in Table 3-4 below.

Table 3-4: Heat transfer calculations parameters and results

Parameter	Value	SI Unit
Input		
Braking time	15	s
Times breaking per hour	15	-
Air Temperature	298.15	K
Output		
Maximum Temperature	340	K

3.9.3 Piston spring return

The disc brake calliper in the system is a single acting piston. Therefore, once the hydraulic system pressure is removed from the calliper piston, the piston does not return to its original position. This causes undesirable residual pressure on the disc. To counteract the residual pressure, a spring return was designed for the disc brake. The design features a threaded

rod, compression spring, washer and nut. The assembly can be seen in Figure 6-28 and Figure 6-41: the spring is placed over the disc brake calliper connection shaft, and the threaded rod is placed through the hole drilled into the shaft, the threaded rod is screwed into the brake pad securing it for the retraction. The washer and nut holds the spring in place.

In the spring return system, there will be a tensile stress on the threaded rod. This will be calculated as follow,

$$T = \frac{F}{A} \quad (30)$$

Where T is the tensile strength in MPa, F the force in Newton and A the cross-sectional area in mm². For a M3 threaded rod the nominal stress area is 5.03mm, as there are two rods the total area is 10.06mm assuming a maximum force of 700N on the system, the tensile stress is calculated as,

$$T = \frac{700}{10.06} = 69.5825 \text{ MPa}$$

For stainless steel the yield tensile strength is 215MPa. Therefore, the safety factor for the M3 rod is,

$$\text{Safety Factor} = \frac{T_{yield}}{T} = \frac{215}{69.5825} = 3.09$$

3.10 Hydraulic system detailed design

The previously implemented hydraulic system forms Appendix A of the report. The hydraulic system was designed to be controlled electrically by an XMD-01 controller. The schematic of the hydraulic control block design for the test bench consists out of several basic components. The components are the valves, pump, controller, filter element, induction motor driving the oil pump, tank, pressure gauge and calliper piston.

The way the hydraulic system is currently configured is causing the hydraulic system to supply too much pressure to the disc brake calliper. This was determined during testing and evaluation in Chapter 5. From the testing and evaluation, the required pressure for the disc brake calliper was determined as 0.5 Bar to 8 Bar. There are several aspects in the design that may have caused the system not to operate as expected. Firstly, the setup of the hydraulic block may have been faulty. Secondly, the motor driving the oil pump may be too powerful for the hydraulic system. Alternatively, the diameters of the oil pipes in the hydraulic system could affect the system pressure. It was also possible that a miscommunication previously occurred when the hydraulic systems specifications were discussed.

After investigation of the system the first problem identified was that the system is designed to operate between 10.5 and 105 Bar. Considering the whole design, the motor driving the

hydraulic system oil pump is an 80 V 3KW induction motor, pipes with large diameters, an OT200 series oil pump with pressure range up to 260 Bar and valves with operation range of 10.5 Bar to 105 Bar. Therefore, it is clear from these aspects that the specification for the design were incorrect. The XMD-01 is used to control the hydraulic system electronically. The XMD-01 is detailed in section 3.11.

There are three valves in the hydraulic system design schematic: the proportional pressure relief valve, configurable directional valve and the sequence check valve. The DMDA-MNN valve is a 2-position, 3-way spool directional valve shown in Figure 6-2 in Appendix A.1. The valve is normally open port 2 to 3 and closed port 1 to 2. The DMDA requires no minimum hydraulic pressure to operate. The RBAP-MBN is an electro-proportional relief valve shown in Figure 6-3, in Appendix A.1. The RBAP-MBN regulates the pressure of the system and operates between 10.5 and 105Bar. The SCCA-LAN is a direct-acting sequence valve with reverse flow check, depicted in Figure 6-4 in Appendix A.1. The valve allows flow in the circuit when the circuit exceeds the valve pressure settings. When the pressure at port 2 is higher than the pressure at port 1 the sequence valve opens to the tank.

The design was created for a two-way acting piston therefore two directional valves A and B were selected to work together. The design would allow the piston to move in one direction when valve A is selected and the other direction when valve B is selected. However, the disc brake implemented is a one-way acting piston. Therefore, only one proportional relief valve's output connects to the disc brake calliper and there is no way to retract the piston. The second proportional relief valve's output is plugged.

The XMD-01 controller was chosen to control the proportional pressure relief valve. Therefore, the XMD-01 controller controls the pressure of the system, as the proportional pressure relief valve throttles the fluid flow. The ports are used to change the flow direction. From the previous implementation the valves are controlled by 24V coils.

According to the design the pressure is measured at port A with a pressure gauge. The pressure gauge should thus measure the pressure after the configurable directional valve, meaning that the pressure measured is the pressure supplied to the calliper piston. However, as the design was changed, the pressure measured with the pressure gauge does not reflect the pressure to the disc brake calliper. Therefore, a new pressure gauge was connected before the disc brake calliper to measure the pressure to the calliper.

In the Figure 6-29 in Appendix A.2 the flow diagram of the hydraulic system is depicted when DMDA valve A is powered. The red line shows the flow path of the hydraulic fluid during this state. The hydraulic fluid flows from the oil pump through DMDA valve A to the piston calliper.

In the following Figure 6-30 in Appendix A.2 the flow path of the hydraulic fluid can be seen in red. The hydraulic fluid flows from the oil pump to the sequence valve and through the sequence valve to port 1 of the DMDA. The path is thus blocked and if the pressure set by the RBAP is higher than the pressure at port 2 of the sequence check valve, said valve will release the pressure to the tank. Port 2 and 3 of DMDA valve A are connected, therefore the hydraulic fluid in to the piston will flow back to the tank.

Hydraulic system solutions investigated

The disc brake requires 0.5-8 Bar from the system (determined during testing and evaluation, documented in Chapter 5); however, the installed valves operate between 10.5-105 Bar. In order to solve the pressure problem in the hydraulic system the following solutions were investigated.

1. Reduce the calliper size of the brake's piston
2. Reduce the brake pad area size
3. Position another pressure relief valve between the hydraulic system and disc brake piston calliper
4. Reduce the oil pump size

3.10.1 Reduce calliper size of brake's piston

Purpose

By reducing the size of the disc brake piston's calliper, the force applied to the disc is reduced for the same amount of pressure from the system.

Procedure

The calliper size can be reduced by sleeving the calliper. This is done by manufacturing a calliper of the desired diameter and fitting it into the calliper and blocking the excess space.

Calculations

The basic relationship between power and force is,

$$F = PA$$

Where F is the force in Newton, P the pressure in Pascal and A the area in meter squared. From this equation it is clear that by reducing the area the force applied is reduced. The valve installed in the system is a RBAP MBN proportional relief valve. This valve operates between 10.5-105 Bar. However, Sun Hydraulics has available an alternative electro proportional relief RBAP MDN valve which operates between 3.5-50 Bar. The calculations are done for both valves. The calliper in the disc brake piston is 48 mm.

Firstly, one needs to calculate the maximum and minimum pressure applied during the tests with the 48 mm piston.

Maximum force at 8 Bar

$$F_{max} = 243.8N$$

Minimum force applied at 0.5 Bar

$$F_{min} = 15.24N$$

Calculating for the RBAP MBN the minimum calliper diameter to reduce the pressure from 10.5 Bar to the 0.5 Bar is

$$\phi_{min\ MBN} = 10.598mm$$

For the RBAP MDN the minimum calliper diameter to reduce the 3.5 Bar to 0.5Bar is

$$\phi_{min\ MDN} = 14.89mm$$

Design

Reducing the calliper size requires the design of two new parts for the piston, the calliper sleeve and a new calliper. The calliper sleeve can be seen in Figure 6-49, the calliper sleeve will have a slide fit H7 tolerance. The new calliper designed from the calculations above can be seen in Figure 6-48 in Appendix B.1.

3.10.2 Reduce brake pad size

Purpose

To reduce the force on the disc in the disc brake by reducing the brake pad area.

Procedure

Manufacture a smaller brake pad with a smaller area to fix to the existing brake pad.

Calculations

Assuming brake pads with the following parameters in Table 3-5 and a calliper with 39.4mm diameter.

Table 3-5: Parameters of brake pad

Parameter	value	SI unit
Inner radius	0.078	m
Outer radius	0.118	m

Varying the angle, the area of the disc pad is varied. By varying the area of the brake pad the calliper pressure required to brake the motor is varied. This can be seen in Table 3-6 below.

Table 3-6: Brake pad area reduction calculation results

Angle [°]	Required Calliper pressure [Pa]	Required Calliper pressure [Bar]
5	541635	5.41635
30	90272	0.90272
49.6	54595	0.54595
100	27082	0.27082

Results

From the calculations it is clear that reducing the disc brake size will not increase the pressure requirement as much as required to be effective.

3.10.3 Reduce pump size

Purpose

To reduce the overall pressure in the hydraulic system the oil pump size can be reduced.

Method

Remove the 100 Bar pump from the system and replace with a smaller oil pump that only produces up to 10 Bar.

Result

By reducing the oil pump size, the pressure through the valves will be reduced. The electronic valves in the system can only operate between 10,5 to 105 Bar. Therefore, it would not be possible to reduce the oil pump without rendering the valves unusable.

3.10.4 Pressure relieving(reduction) valve

Purpose

To reduce the pressure from the hydraulic system before the brake piston calliper a pressure relieving valve can be placed before the calliper.

Method

Connect a pressure relieving valve between the calliper and hydraulic system block connected to the calliper.

Result

The pressure relieving valve with the smallest minimum control pressure is PVDA – 8DN. The minimum control pressure of a Sun Hydraulics pressure relieving valve is 1.7 Bar with a maximum pressure difference of 140 Bar. The 1.7 Bar is still too large to apply to the disc

brake. Therefore, some other form of reduction will still need to take place after the pressure relieving valve.

3.11 Controller detailed design

The previous control system is controlled via manual variable speed control of the hydraulic system.

3.11.1 Controller design V1.0 ESP 32 WROOM

The ESP 32 was researched in chapter 2 of this report. No form of automatic or electronic control was implemented in the previous year's design. The ESP 32 was chosen as it has strong processing capabilities, is relatively inexpensive and can be programmed in Arduino studio. The ESP 32 chip is already installed on a developed kit namely ESP 32 WROOM. The ESP 32 acts as the PI controller for the system. The ESP 32 devkit has the following pin layout shown in Figure 6-9 in Appendix A.1. The ESP 32 will be connected as shown in Figure 6-31.

Due to 5V requirements throughout the circuit the 3.3V IO pins of the ESP 32 were undesirable and the ESP 32 was replaced with an Arduino Uno®.

3.11.2 Controller design V2.0 Arduino Uno®

The Arduino Uno® was implemented to replace the ESP 32, in order to allow the 5V applications required. The pin assignment of the Arduino Uno® can be seen in Figure 6-10 in appendix A.2. The detailed design for the controller circuit is shown in section 3.17.2.

3.12 XMD-01 valve control detailed design

The Sun XMD-01 shown in Figure 6-11 in Appendix A.2, will be implemented to control the hydraulic system electrically. The XMD-01 is programmed via Bluetooth and the Sun XMD mobile app. The XMD-01 is most often used for CANBUS applications. CAN will not be used in this project as it does not provide the required function.

The mobile app interface can be seen Figure 4-3. The interface can be used to change the input settings between 0-10V and 0 to 5V. The input can be done as a signal or be pre-set as a graph. The output from the XMD-01 to the DMDA valve is a current signal, which will control the valve's operation.

3.13 Voltage Signal control detailed design

The Arduino Uno® will send a voltage signal to the XMD-01 to control the output to the valves. The valves will then control the hydraulic system, consequentially controlling the load of the disc brake on the motor. The signal from the Arduino Uno® to the XDM-01 is a 0-5V signal to pin 11 on the XDM-01.

The MCP41010 digital potential meter will be used to control the circuit. The potentiometer operates between 100 Ohm and 10K Ohm. The pin assignment for the MCP41100 can be seen in Table 3-7 below.

Table 3-7: Pin assignment MCP41100 [22]

MCP41100 Pin	MCP41100 Pin number	MCP41100 Pin Function
PA0	5	Potentiometer Terminal A
PB0	7	Potentiometer Terminal B
PW0	6	Potentiometer Wiper
CS	1	Chip Select
SCK	2	Serial Clock
SI	3	Serial Data Input
VDD	8	Power supply terminal (2.7 V–5.5 V)
VSS	4	Power supply terminal (2.7 V–5.5 V)

The pin connection of the MCP41100 to the Arduino Uno® can be seen in Figure 6-47 below. From the graph depicted in Figure 6-12 in Appendix A.1 it is apparent that the normalized resistance to the end terminal resistance is linearly related to the code decimal value [22]. There are 256 taps for the potentiometer. The output is calculated as depicted in Figure 6-13, Appendix A.1.

3.14 Torque Transducer Signal Measurement Detailed Design

3.14.1 Torque Transducer Signal Measurement V1.0

The HBM T40B torque transducer produces a 0-5V output for the frequency, torque or speed measured by the torque transducer. The output signal will originate from Pin 12 of the torque sensor and pin 13 will be connected to a common ground. The ESP 32's maximum voltage for the I/O pins is 3.3V therefore, a voltage divider will be used to reduce the voltage range.

$$V_{out} = \frac{V_s R_2}{R_1 + R_2} \quad (31)$$

Where the source is 5 V and the output is taken as 3V. The circuit can be seen in Figure 6-43.

However, it was determined that this signal should be interpreted by the G070A adapter and is sent as a RS422 signal therefore cannot be measured directly.

3.14.2 Torque Transducer Signal Measurement V2.0

The G070A torque adapter sends an output signal of the torque and speed measurements via RS422. The pin assignment of the RS422 connection from the G070A torque adapter is shown in Figure 6-14 in Appendix A.1.

RS422 adapter chips are uncommon and would be slow to ship to South Africa. A RS485 adapter was selected as RS422 can be received with a RS485 adapter. Therefore, a RS485 shield was selected to convert the RS422 signal to UART that can be processed by the Arduino Uno®. The RS485 pin assignment can be seen in Figure 6-15 in Appendix A.1.

The shield is powered by the 5V connection of the Arduino Uno® and therefore the Vcc is not connected to power. The shield communicates with the Arduino Uno® through the TX and RX pins 0 and 1 on the Arduino Uno® board. The connection between the RS422 and the shield is as follows in Table 3-8 below.

Table 3-8: Connection between G070A and Shield

G070A adapter RS422 output				RS485 Shield pin	
Torque output		Speed output			
Output	Pin	Output	Pin		
GND	8	GND	8	GND	
+ Torque signal	12	+ Signal	12	B	
- Torque signal	13	- Signal	13	A	

The expected frequency range for the G070A torque adapter RS422 output is 60kHz at zero load, 61kHz at minimum positive torque, 90kHz at maximum positive torque and the required sampling rate would be 150kHz. The Arduino Uno® does not sample fast enough in order to measure this signal therefore a new design was required.

3.14.3 Torque Transducer Signal Measurement V3.0

Plug 3 on of the T40B torque transducer provides the torque measured as a +10V output. Figure 6-16 in Appendix A.1 reflects the pin assignment of plug 3, pin 1 and 4 providing the torque measurement signal.

From the test done in subparagraph 5.3.5 it is clear that the voltage will range between +15 mV and -500mV where + 15mV may occur at no load applied and -500mV at greatest load applied. The Arduino Uno® can measure 1024 voltage points. Therefore the 0-5V will be divided into 4.8828 mV increments. In the concept design it was suggested to use a voltage divider to reduce the 0 to 10V to a 0-5V. However, this would divide the signal into 10mV increments, which will not provide the required control.

In order to measure the positive and negative voltage output a summing operational amplifier was designed.

The output voltage is calculated with the following equation,

$$V_{out} = \left(V_1 \frac{R2}{R1 + R2} + V_2 \frac{R1}{R1 + R2} \right) \left(1 + \frac{R4}{R3} \right) \quad (32)$$

The circuit in Figure 6-44 was designed, with voltage regulators for the voltage inputs of the system. The op amp selected was the UA741 being readily available. The circuit was initially designed with 10V rail supply for the op amp, however, due to time constraints only 5V

regulators could be found and the circuit was redesigned with 5V rail supply to the op amp. The positive voltage regulator selected is the L7805CV and the negative voltage regulator is the MC7905CD. The IC pin assignment is as follows in Table 3-9 below.

Table 3-9: Op amp circuit IC pin assignment

Pin in schematic	UA741	L7805CV	MC7905CD
1	Non-inverting input	Input	Input
2	Inverting input	Ground	Ground
3	Positive power supply	Output	Output
4	Negative power supply	-	-
5	Output	-	-

Taking the reference as negative torque is the greatest torque and positive torque is the smallest output. The voltages will then be represented as follow in the Table 3-10 below.

Table 3-10: Voltage output after op amp

Input voltage [V]	Output voltage [V]	Torque relation
+0.5	+3.005	Motor positive torque upper range according to tests
+ 0.015	+2.742	Positive variance around no load
0	+2.705	Ideal no load zero torque measurement
-0.015	+2.668	Negative variance around no load
-0.5	+1.475	Motor negative torque upper range according to tests

3.15 Control loop design

The control loop will be implemented with an Arduino Uno®. The user will provide a torque set point and the time that the motor has to be kept at the set point. The torque is measured with the HBM T40B which gives a +10V signal representing the torque output. The output voltage is shifted up with an op amp circuit in order to accommodate the Arduino Uno® ADC voltage restrictions. The control loop flow diagram can be seen in Figure 6-32 in Appendix A.2.

In order to find the setpoint and input correlation, the relation between the torque measurement and the T40B voltage output, and between the T40B output voltage and the op amp output to the Arduino ADC, have to be calculated. The relationship between the torque and the voltage output of the T40B was determined with linearization in the test and evaluation in subparagraph 5.3.5 below. From the linearization we find,

$$V_{T40B} = 0.0934 * \text{Torque} + 0.0066 \quad (33)$$

Substituting the circuit values in to equation 32 it can be reduced as follow.

$$V_{out \ op \ amp} = \left(V_{T40B} \frac{10400}{12600} + 5 \frac{2200}{12600} \right) (3) \quad (34)$$

These two are then combined to calculate the relation between the torque and the output voltage to the Arduino Uno®.

$$V_{out \ op \ amp} = \left((0.0934 * Torque + 0.0066) \frac{10400}{12600} + 5 \frac{2200}{12600} \right) (3) \quad (35)$$

With this formula and the PID Arduino IDE library the control loop for the load system can be implemented.

During testing and evaluation, the PID control did not operate as expected. It was determined that there was too much noise input to the system as can be seen in Figure 6-55. By elimination it was determined that most of the noise was caused by the induction motor being controlled with the VSD. The power supply of the induction motor was changed to the Variac power supply. This reduced the noise drastically as can be seen in Figure 6-59. However, there was still some noise due to the Grundfos motor as well as general noise from the heavy current laboratory. To reduce this a RC filter was designed with the following equation,

$$f_c = \frac{1}{2\pi RC} \quad (36)$$

The RC filter was designed for 66Hz and 15uF, which design can be seen in Figure 6-45 in Appendix A.2.

However, there was still some noise after the filter was installed. To filter out the noise an averaging digital filter was coded to reduce the remaining noise. Further testing showed some oscillation in the system, that can be accounted for by the operating ranges of the MCP41100 potentiometer, XMD-01 and RBAP valve. This can be seen in Figure 6-33 in Appendix A.2.

To increase the range, the XMD-01 measurement input settings are changed to 0-10V input so that the operation range becomes 0-2.22V. To increase the operating range of the MCP41100 digital potentiometer, a voltage divider circuit, as per Figure 6-46 in Appendix A.2, was designed to reduce the output voltage and thereby increase the range.

Therefore, as can be seen in Table 3-11 below, the increments per Bar has increased drastically and will reduce the oscillation in the system PID control.

Table 3-11: Operating range improvements

Parameter	Before design changes	After design changes	Unit
Valve	10-30	10-30	Bar
XMD-01	0-1.11	0.2.22	V

MCP41100	0-57	0-227	Setpoints
Pressure to MCP41100 relation	2	11	Increment/Bar

3.16 Motor coupling detailed design

The motor coupling is divided into two segments: the motor under test to the test bench and the motor to the shaft. The designs for the couplings are drawn on Solidworks. The detailed drawings are provided in Appendix A.2 coupling.1. The manufacturing will be done in the NWU laboratory.

3.16.1 Test bench couple

The motor couples to the test bench with the design in Figure 6-40 in Appendix A.2. The outer section holes couples to the test bench stand with bolts. The inner diameter section couples to the motor. The coupling can be seen in Figure 6-40 in the Appendix of the document. The couple will be cut from 8mm mild steel in order to carry the weight of the motor and to withstand the vibrations of the system.

3.16.2 Motor spacers

The new Grundfos motor implemented and tested in the circuit was larger than the previous motor and accommodation had not been made for its size in the stand. Therefore, the plates had to be switched around in order to fit the motor. Switching around the coupling plate left a space between the stand and the motor coupling plate. Therefore, there would be moments on the bolts fastening the motor to the coupling. These moments on the bolts would weaken the bolts and cause failure over time. To prevent this, spacers where designed to fit between the coupling and the mounting. The spacers where designed to fit snugly between the plate and the coupling.

3.17 Integrated system detailed design

The following is the integrated system of the detailed designs defined in the preceding paragraphs.

3.17.1 Combined electronic system V1.0

In Figure 6-35 below the process of the XMD-01 can be seen. A voltage input of 0-10 V is provided at pin 11 of the XMD-01 from the ESP32 via a voltage divider as shown in Figure 6-34 in Appendix A.2.

This voltage signal will then have a corresponding current output depending on the programming of the XMD-01 via the Bluetooth connection and the SUN app. The corresponding current output from the XMD-01 is sent to the valve electronic input. The current input to the valve coil will then result in a pressure change in the valve that will control the hydraulic system pressure. The pressure change in the hydraulic system will control the pressure change on the disc brake clipper.

3.17.2 Combined electronic system V2.0

The following figure shows the combined electronic circuit. The Arduino Uno® controls the pressure in the hydraulic system between 10 and 100Bar with a 0-5V. The 0-5V is varied through a digital potentiometer MCP41100 that is powered by the 5V pin of the Arduino Uno®. The combined circuit was designed in Proteus and can be seen in Figure 6-47 in Appendix A.2.

3.17.3 Combined electronic system V2.1

The torque and speed input to the Arduino Uno® was determined to be a RS422 signal input therefore the Arduino Uno® cannot measure it directly. A RS485 adapter was added to convert the signal to serial communication. The design stays similar to that of Figure 6-47 with the exception that the torque and speed no longer connects to pin A1 and A2 but to the RS485 shield, which connects to RX, TX and 5V pin of the Arduino Uno®, as depicted in Figure 6-36 Appendix A.2.

3.18 Combined electronic system V2.2

Design V2.2 shown in Figure 6-37 in Appendix A.2 is similar to V2.1 with the exception that the torque measurement input is no longer RS422 frequency signal from the G070A torque adapter but a +10V signal from the T40B torque transducer's plug 3. The voltage signal is converted to an appropriate 0-5V with an op amp circuit. The output of the op amp circuit is connected to the ADC input pin A0 of the Arduino Uno®. The rest of the design remains the same as V2.1.

3.19 Conclusion

This chapter focused on the design solution of the project. From the detailed design, improvements to the current design is made and the required aspects of the new design can be constructed and implemented. An iterative design process was followed in order to improve the designs throughout the project life cycle. All the detailed designs were implemented; however, the final implementation of the test bench can be seen in the system breakdown structure in Figure 3-2.

Chapter 4. Implementation

4.1 Introduction

In the following chapter the detailed designs for the system are implemented. Some prototypes of subsystems were built on a breadboard in order to test the functionality before implementation. If it was determined during implementation that the design was not functioning as required a new detailed design was made and implemented.

4.2 Disc brake piston and sleeve

The piston and sleeve designed in subparagraph 3.10.1 was manufactured and implemented. The original piston was removed from the disc brake calliper. As per the design an O-ring was placed over the piston shaft to fit in the seal groove. The sleeve was slid into the disc brake calliper and locked in place with a circlip. Finally, the piston with the O-ring was slid into the sleeve and the disc brake was reattached to the test bench. After implementation, testing and evaluation was done to determine that the design functioned as required. The piston was implemented in the disc brake calliper; the calliper can be seen in Figure 4-1.



Figure 4-1: Disc brake calliper

4.3 Spring return

The spring return system was designed to retract the piston to its original position when pressure is reduced in the system. The spring return system consists of a 3mm threaded rod, a 15mm diameter spring, a 20mm diameter washer and a M3 nut. Holes were drilled into the brake pad whereupon the piston presses. The holes were then threaded to allow the threaded rod to be screwed into the brake pads. A 3.5 mm hole was drilled into the shaft connection of the disc brake body that is situated approximately over the middle cross section of the brake pad. It is accordingly ideally situated to retract the piston in a balanced manner. On the outside of the disc brake body the spring is placed over the threaded rod and secured with a washer and nut. The spring return system can be seen in Figure 4-2. The testing results are presented in subparagraph 5.3.8 of the report.



Figure 4-2: Spring return system implemented

4.4 Hydraulic system

As per the Axiom design specifications the hydraulic system operates between 10.5 and 105 Bar. The induction motor drives the oil pump at a constant rate of 1200 RPM. The pressure in the system is controlled by the RBAP electro pressure relief valve, which is controlled by the XMD-01. The XMD-01 configuration is controlled by the mobile app shown in Figure 4-3.



Figure 4-3: XMD-01 App interface

A pressure gauge was added between the valve block and the disc brake calliper system. The XMD-01 0-5V input can either be done manually with a dial to control the pressure or it can be switched to digital control where the Arduino Uno® will control the load, as a result of the changes made to the control system. For the tests the pressure in the system required is 10.5-30 Bar. At 10.5 Bar there is no force applied to the disc brake pads. When the motor is tested

above 30 Bar, the load applied to the motor is too high and causes the motor to stop. The test bench system can accordingly be applied to both a weaker and stronger motor depending on the test requirements.

4.5 Controller

4.5.1 ESP 32 WROOM

Basic functionality was implemented with the ESP 32 using Arduino IDE. However, it was determined that due to the 5V requirements of both the RS422 connection and the XMD-01, the ESP32 is not the best choice and the ESP32 was exchanged for an Arduino Uno ®.

4.5.2 Arduino Uno®

The Arduino Uno® was implemented as the control for the system. The Arduino Uno® is powered through the USB connection of the computer and communicates with the computer via UART. The data measured with the Arduino Uno® is saved to a csv file with Tera Term.

The Arduino Uno® controls the output voltage to the XMD-01 controller, with a MCP41100 digital potentiometer. The potentiometer was at first connected to an LED on a breadboard to test the output of the MCP41100, shown in Figure 4-4. It was also measured with a multimeter to check whether the MCP41100 operated as expected. Once its operation was tested and succeeded, the MCP41100 was soldered onto a strip board with wire connectors to the Arduino Uno®.

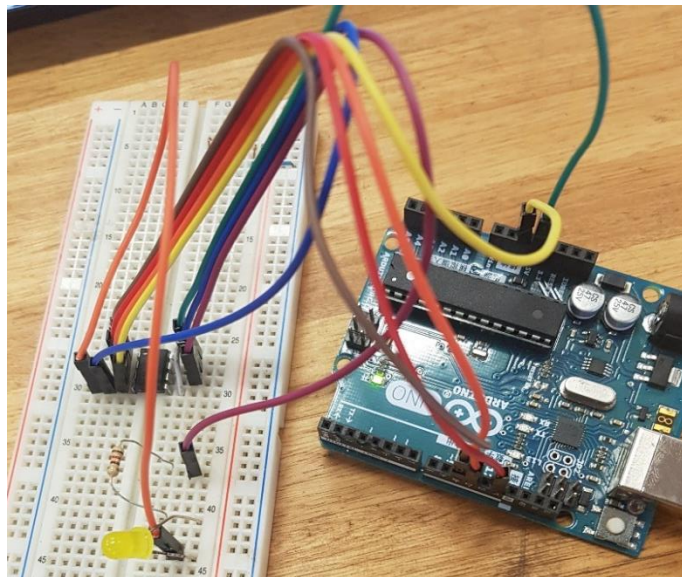


Figure 4-4: MCP41100 LED test circuit

The RS422 was implemented as follows: the Arduino Uno® connects to the G070A torque adapter with a RS485 Shield that converts the RS422 output from the torque adapter to UART. The RS485 connects to the RX and TX and the 5V power pin of the Arduino UNO®. The converted signal is then sent to the IDE serial monitor through serial communication. The measurements are logged with Tera Term to a csv file. During testing and evaluation, it was

determined that the sampling rate required for the RS422 was too high for the Arduino Uno®. Therefore, a different controller is required to measure the RS422 signal. To implement a different, more complex controller falls outside the scope of this project and therefore another solution was required to measure the torque.

The torque measurement signal can be measured directly on the T40B torque transducer at plug 3 as a +10V output. The relation between the torque and the output voltage was determined during testing and evaluation. In order to accommodate the negative voltage output, a summing amplifier circuit was designed and implemented to shift the voltage output up to the required 0-5V voltage range of the Arduino Uno® ADC pins. In order to ensure the voltage supply to the op amp circuit is constant, a voltage regulator circuit was designed and implemented. +5V Rail supply voltage to the op amp was implemented. The only voltage regulators that could be found within the time constraints were positive and negative 5V. However, as per the design +10V rail supply would have been preferable. The +10V rail supply can be implemented, when 10V positive and negative voltage regulators are acquired. The only changes that would be required in the design is to change the voltage regulators' capacitors according to the application notes.

4.6 Grundfos motor replacement

During testing of the piston and sleeve design it was determined that the original motor, the MGE90SC, was not operating as required. The MGE90SC is an electric motor with a built-in drive designed for pump applications. The motor stopped when even the slightest load was applied due to an over voltage error as well as a pump blocked error. Technicians from Grundfos serviced the motor and determined the drive was not operating correctly. The technician was unable to solve the problem with the drive and the motor was replaced with a MGE90SB2 as the motor was still under warranty.



Figure 4-5: Photo of MGE90SB2 Grundfos motor

The implemented MGE90SB2 Grundfos motor can be seen in Figure 4-5. In order to fit, the new motor required spacers to the mountings. Spacers were designed and manufactured and can be seen in Figure 4-6.



Figure 4-6: Photo of spacer implemented

4.7 Software User interface

The user interface consists of three modules the Arduino IDE, HBM Precision software and a Python interface. The HBM Precision user interface displays the current, voltage, input power, torque, speed and mechanical power. This is displayed on a simple interface for the user available as a preview or the ability to save the data.

Two main programs are used to control the load of the system. The first is a user defined pressure on the system and the second is a torque set point with a control loop. The pressure defined load works as follows: In the Arduino IDE a simple array is available for the user to input the desired set points for the test. For the simple load set point, the user types in the pressure in Bar[] in the Bar array and the time period the test should run each pressure in the timeS[] array in the Arduino IDE load.ino file. The code is then loaded onto the Arduino Uno®. The user must then open the Arduino IDE serial monitor window. The user is then prompted to start the test by typing 1 into the serial monitor window. Once the program receives the prompt to start, the MCP41100 potentiometer is controlled to allow the following output as displayed in the Serial monitor window shown in Figure 4-7.

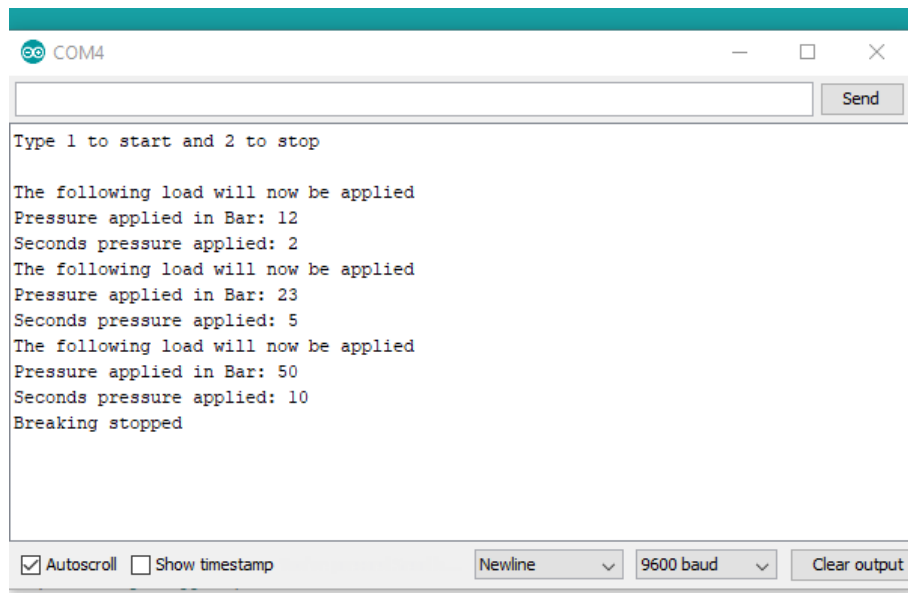


Figure 4-7: IDE serial monitor user interface

The control loop interface is similar to the interface described above. The user inputs the torque in the `setTorque[i]` array and the time the torque must be maintained in the `SetTime[i]` array. The torque measured is written to a csv file which is displayed as a graph by the Python program.

The Python user interface is a simple window that displays the torque and speed measurements read from the csv file created with Tera Term as shown in Figure 4-8. The program is functional and can be implemented once a speed measurement is received. However, as only the torque measurement can be read with voltage output from the T40B, the program is used to display the Torque as a function of time, until the RS422 measurement is implemented with a different controller that is able to sample at the required speed.

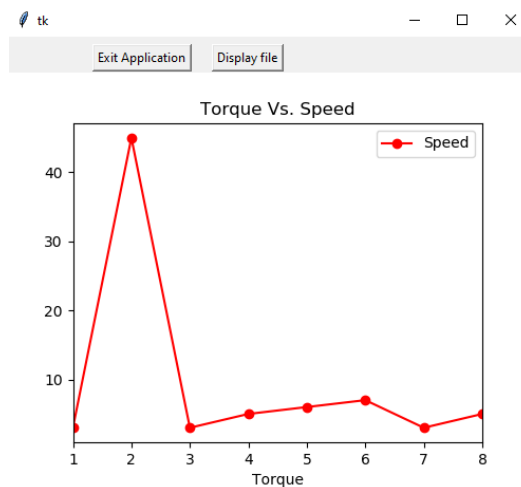


Figure 4-8: Example data output

4.8 Control loop

The control loop could not be implemented for the RS422 output from the G070A torque adapter as the Arduino Uno® is unable to sample at the required speed. The control loop was implemented with the T40B torque transducer voltage output as reference signal. The tests were first done on a breadboard as can be seen in Figure 4-9 to allow changes to the circuit.

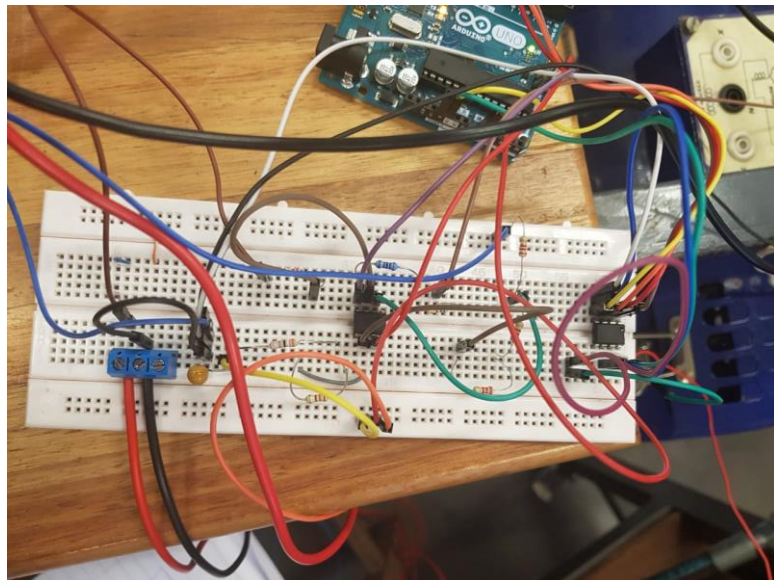


Figure 4-9: Photo of combined circuit implemented on a breadboard

Once the circuit was connected the first tests were done as documented in the test and evaluation section. The PID control did not operate as expected, changes were made to the code and the PID gain values, but no improvement could be made to its operation. Analysis was done to determine the source of the issue. After evaluation it was determined that the input to the control loop had too much noise. The cause of the noise was investigated in the test and evaluation section. It was concluded that the induction motor VSD control was causing the bulk of the noise. To reduce the noise the induction motor's power input was changed to the variac. However, there was still some noise on the system to reduce the noise a RC filter was designed and implemented as can be seen in Figure 4-9.

This reduced the noise significantly; the little noise remaining was reduced by implementing an averaging filter in the code. Once this was implemented the PID control improved drastically. However, there was still some oscillation due to the delay in the system and the MCP41100, XMD-01 and valve increments not being small enough.

4.9 Conclusion

In this chapter the detailed design was implemented. The force applied to the disc brake was reduced by implementing a piston and sleeve in the disc brake calliper. A spring return system was implemented to retract the calliper when pressure is reduced. The combination of the spring, piston and sleeve allows the system to operate between 10 and 30Bar, therefore the

RBAP valves can be controlled electronically to control the system. The digital control was implemented, the user provides pressures as a setpoints and the load will be digitally controlled. The PID control was implemented and tested, there remained some oscillation with the PID due to the delay in response from the elements in the system.

Chapter 5. Testing and evaluation

5.1 Introduction

Important aspects of the engineering design process are testing and evaluation. Testing and evaluation are done to determine whether the aspects of the design are functioning as required and to determine characteristics of components in the design. The test breakdown structure can be seen in Figure 5-1.

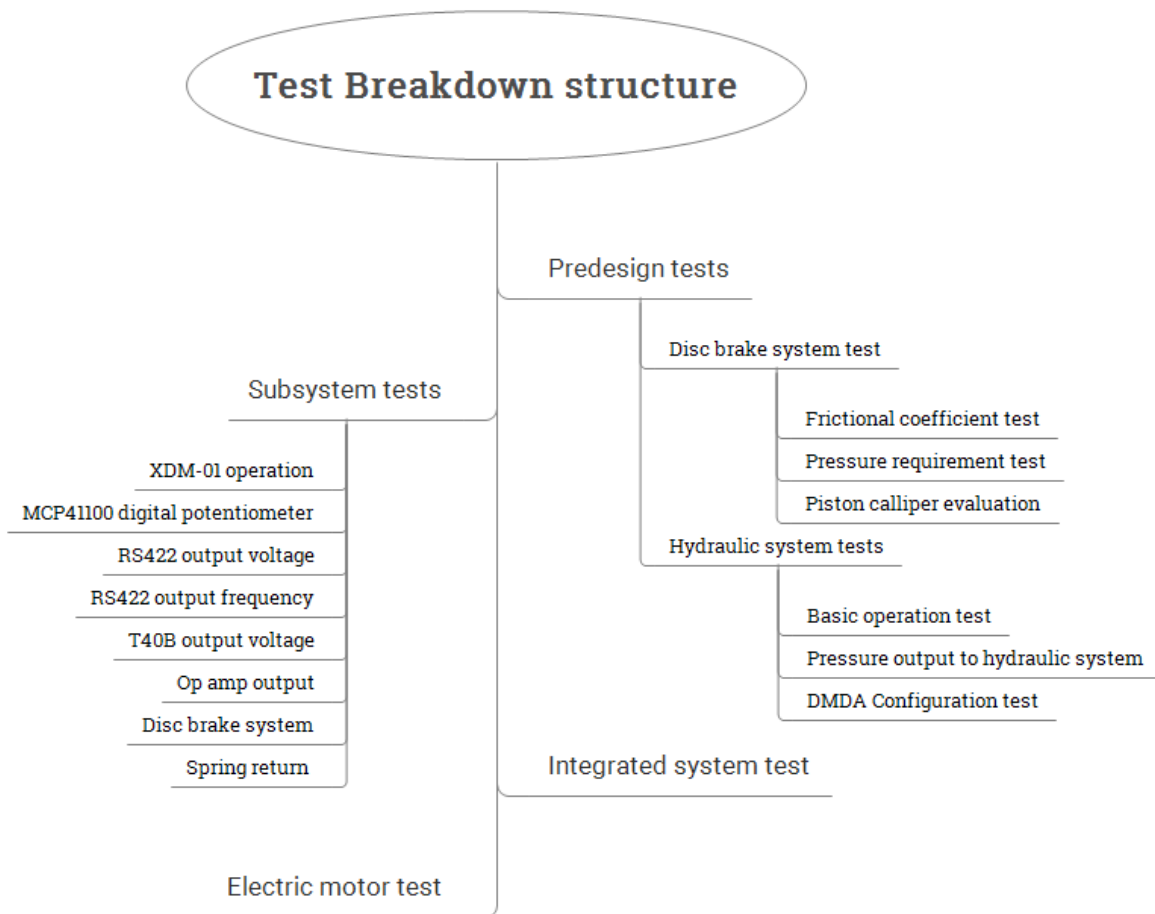


Figure 5-1: test breakdown structure

5.2 Predesign tests

Several tests were done on the disc brake and hydraulic system to determine the operational properties.

5.2.1 Disc brake predesign experiment 1: Frictional coefficient of brake pads

Purpose

Determine the frictional coefficient of the brake pads and the disc in order to calculate the pressure required to brake the motor.

Method

The frictional coefficient as discussed in the literature study is determined from the angle at which the brake pad slides down the disc brake as shown in Figure 5-2.

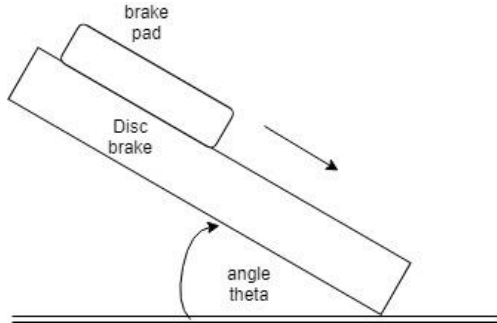


Figure 5-2: disc and brake pad frictional coefficient

From the literature study,

$$\tan(\theta) = \mu_s$$

Results

Therefore, the frictional coefficient is calculated as follow for the disc and brake pad,

$$\tan(22.3^\circ) = \mu_s$$

$$\mu_s = 0.41013$$

5.2.2 Disc brake predesign experiment 2: Disc brake pressure required Purpose

The following test was done in order that the calculations could be done in the detailed design to determine the pressure requirements to operate the disc brake.

Method

The disc brake was disconnected from the system and disassembled to measure the aspects of the disc brake.

Results

Once the disc brake was disassembled the following characteristics were determined in Table 5-1.

Table 5-1: Disc brake measured parameters

Parameter	Value	SI Unit
Calliper diameter	48	mm
Disc outer diameter	235	mm
Disc inner diameter	144	mm

Brake pad inner radius	78	mm
Brake pad outer radius	118	mm
Calliper type	Single hydraulic calliper	-

From these results the maximum required pressure was calculated as 7,2 Bar where brake pad 1 is the brake pad on which the pressure is applied from the calliper. Therefore, it is reasonable to assume that the hydraulic system should operate between 0-7,2 Bar. The implemented hydraulic system operates from 10 Bar.

5.2.3 Disc brake predesign experiment 3: Disc brake calliper

Purpose

To determine the disc brake calliper characteristics in order to design a sleeve and new calliper in order to increase the pressure requirement of the disc brake calliper.

Method

The disc brake was disconnected from the system and disassembled. Once the disc brake was disassembled the calliper was detached from the piston.

Results

The piston has the following characteristics that must be taken into account when designing the sleeve and the calliper.

- There is an inlet at the side of the calliper 12 mm above the base of the primary inlet. The sleeve must accommodate for pressure release through the connection if required, for example when bleeding the system.
- The pressure inlet at the base requires a 1mm gap for the pressure of the hydraulic fluid to disperse along the surface area.
- The groove just below the top of the calliper will be able to accommodate a circlip to secure the sleeve.

5.2.4 Hydraulic predesign experiment 1: Basic operation

Purpose

To assess how the hydraulic system is set up in order to determine the problem with its operation.

Method

This test is conducted by running the hydraulic system as defined in Mr Zaaiman's report. Therefore, the hydraulic system was not used in control. The pressure in the system was controlled by controlling the speed of the induction motor using variable speed drive. The

speed control of the motor controls the oil pump and thereby the pressure of the system. A new pressure gauge of 0 to 10 Bar was connected at the inlet of the disc brake calliper.

Results

From the experiment it was determined that the required pressure on the disc brake calliper is 0.5 Bar to 8 Bar maximum.

5.2.5 Hydraulic predesign experiment 2: Pressure output to the hydraulic system

Purpose

To determine the pressure range of the system, in order to assess whether the valves will be able to operate if the system is operated at normal capacity.

Method

This is conducted by setting up the experiment as in hydraulic experiment 1. For the test the induction motor is operated at 1200RPM and the hydraulic system is switched to DMDA valve A. The minimum and maximum pressure of the system is tested by operating the DMDA valve at maximum and minimum pressure.

Results

The minimum pressure measured at the disc brake calliper was 10Bar and the maximum was a 100 Bar. According to the calculations the pressure should not exceed 7,2 Bar. Therefore, the pressure range of the system when the valves are used is too high.

5.2.6 Hydraulic predesign experiment 3: DMDA Configuration test

Purpose

The piston calliper of the disc brake presses on the disc brake when the hydraulic system is switched off. The purpose is to determine whether the disc brake will be able to move freely if the DMDA-MNN valve configuration is varied.

Method

The experiment is set up as in hydraulic experiment 2. It is extended by varying DMDA valve A and B configurations to test whether the disc can move freely once the pressure is relieved.

Results

If DMDA valve B is selected the hydraulic fluid drains to the tank. Therefore, the pressure on the piston drops to zero, allowing the shaft to turn freely. However, the piston does not return to its start position and there is still some friction on the disc.

5.3 Subsystem tests

5.3.1 XMD-01 operational test

Purpose

To determine the pressure output in the system in relation to the input voltage to the XMD-01.

Method

The test consists of the following steps: varying the input voltage to the XMD-01, documenting the voltage measurement displayed in the Sun Hydraulic mobile application for the XMD-01 and the pressure output displayed on the pressure gauge connected between the hydraulic system and the disc brake calliper.

Results

The measurements of the voltage input to the XMD-01 in relation to the pressure is tabulated in Table 6-1 in appendix B.3 of the report. The measurements read from the pressure gauge at 10 to 20 Bar are probably inaccurate as they were taken in small increments and the pressure gauge is calibrated from 0-240 bar. The 10 to 20 Bar increments were mostly illegible. Making provision for the inaccuracy of the pressure reading in small increments, it can be deduced from the Figure 5-3 below, that the relation of the voltage to pressure is linear.

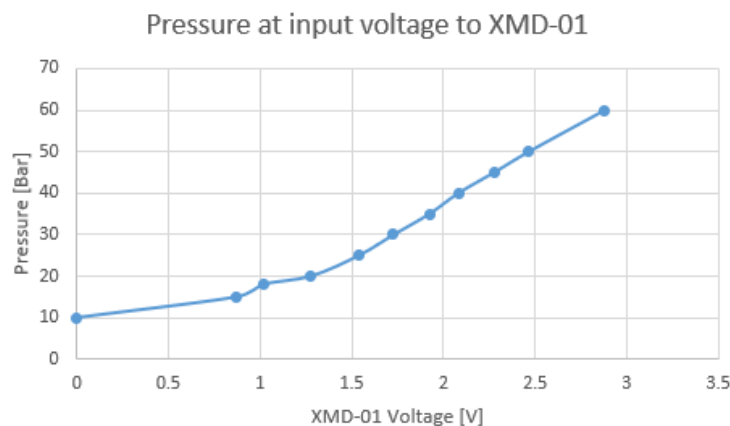


Figure 5-3: Pressure to XMD-01 voltage relation

5.3.2 MCP41100 digital potentiometer test

Purpose

The purpose is to determine if the output voltage is as expected from the digital potentiometer as per the datasheet.

Method

The test was done by setting the value for the digital potentiometer between 0 and 255 in the Arduino IDE code. The expected voltage output at PW0, the wiper terminal of the MCP41100,

was calculated. A comparison between the calculated voltage and the measured voltage at PW0 followed.

Results

The voltage is calculated as follows: Firstly, the resistance between terminal A and the wiper is [22],

$$R_{WA}(D_n) = \frac{R_{AB}(256 - D_n)}{256} + R_W \quad (37)$$

Where D_n is the data value from the code, R_{AB} is the overall resistance which is $100\text{k}\Omega$ and R_W is the wiper resistance of 128Ω . The resistance between B and the wiper is calculated as follows [22],

$$R_{WB}(D_n) = \frac{R_{AB}(D_n)}{256} + R_W \quad (38)$$

The voltage output is then calculated as,

$$V_{out} = V_{in} \frac{R_{WB}}{R_{WA} + R_{WB}} \quad (39)$$

The input voltage is the 5V pin from the Arduino Uno®. Therefore, the expected output is calculated as follows in Table 5-2 below. It is clear from Table 5-2 that the measured output corresponds with the calculated voltage output.

Table 5-2: MCP41100 test results

Code setpoint	$R_{WA}(D_n)$	$R_{WB}(D_n)$	Expected output [V]	Measured output [V]
0	100128	128	0.006384	0.0003
10	96221.75	4034.25	0.201197	0.201
50	80596.75	19659.25	0.980453	0.986
100	61065.5	39190.5	1.954521	1.96
200	22003	78253	3.902659	3.93
255	518.625	99737.38	4.974135	5.02

5.3.3 G070A torque adapter RS422 output voltage test

Purpose

The purpose is to determine the output signal from the G070A torque adapter.

Method

The method is measuring output voltage differentially between the + Torque signal and – Torque signal of the RS422 with TiePie oscilloscope.

Results

The output signal voltage measured with TiePie was taken at 0.43Nm torque. The + Torque signal and – torque signal was measured at 50kHz for 10kS as can be seen in Figure 6-50 in Appendix B.3. The output signal was measured as a pulse of -6V to -2V.

5.3.4 G070A torque adapter RS422 output frequency test

Purpose

The purpose is to compare measured Arduino Uno® UART output with expected frequency output from G070A RS422 signal shown in Figure 6-51, in Appendix B.3.

Method

The test is done by connecting RS422 to the RS485 shield plugged into the Arduino Uno®. The serial plotter is used to plot output at 2000 000 and 1000 000 Baud rate, with no delays in the code, therefore sampling as fast as possible.

Results

At a Baud rate of 1000 000 the output depicted in Figure 6-52 in Appendix B.3, was plotted on the serial plotter. The output plotted reflects spikes between 120 and 250, not the square signal expected. This is a result of the Arduino Uno® being unable to sample at sufficiently fast speed to read the signal correctly. The serial plotter output at 2000 000 Baud rate was of no use. The serial monitor output was taken and plotted in the Excel program to provide a graph. This output signal can be seen in Figure 6-53 in Appendix B.3 of the report. The output signal is spikes between 0 and 7 which is not the expected output. Therefore, the RS422 connection cannot be used to measure the torque and speed output with the Arduino Uno®.

5.3.5 T40B torque transducer voltage output test

Purpose

The purpose is to determine the relation between the torque and the +- 10V voltage output signal at plug 3 of the T40B torque transducer.

Method

The test is done by measuring the voltage output at pin 1 and 4 of plug 3 on the T40B torque transducer at incremental torque points.

Results

The relation between the torque and the voltage output can be seen in Table 6-2 in Appendix B.3. During testing of the Grundfos electric motor it was determined that the torque never exceeds 5Nm, as the load is then too great for the motor and the motor's control system will switch off the motor. Therefore, from the relation in Table 6-2, we can estimate that the voltage

range of outputs from the torque transducer will be between 0 to -500 mV. However, some deviation exists, as to the zero-load torque output, at no load the torque measured is between -0.19 and +0.19 Nm. This is the case even after the torque has been zeroed with the Precision software. Therefore, the output voltage will fluctuate between +15 and -500mV for this motor. The data in Table 6-2 was plotted as a scatter plot and a linearization line was drawn in Figure 5-4, in order to determine the mathematic relation between the torque and the voltage output. This equation is used in the PID control code.

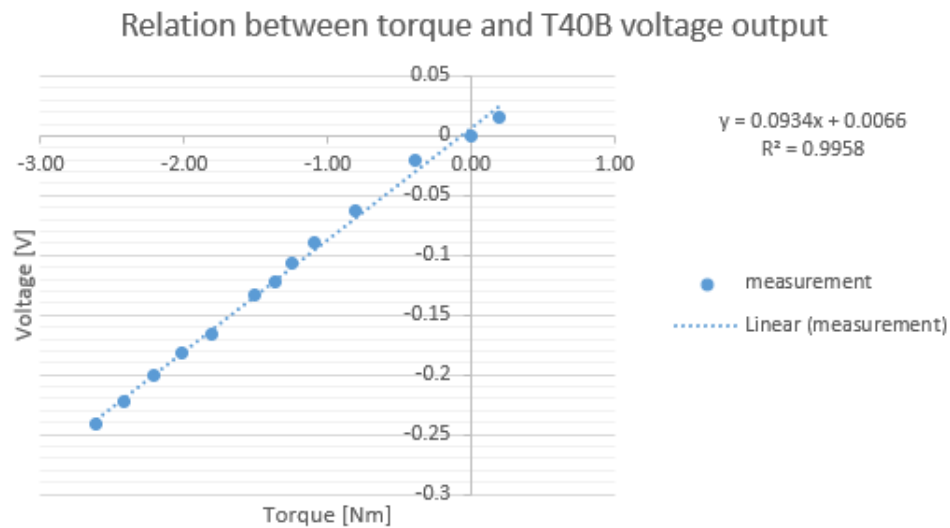


Figure 5-4: Relationship between torque and voltage of the T40B linearization

5.3.6 Operational amplifier test

Purpose

The purpose is to compare the simulated values of the designed op amp to the measured output of the circuit implemented.

Method

The set-up to test the op amp is reflected in Figure 6-54, where the reference voltage is 5V, and the input voltage is varied from -1V to 0.8V. The +- 10V rail voltage was compared to the +5V rail voltage, as the design was changed to +5V rail voltage in order to use available voltage regulator chips.

The pin assignment of the op amp UA741 pin output is as defined in the detailed design.

Results

The simulated and measured outputs are tabulated in Table 6-3 in Appendix B.3. From the Table 6-3 the results were graphed on Figure 5-5 below. From Figure 5-5 it is apparent that there is a small deviation between the measured output voltage of the op amp circuit with the

+10V rail supply, and the simulated output of the op amp with +10V rail supply. This deviation is amplified as the voltage is amplified. This is due to the op amp offset, which can be compensated for in the Arduino Uno® code. It is also clear that the op amp circuit with +5V rail supply's output plateaus at 3V when the input voltage rises above 0.3V. This is acceptable as the operation range is within the 0-3V bounds.

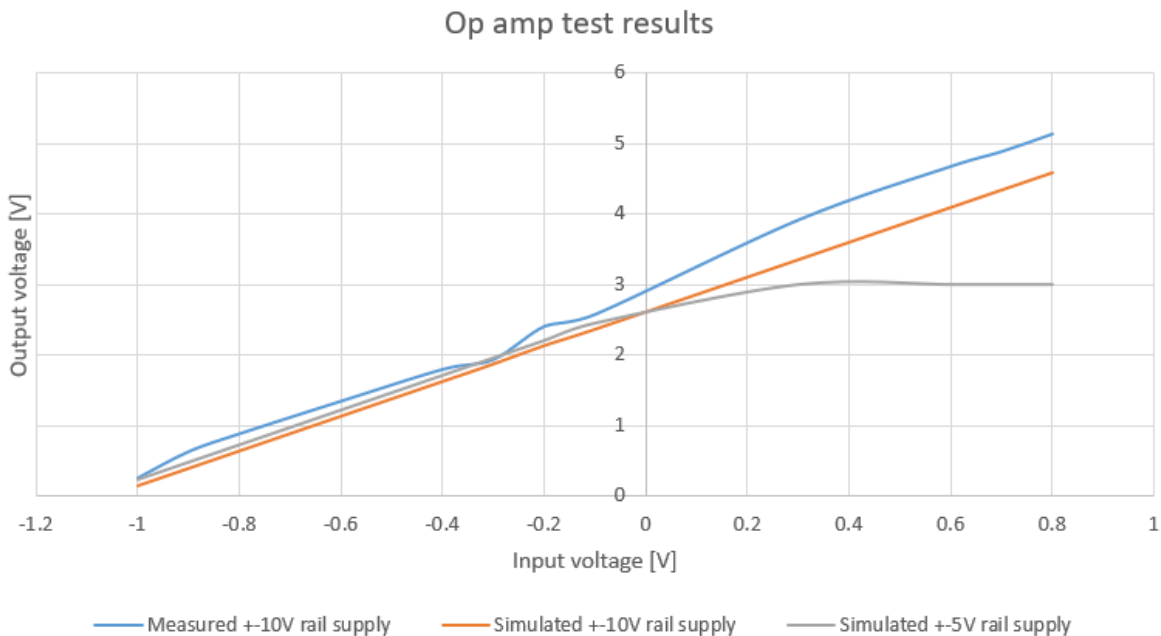


Figure 5-5: op amp test results

5.3.7 Disc brake system test

Purpose

The purpose is to determine whether the designed piston and sleeve operate as required.

Method

The test involves the implementation of the designed piston and sleeve in the disc brake calliper. Pressure of 0-100 Bar is applied on the system.

Results

The piston and sleeve meet all the requirements set in the Table 5-3 below.

Table 5-3: Piston and sleeve operation results

Function	Operating correctly
No leakage at 100 Bar	Yes
O- ring stays in place	Yes
Reduces the force output as required	Yes

5.3.8 Spring return system

Purpose

The purpose is to determine whether the designed spring return system operates as per design requirements.

Method

The test was done by implementing the designed spring return system on the disc brake body. Pressure of 0-100 Bar is applied on the system.

Results

From the results in Table 5-4 below it is clear that the spring return system fulfils the requirements for the system.

Table 5-4: Spring return system test results

Function	Operating correctly
Return piston to start position when pressure 10 Bar	Yes
Rod stays in place in brake pad at 100 Bar	Yes
Spring system does not prevent disc brake functionality	Yes

5.4 Integrated system test

Purpose

To test the operation of the integrated circuit including the PID control.

Method

Implement the PID control with the combined system.

Result

Once implemented the PID control did not operate as expected. Random spikes occurred during the control. No change in the output spikes occurred when the PID gain values were changed. The input to the PID program was analysed by plotting the input values as can be seen in Figure 6-55. From this it was clear that the issue with the PID was due to the extreme noise on the input.

To determine the cause of the noise the following tests were done, the laboratory noise, Grundfos motor noise and induction motor VSD noise. The measurements were taken directly on the output voltage of the T40B torque transducer to ensure that it is not noise on the circuit itself. All the measurements were taken with TiePie oscilloscope. From Figure 6-56, it is clear that there is some noise caused by the machines in the vicinity, however the noise can be reduced with the RC filter design set out in subparagraph 3.15. The noise caused by the Grundfos motor was measured in Figure 6-57, which made it clear that the Grundfos motor causes some noise, but that it can also be reduced with the RC filter. Finally, the effect of the

VSD controlled induction motor was measured in Figure 6-58. It became apparent that the primary source of the noise is the VSD. To prevent this, the induction motor is connected directly to the variac. From Figure 6-59 it is clear that connecting the induction motor to the variac reduces the noise considerably.

To reduce the remaining noise on the system the RC filter was implemented. The impact of a 66Hz and 994Hz filter can be seen in Figure 6-60 in comparison to the unfiltered output. There clearly remain some noise, and to reduce it an averaging filter was implemented in the Arduino IDE code. The effect can be seen in Figure 5-6 below.

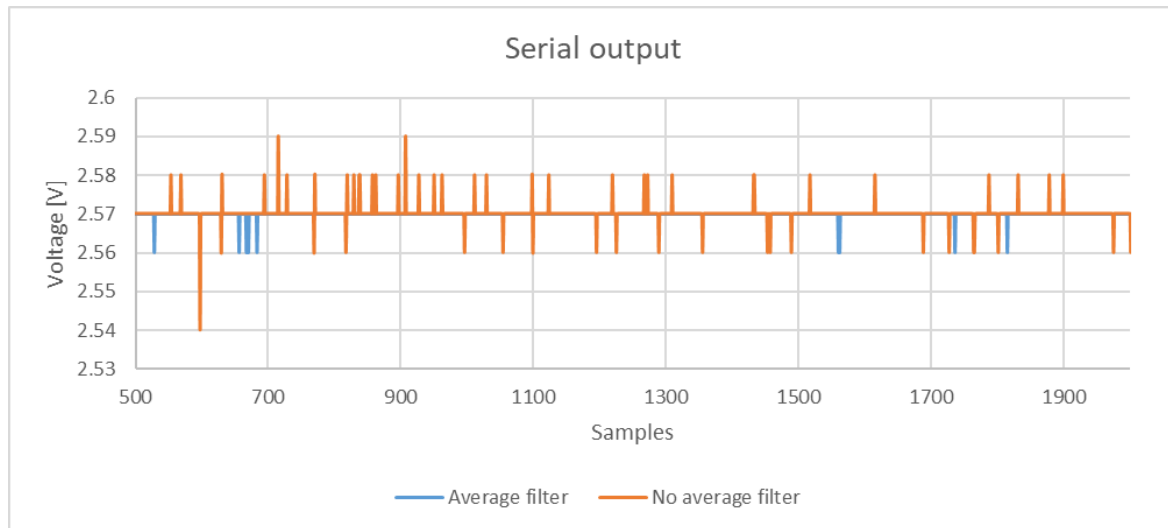


Figure 5-6: Input voltage average filter

Once the filters were implemented there was still some oscillation in the circuit, however it was much improved. The remaining oscillation may be due to the MCP41100, XMD-01 and RBAP valve ranges, as discussed in the detailed design in subparagraph 3.15.

5.5 Electric motor test

Purpose

The purpose is to test the Grundfos motor and draw an efficiency map for the motor at different speeds and loads.

Equipment set up

The equipment was set up as follows:

1. HBM system connection
 - a. Set up Precision software
 - i. Connect licence USB dongle to computer
 - ii. Open Precision software
 - iii. Open virtual workbench

- b. Connect GEN3t to G070A adapter
 - c. Plug in GEN3t power cable
 - d. Connect GEN3t with LAN cable to computer
 - e. Connect GEN3t measuring current clamps to power source of the electric motor under test as depicted in the virtual workbench.
 - f. Connect GEN3t measuring input to power source of motor under test to measure the voltage as described in the virtual workbench.
2. Grundfos motor connection
 - a. Connect to bench 3 phase power
 - b. Switch power on
 3. Hydraulic system set up
 - a. Connect induction motor to test bench siemens VSD.
 - b. Set control box dial to zero
 - c. Switch control box to coil A on
 - d. Switch control box on
 - e. Switch on bench 3 phase power source to VSD
 - f. Turn on VSD switch to manual setting and turn on to 1200rpm

Method

The following method was followed during the testing of the system:

1. Set up equipment as stated above
2. Ensure all settings are at zero
3. Increase the pressure incrementally and take measurements from Precision software and pressure gauge.

Results

The measurements taken of the complete system can be seen in the Table 6-4 in Appendix B.3. In the Figure 5-7 below the mechanical power and the input power for several motor speeds are plotted against the pressure applied to the disc brake calliper. From this scatter plot the following became clear: Firstly, mechanical power increases significantly as the load on the system increases. Secondly, the percentage efficiency of the system cannot be calculated by the formula: mechanical power divided by the input power. The reason is that the measurement system applies some internal multipliers for the mechanical power and/or the input power that results in the mechanical power being greater than the input power in some instances.

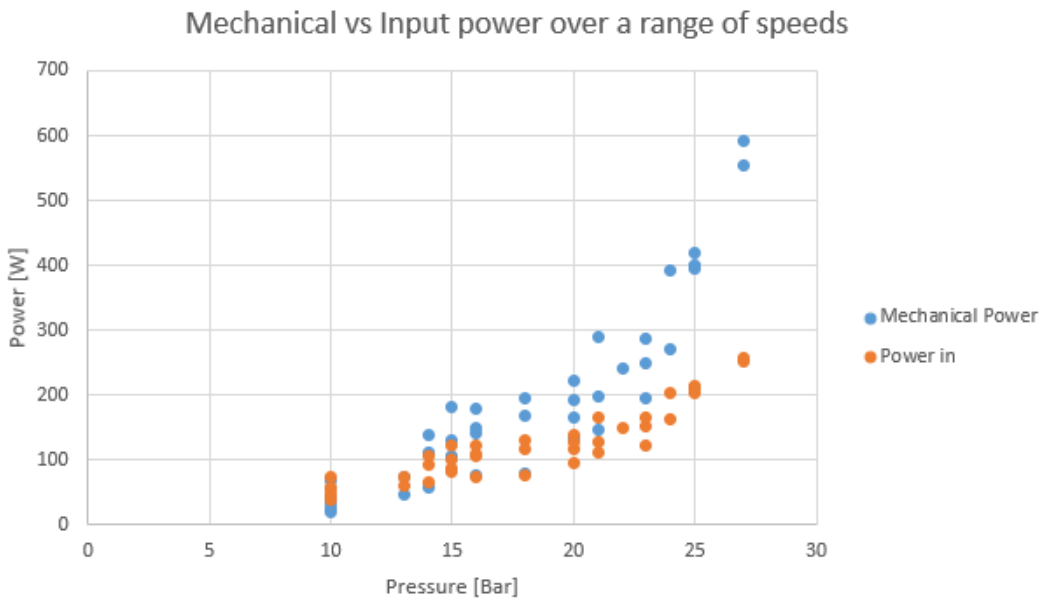


Figure 5-7: Mechanical vs Input power measured with HBM system

In the Figure 5-8 below the torque, speed and pressure is represented in a 3D graph. From this graph the following is apparent: Firstly, as expected, the torque increases as the pressure applied to the system increases. Secondly, the torque is greater at lower speeds. For example, the measurements at 23 Bar for 760 RPM the torque is 2.467 Nm whilst at 1600 RPM the torque is 2.112 Bar.

Torque and speed in relation to the pressure applied

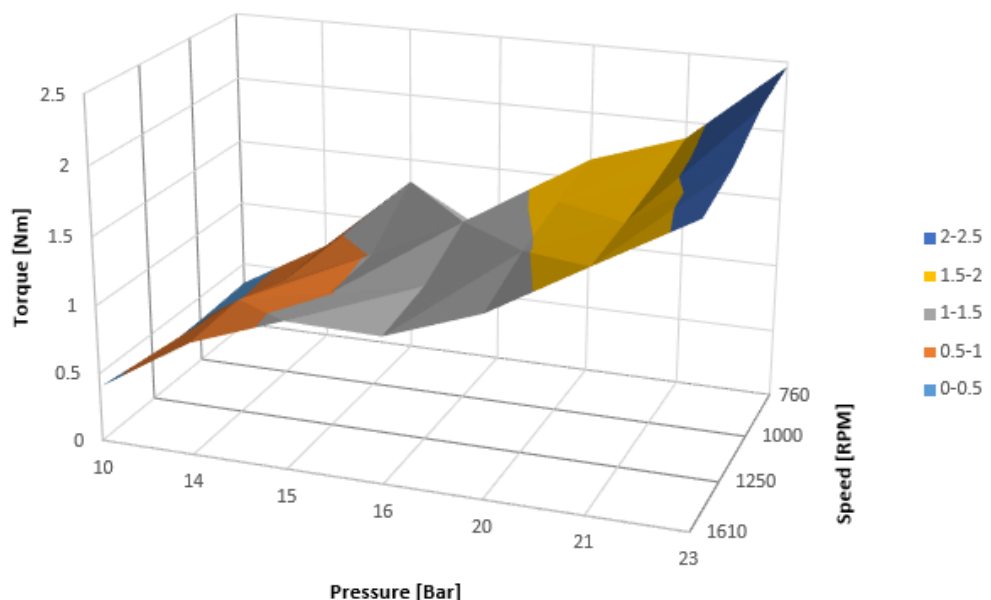


Figure 5-8: Torque and speed in relation to the applied pressure

The total motor efficiency points produced in the Precision software program, were used to draw the efficiency map below in Figure 5-9. The efficiency map was drawn using Matlab.

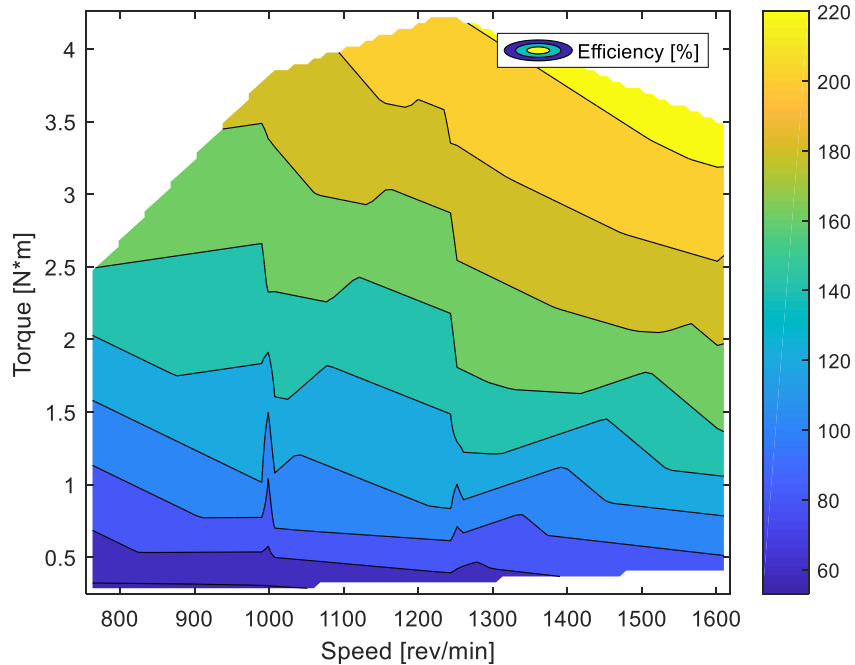


Figure 5-9: Grundfos motor efficiency map

The details of the map correspond with the calculated efficiency as in Table 6-4. It is clear from the efficiency map that the motor is most efficient at high speeds and greater loads. The tests on the electrical motor set out above, were run for more than four hours without any negative impact.

5.6 Conclusion

From the predesigned tests and evaluation, the following are concluded: The disc brake test lead to the design of the spring. The hydraulic system tests proved that its operation was between 10-100 Bar, whilst the need was for 0,5 to 8 Bar. The design for the sleeve and piston was derived from the results of these tests.

From the subsystem tests design changes were made to improve the designs. From the XMD-01 test the operating aspects where determined. The operation of the MCP41100 was tested and the output was within the expected range. From the RS422 output frequency test it was determined that the sampling rate of the Arduino Uno® is too slow to use the RS422. From the T40B output voltage the operational range was determined and used to design the operational amplifier circuit. The operational amplifier test showed that the amplifier worked as expected from the simulations.

The integrated system test was used to test the combined system including the PID control. From the test it was determined that the VSD controlling the induction motor caused too much

noise to the input of the PID control. The VSD was changed to direct connection to the variac. The Grundfos motor, variac and laboratory produced noise that was addressed with a RC filter and an averaging filter. Finally, it was determined that the delay in the system response caused oscillation in the PID control.

The electric motor test was used to analyse the Grundfos electric motor through an efficiency map. The efficiency map was drawn up from the input power and the mechanical power output. The efficiency map illustrates that the motor is most efficient at high speeds and higher loads.

Chapter 6. Conclusion and Recommendations

6.1 Introduction

This chapter gives an overview of the completed project. It is followed by recommendations to improve the weaknesses of the project. Finally, it demonstrates how each ELO required for this project is met.

6.2 Project Overview

The aim of the project was to design a test bench to digitally control the load applied to the electric motor shaft. This goal was reached by providing proper control by designing and manufacturing a new calliper piston for the disc brake to reduce the force applied to the brake pads. This allowed the use of RBAP valve to control the pressure in the system between 10-100Bar. To reduce the impact of the piston when the load is not applied, a spring return system to return the piston to its neutral position was designed, manufactured and implemented. To digitally control the load an Arduino Uno® was implemented to control the voltage output to the XMD-01 controller, which controls the RBAP valves which controls the system's pressure output. This created an automatic control system.

A PID controller was designed and implemented to allow the user to input a torque they want to test at and the system would then keep the torque of the motor at that set point. The T40B torque transducer provides a voltage output signal proportional to the torque measured. The voltage output is shifted up with a summing amplifier to the required range and protecting against reverse voltage. The op amp output is filtered with an RC hardware filter and an averaging digital filter to filter out the noise of the Grundfos motor, variac and the laboratory. The PID controller does not operate satisfactorily due to delays in the system causing oscillations. However, as per the scope of the project, a digital control is required to draw an efficiency map. This goal is reached with the pressure control program as the required ranges can be set digitally and the map can be drawn at several pressures. The PID control is not a requirement of the system.

An efficiency map of the Grundfos electric motor was drawn from the data collected. The test bench system can be used to test the motor of the solar car, and its own efficiency map can be drawn with the Matlab program Motor_Efficiency_Map.m using the data collected.

6.3 Recommendations

Although the project was successful, it can be further improved and extended. It is recommended that the G070A torque adapter's RS422 communication be used to measure the speed and torque. This can be done by implementing a microcontroller with faster sampling capabilities. Another recommendation is to replace the +- 5V rail supply to the op amp with a +-10V rail supply. This can be done once the voltage regulators in the op amp circuit are replaced with the appropriate positive and negative 10V voltage regulators. The

tests condition input to the digital control for the test bench can be refined in order to simplify its use during testing. Finally, the PID controller can be improved with control theory to prevent the oscillation due to the delay from the valves, MCP41100 and the torque output.

6.4 ECSA ELOs

The ECSA exit-level outcomes of a Qualification Standard for Bachelors of Engineering met in this project are ELO 1, ELO 2, ELO 3, ELO 4, ELO 5, ELO 6, ELO 8 and ELO 9. The ELOs are met by the project as follow.

ELO 1: Problem solving

In order to complete the digital controllable load system, several design problems had to be solved. These problems included finding a way to operate the disc brake while maintaining the hydraulic valve system implemented, designing a retraction system for the single acting hydraulic piston brake system, as well as designing and implementing the digital control system. To solve the hydraulic system pressure problem, analysis was done of the system and it was determined that a new piston with a smaller surface area would solve the issue, calculations were done and a new piston was designed and implemented in the disc brake. This solved the pressure issue in the system. To prevent the brake pad from applying a load on the disc when no pressure is applied, a spring return system was designed and implemented. The spring return system works for the required pressure range of the system. To allow automatic testing with the test bench, digital control was designed and implemented with an Arduino Uno® using the torque transducer input voltage. Several problems presented throughout the design process that had to be solved e.g. the frequency of the RS422, the ESP32 supply voltage, the T40B negative output voltage and the excessive noise on the input of the PID by the VSD.

ELO 2: Application of scientific and engineering knowledge

Science and engineering knowledge were constantly applied during the project, particularly in the following aspects:

- to design the piston and sleeve for the disc brake calliper to reduce the force applied on the disc
- to design the electronic controller circuit and the coding required to control the system
- identify the relevant mathematical equations

The application of scientific and engineering knowledge was required to analyse the disc brake operation for both the heat transfer and the pressure and force calculation in order to determine the required pressure on the disc brake to test the motor.

ELO 3: Engineering design

The engineering design process was followed throughout the project life cycle. The first step of the engineering design process is to identify and define the complex problem of the project. Once the problem was identified the requirements and scope of the project was defined as set out in Chapter 1 of his document. Research was done on the pertinent aspects of the system and documented in the literature study. Each time new technology or any aspect of the design became relevant, it was researched and documented. In the following step, concept designs were created as possible solutions for the problems in the system. These designs were analysed and if no clear solution could be found, a trade-off study was done to determine the design to pursue. From the selected concept designs, detailed designs were created. Thereafter the detailed designs were implemented, tested and evaluated. Where problems came to the fore, research was done, solutions were considered and new detailed designs were created, implemented, tested and evaluated.

ELO 4: Investigations, experiments and data analysis

In order to find possible solutions for the project problems, the existing system had to be investigated through experiments and tests, as documented. The data from the experiments were then analysed in order to determine the functionality and operation of the subsystems of the test bench. From this investigation possible solutions for the different problems were identified and evaluated. Several other experiments were also conducted to test the subsystems built and implemented in this project and the data was analysed.

ELO 5: Engineering methods, skills and tools

Informational technology engineering tools were used throughout the project such as, Proteus to design the electronic circuit, Python to display the torque and speed output, Arduino IDE to program the Arduino Uno® as well as the ESP 32 when it was implemented, Tera Term to log the serial data, Precision software to measure the HBM system output, TiePie to measure the voltage outputs during testing and evaluation.

ELO 6: Professional and technical communication

Professional and technical communication was required throughout the project. These included communication with supervisors and technicians. Scheduled meetings and discussions regarding milestones and progress were held. Professional and technical communication with manufacturers took place during manufacturing of parts. As such, technical communication was required with Grundfos and HBM regarding support services for their products. Professional communication is also required during oral presentation of the project as well as presentation to the public during project day. Finally, the project report is written communication of the project.

ELO 8: Individual, team and multidisciplinary working

The project was accomplished as individual work. However, no such project came into being in isolation, and some team work was required with the project study leaders as the client, and collaboration was required in the process to have the parts manufactured. The project required multidisciplinary work as it is a combination between mechanical, hydraulic, electric and electronic fields.

ELO 9: Independent learning ability

In this project independent learning was required as the project dealt with various disciplines. The student demonstrated independent learning by mastering new programs such as the application of Arduino Uno®, ESP32, Arduino IDE, Python, RS422, and the HBM measuring system. The student also executed independent learning in obtaining the necessary information on the operation of hydraulic systems, the impact of hydraulic valves used in the system, and disc brakes.

BIBLIOGRAPHY

- [1] M. R. Zaaiman, "Controllable rotational load for the testing of motors," NWU, Potchefstroom, 2018.
- [2] HBM, "HBM," [Online]. Available: <https://www.hbm.com/en/0061/company-details/>. [Accessed 26 02 2019].
- [3] HBM, *GEN series GEN3t Data sheet*.
- [4] B. Guru and H. Hiziroglu, Electric Machinery and Transformers, New York: Oxford University Press, 2001.
- [5] A. Belhocine, C. Cho, M. Nouby, Y. Yi and A. R. Abu Bakar, "Thermal analysis of both ventilated and full disc brake rotors with frictional heat generation," *Applied and Computation Mechanics*, no. 8, pp. 5-24, 2014.
- [6] Qingdao Casting Quality Industrial Co, *Grey Cast Iron Composition and Property*, Qingdao Casting Quality Industrial Co.
- [7] E. M. Sparrow, J. B. Abraham and J. M. Gorman, "Advances in Heat Transfer," *Academic Press*, vol. 50, 2018.
- [8] C. Shigley, Standard Handbook of Machine Design, New York: The McGraw-Hill Companies, 1996.
- [9] T. Manjunath and P. Suresh, "Structural and Thermal Analysis of Rotor Disc of Disc Brake," *International Journal of Innovative Research in Science, Engineering and Technology*, vol. 2, no. 12, pp. 7741-7749, 2013.
- [10] R. Limpert, Brake Design and Safety, Warrendale: Society of Automotive Engineering Inc., 1999.
- [11] J. E. Shigley, Shigley's Mechanical engineering design, McGraw-Hill, 2006.
- [12] W. Bolton, Instrumentation and Control systems, Elsevier, 2004.
- [13] R. Dorf and R. Bishop, Modern Control systems, Pearson, 2017.
- [14] ESP32.net, "ESP32.net," [Online]. Available: <http://esp32.net/>. [Accessed 18 March 2019].

- [15] ARDUINO, *A000066 Datasheet: Arduino UNO Rev3*, ARDUINO.
- [16] B. Trinkel, “Hydraulics and Pneumatics,” Informa PLC, 16 October 2006. [Online]. Available: <https://www.hydraulicspneumatics.com/other-technologies/chapter-5-pneumatic-and-hydraulic-systems>. [Accessed 18 May 2019].
- [17] “Electronics projects focus,” Elprocus, [Online]. Available: <https://www.elprocus.com/stepper-motor-types-advantages-applications/>. [Accessed 5 May 2019].
- [18] Mouser electronics , “Mouser,” TTI and Berkshire Hathaway, [Online]. Available: <https://www.mouser.co.za/applications/motor-control-stepper/>. [Accessed 8 May 2019].
- [19] electronics notes, “Electronics notes,” Incorporating Radio Electronics, [Online]. Available: <https://www.electronics-notes.com/articles/connectivity/serial-data-communications/rs422-basics-tutorial.php>. [Accessed 8 October 2019].
- [20] A. S. Nastase, “Mastering electronics design,” Mastering electronics design, [Online]. Available: <https://masteringelectronicsdesign.com/design-a-bipolar-to-unipolar-converter/>. [Accessed 15 October 2019].
- [21] M. Haller, *T40B with Rotational Speed Measuring System and Reference pulse*, HBM Test and Measurement.
- [22] Microchip Technology Inc, *MCP41XXX/42XXX single/dual digital potentiometer with SPI interface*, 2003.
- [23] sunhydraulics, “sunhydraulics,” sunhydraulics, [Online]. Available: <https://www.sunhydraulics.com/model/RPEC8>. [Accessed 7 May 2019].
- [24] “Microcontrollers Lab,” 13 February 2019. [Online]. Available: <https://microcontrollerlab.com/esp32-pinout-use-gpio-pins/>. [Accessed 21 May 2019].
- [25] Components101, “Components101,” 18 February 2018. [Online]. Available: <https://components101.com/microcontrollers/arduino-uno>. [Accessed 20 June 2019].
- [26] HBM, *B4229 - 2.0 GEN series G070A*, HBM.
- [27] DFRobot, “DFRobot,” [Online]. Available: https://wiki.dfrobot.com/Arduino_RS485_Shield_SKU__DFR0259. [Accessed 1 September 2019].

[28] HBM, *HBM T40B Mounting Instructions*.

APPENDIX A.1: SCHEMATICS AND FLOWCHARTS FROM OTHER SOURCES

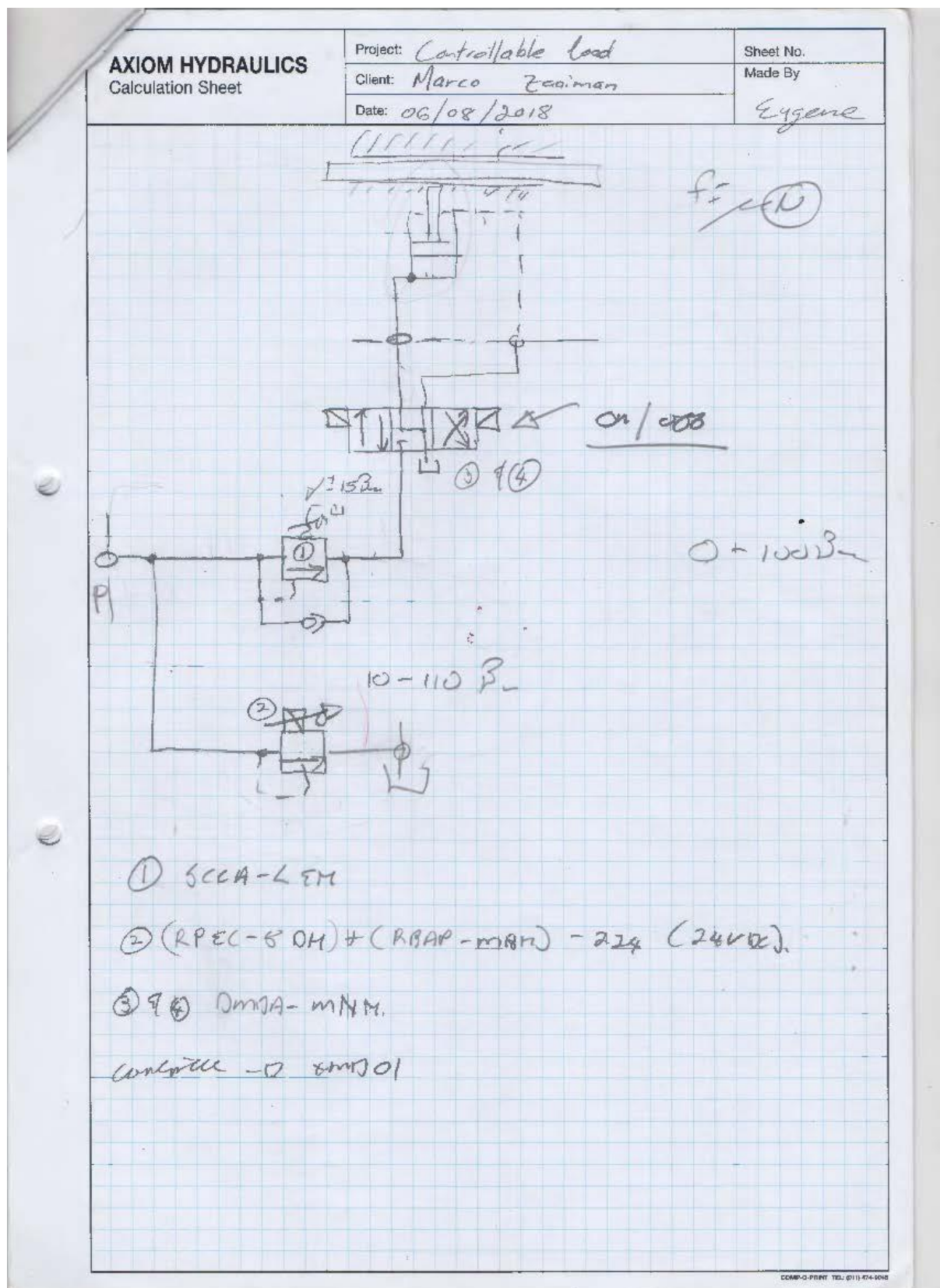


Figure 6-1: Axiom hydraulic schematic [1]

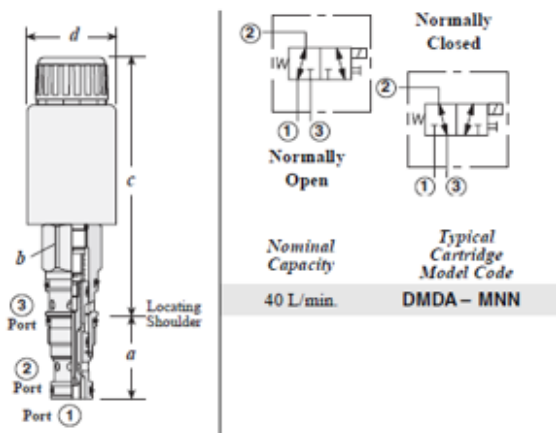


Figure 6-2: DMDAMNN directional valve [23]

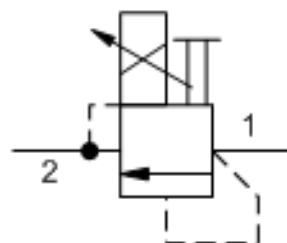


Figure 6-3: RBAPMBN [23]

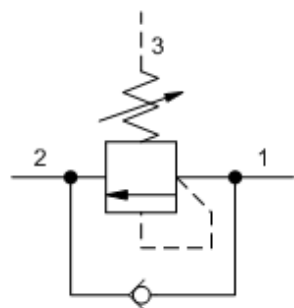


Figure 6-4: SCCALAN [23]

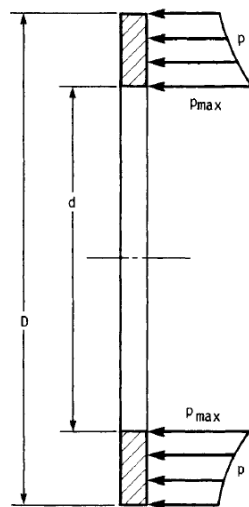


Figure 6-5: Contact-pressure distribution on the face of the cone after the wear-in period [8]

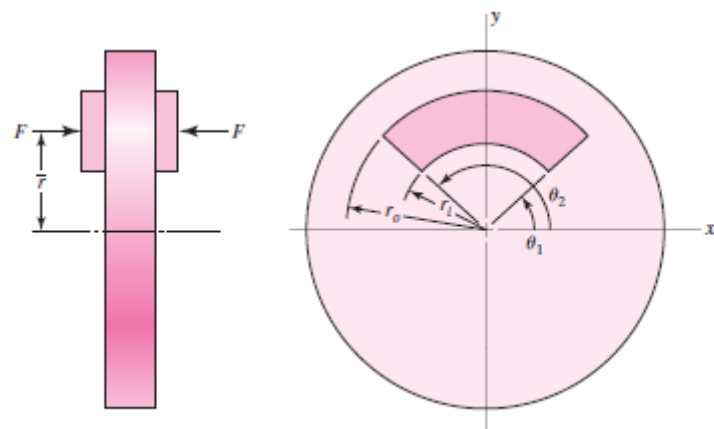


Figure 6-6: Geometry of the contact area of an annular-pad segment of a calliper brake [11]

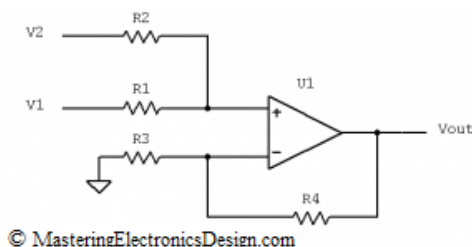


Figure 6-7: Summing amplifier [20]

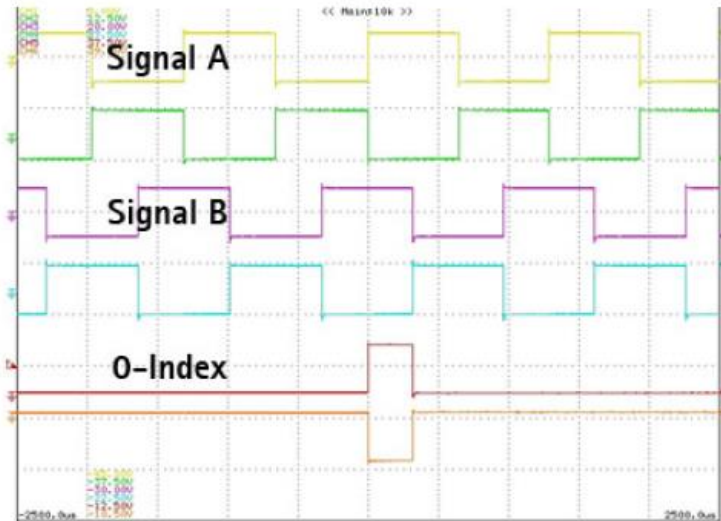
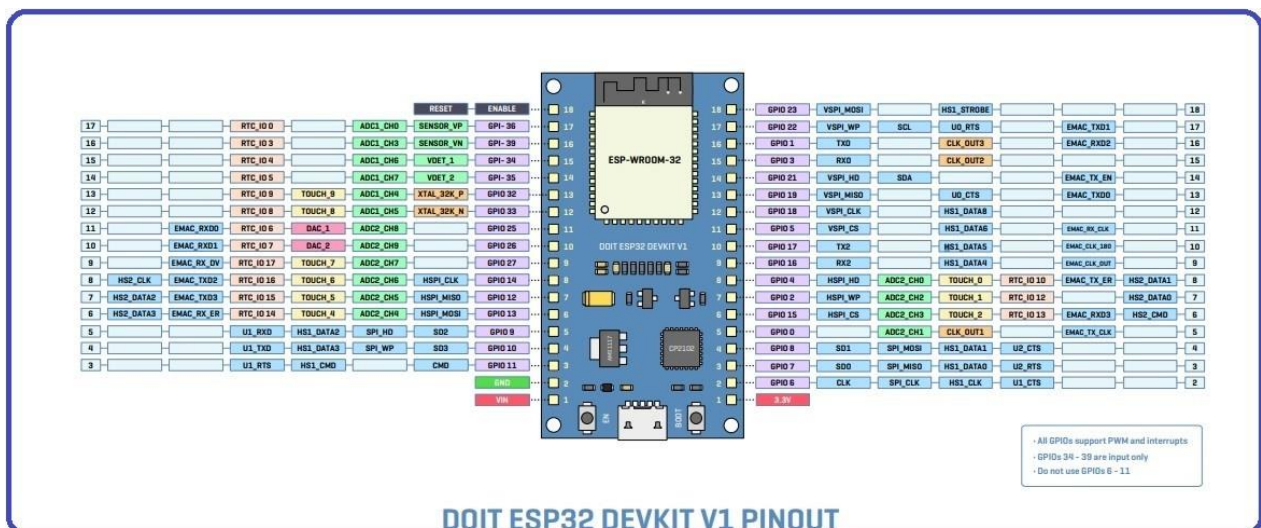
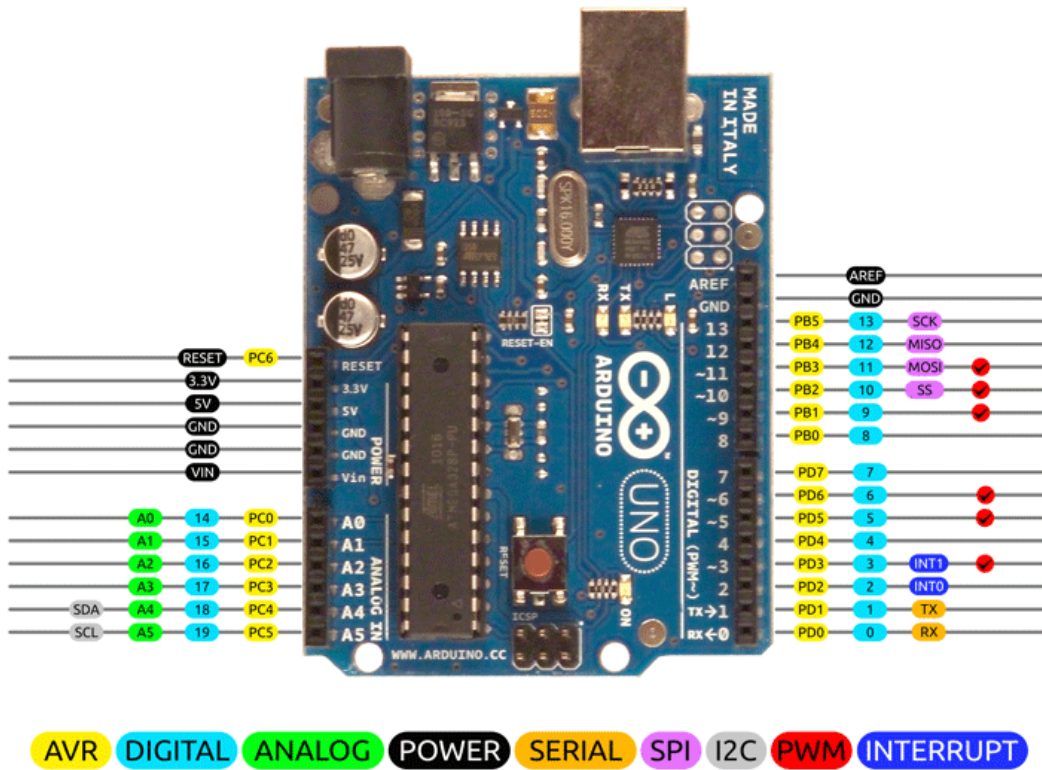


Figure 6-8 Square wave signals A/B and reference signal (0-index) [21]





AVR DIGITAL ANALOG POWER SERIAL SPI I2C PWM INTERRUPT

2014 by Bouni
Photo by Arduino.cc

Figure 6-10: Arduino Uno® pinout [25]

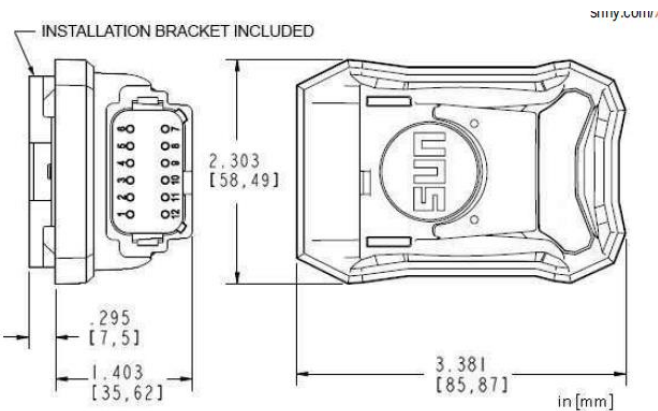


Figure 6-11: XMD-01 data sheet schematic [23]

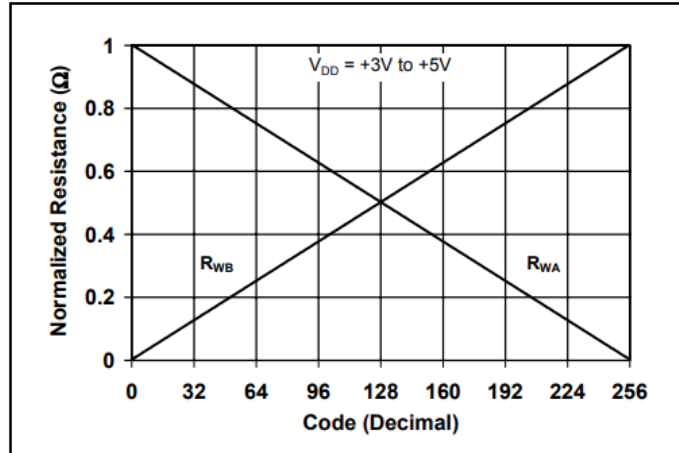


Figure 6-12: Normalized resistance to End Terminal resistance vs code [22]

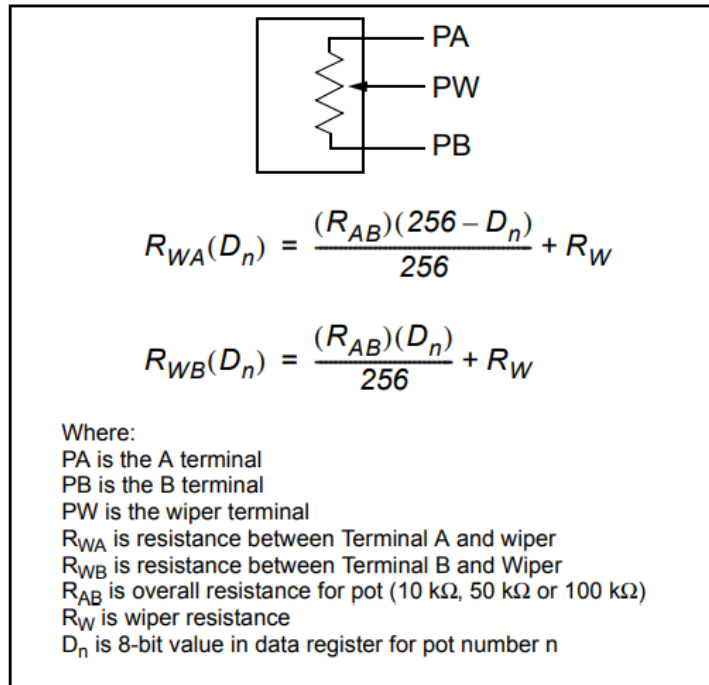
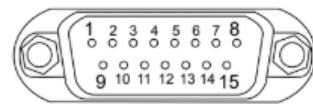


Figure 6-13: Potentiometer resistance are as function of code [22]

Torque Sensor Connector Pin Assignment

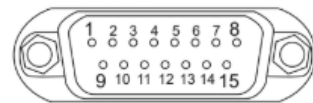
Pin 5 : Supply voltage ground (not connected to signal ground)
 Pin 6 : Supply voltage 18 V to 30 V
 Pin 8: Ground
 Pin 12: + Torque Signal
 Pin 13: - Torque Signal
 Pin 14: Shunt Signal trigger 5 V to 30 V



Shielding connected to connector housing
 All other pins not connected

Figure 1.4: Torque IN and OUT connector pinning

Pin 2: + Reference Signal
 Pin 3: - Reference Signal
 Pin 8: Signal ground
 Pin 12: + Rotational Speed 0° Signal
 Pin 13: - Rotational Speed 0° Signal
 Pin 14: - Rotational Speed 90° Signal
 Pin 15: + Rotational Speed 90° Signal



Shielding connected to connector housing
 All other pins not connected

Figure 1.5: Speed IN and OUT connector pinning

Figure 6-14: Torque sensor connector pin assignment [26]

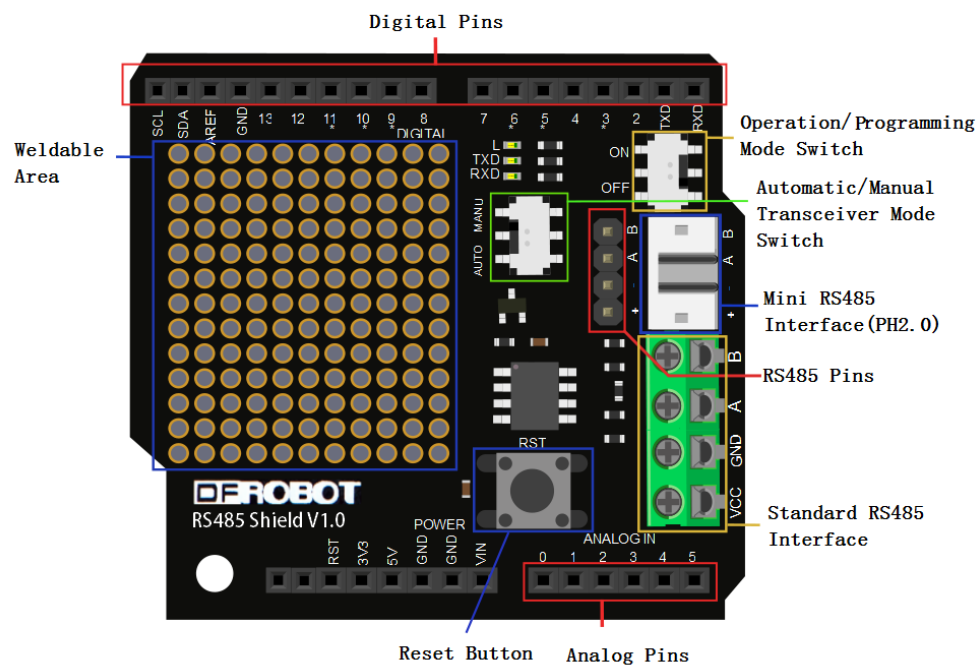


Figure 6-15: RS485 Shield [27]

Plug pin	Assignment
1	Torque measurement signal (voltage output; 0 V) 
2	Supply voltage 0 V; 
3	Supply voltage 18 V to 30 V DC
4	Torque measurement signal (voltage output; ± 10 V)
5	Not in use
6	Shunt signal trigger 5 V to 30 V
7	Shunt signal 0 V; 
	Shielding connected to housing ground

Figure 6-16: T40B Plug 3 assignment [28]

APPENDIX A.2: SCHEMATICS AND FLOWCHARTS

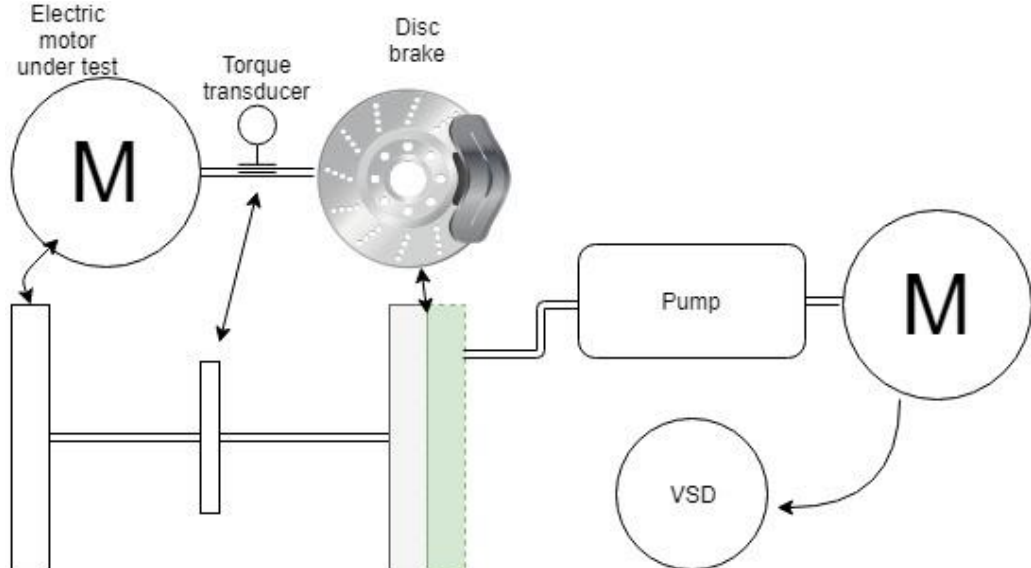


Figure 6-17: Concept design VSD controlled hydraulic Disc brake system

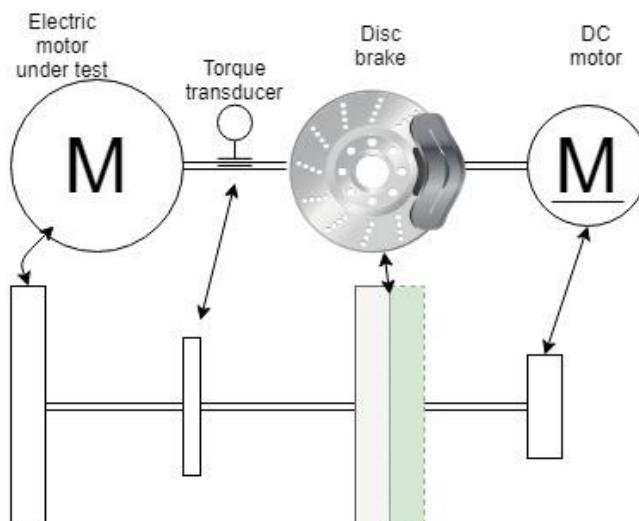


Figure 6-18: Disc brake and DC motor concept schematic

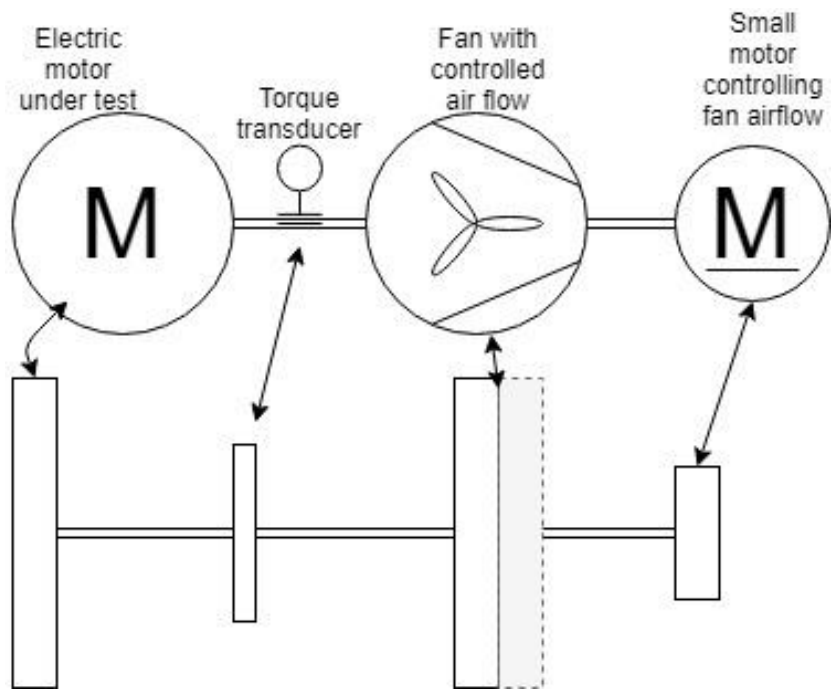


Figure 6-19: Airflow controlled fan concept design

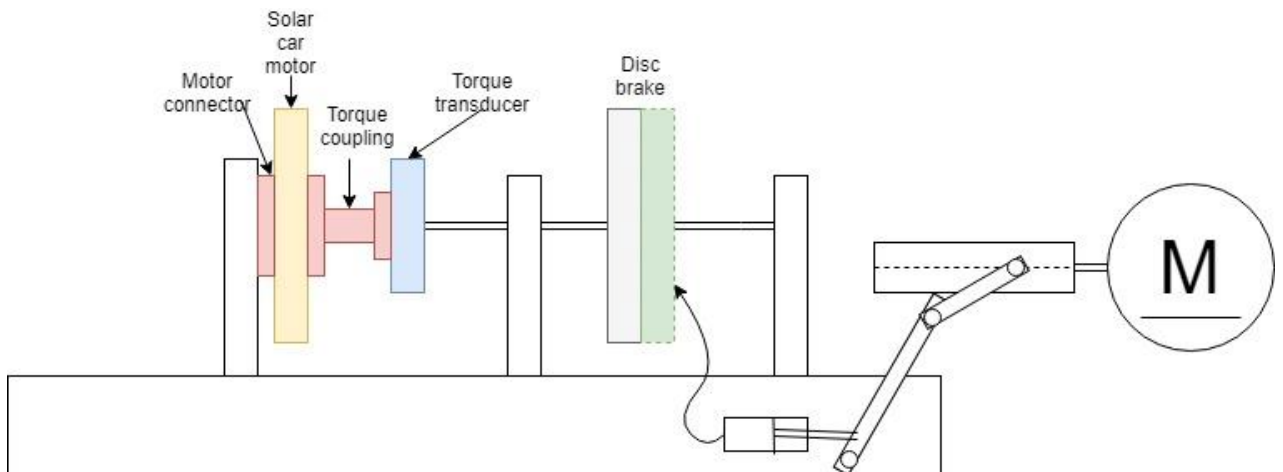


Figure 6-20: Stepper motor-controlled disc brake

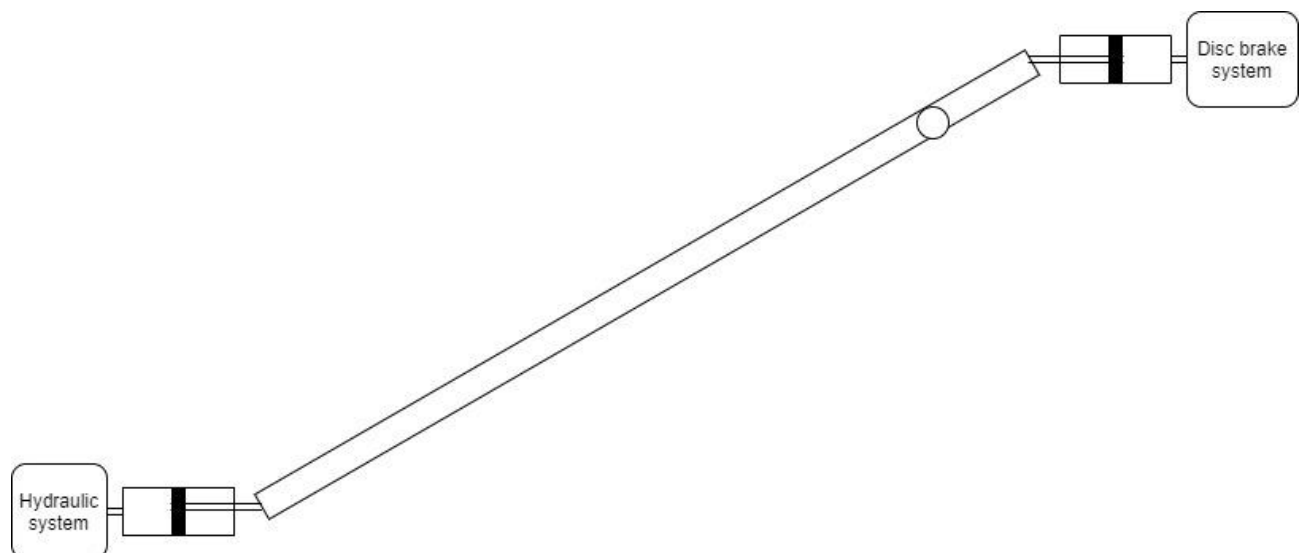


Figure 6-21: lever pressure reduction

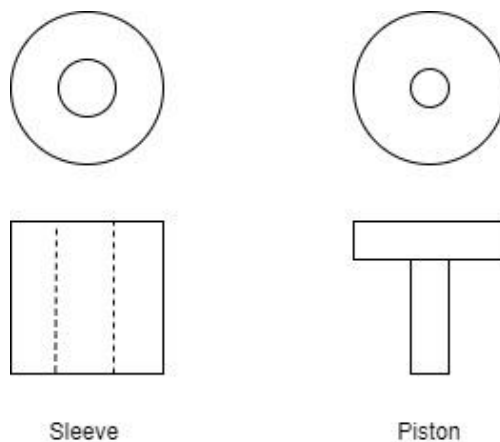


Figure 6-22: Concept design for piston and sleeve

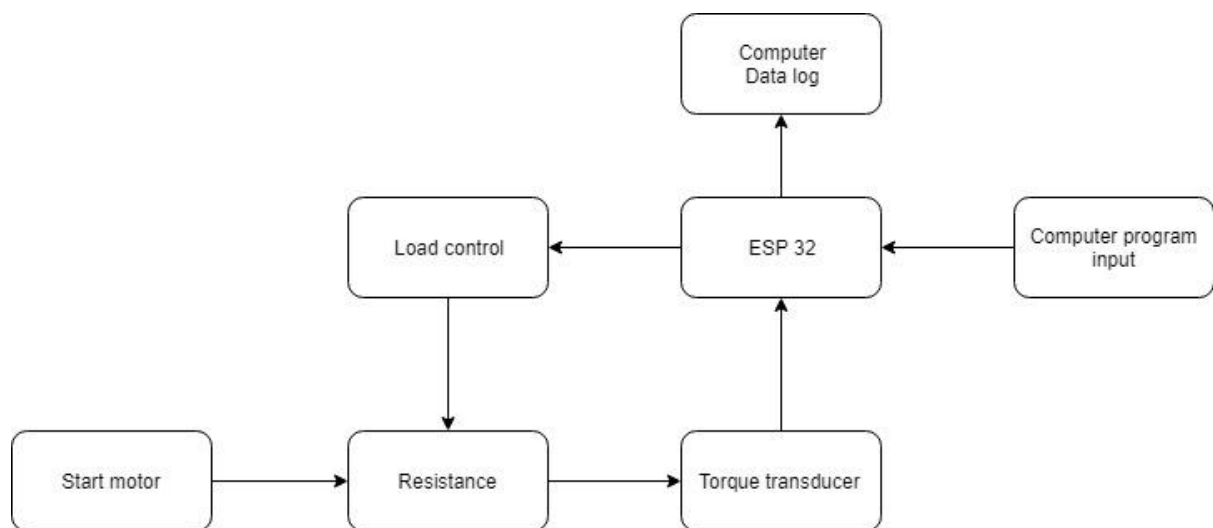


Figure 6-23: Basic flow chart of the control system

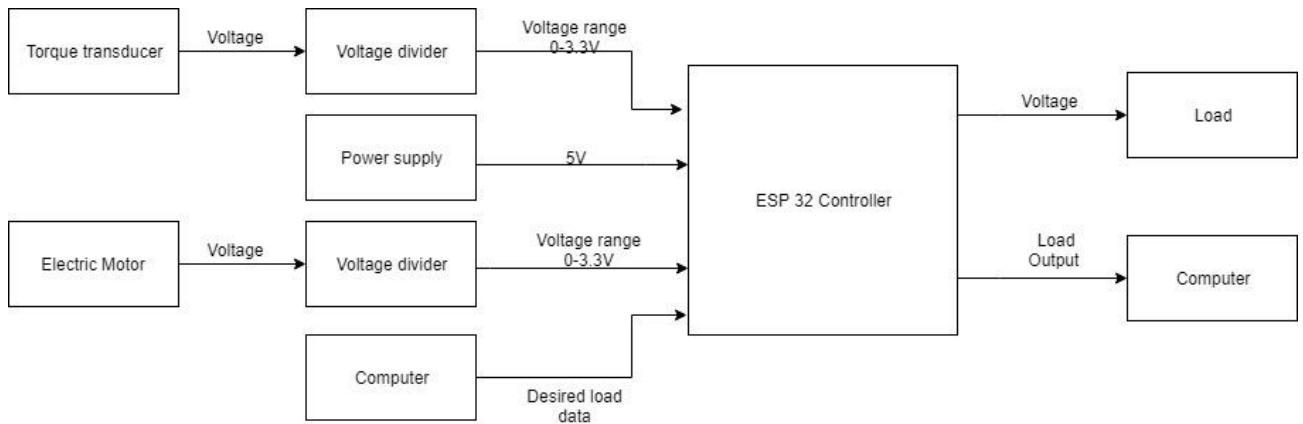


Figure 6-24: Input and output of the ESP 32

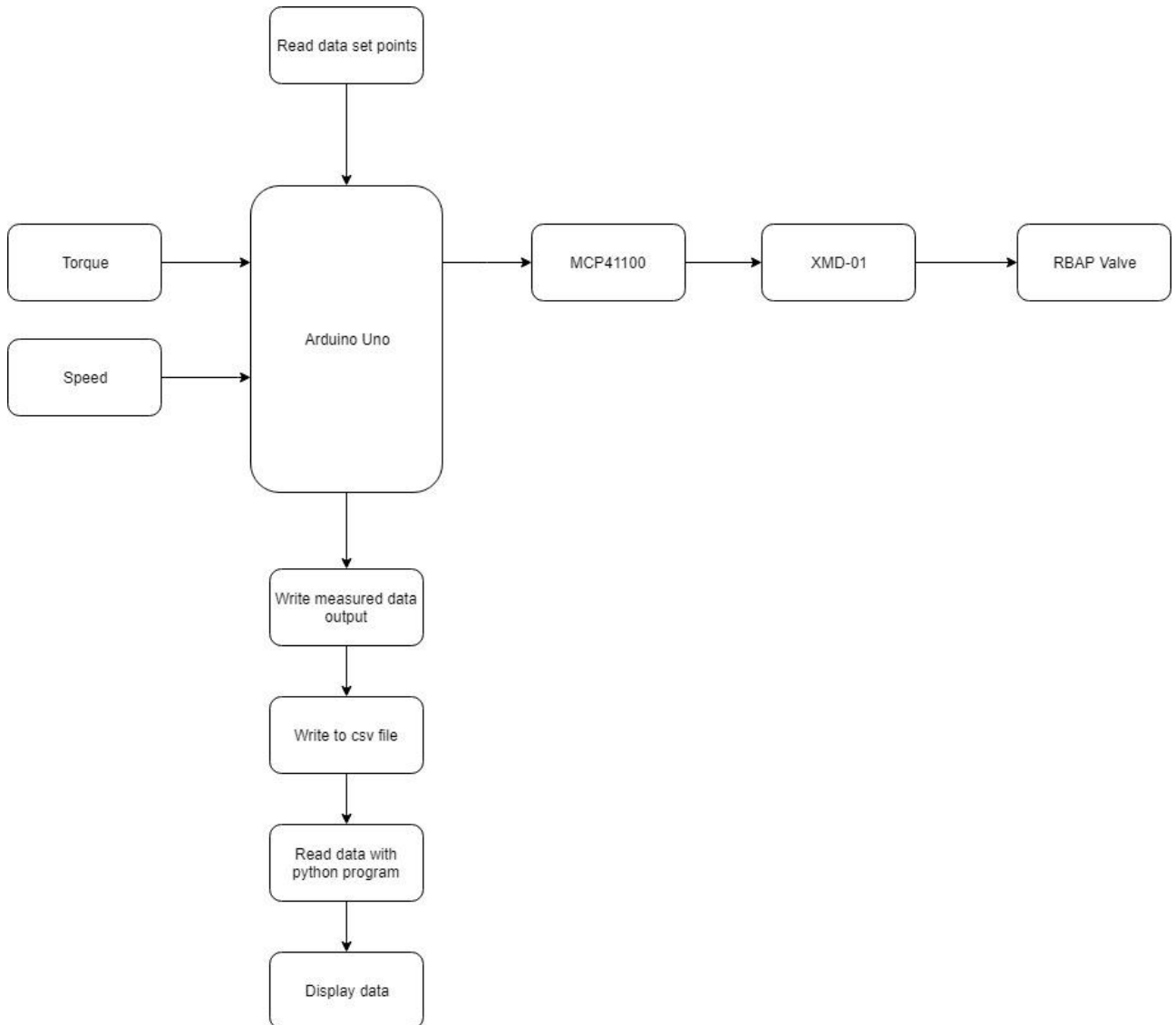


Figure 6-25: Flowchart Arduino Uno®

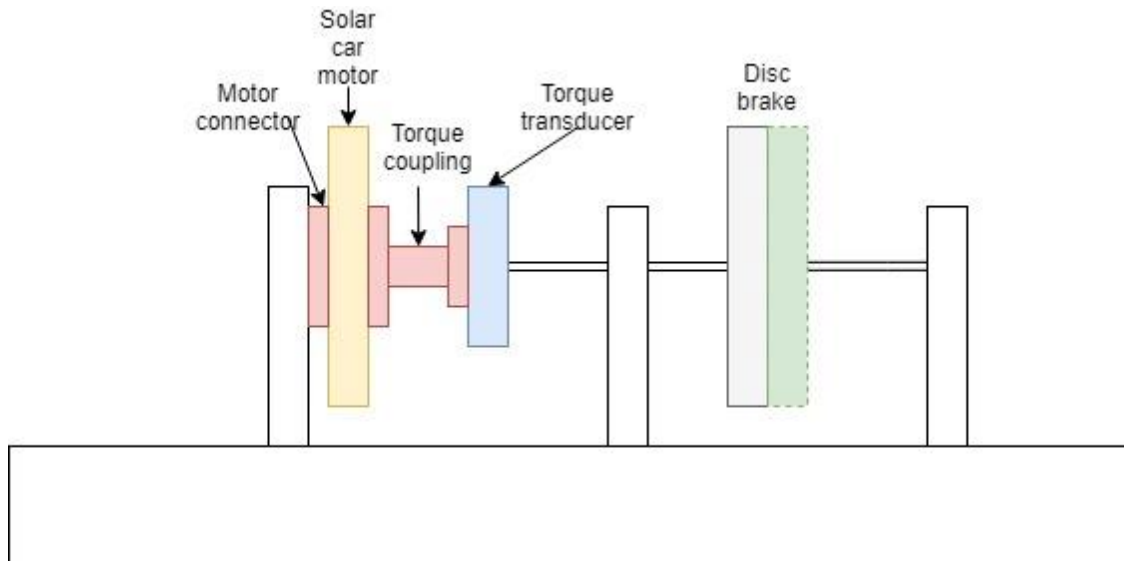


Figure 6-26: Solar car motor connection concept design 2

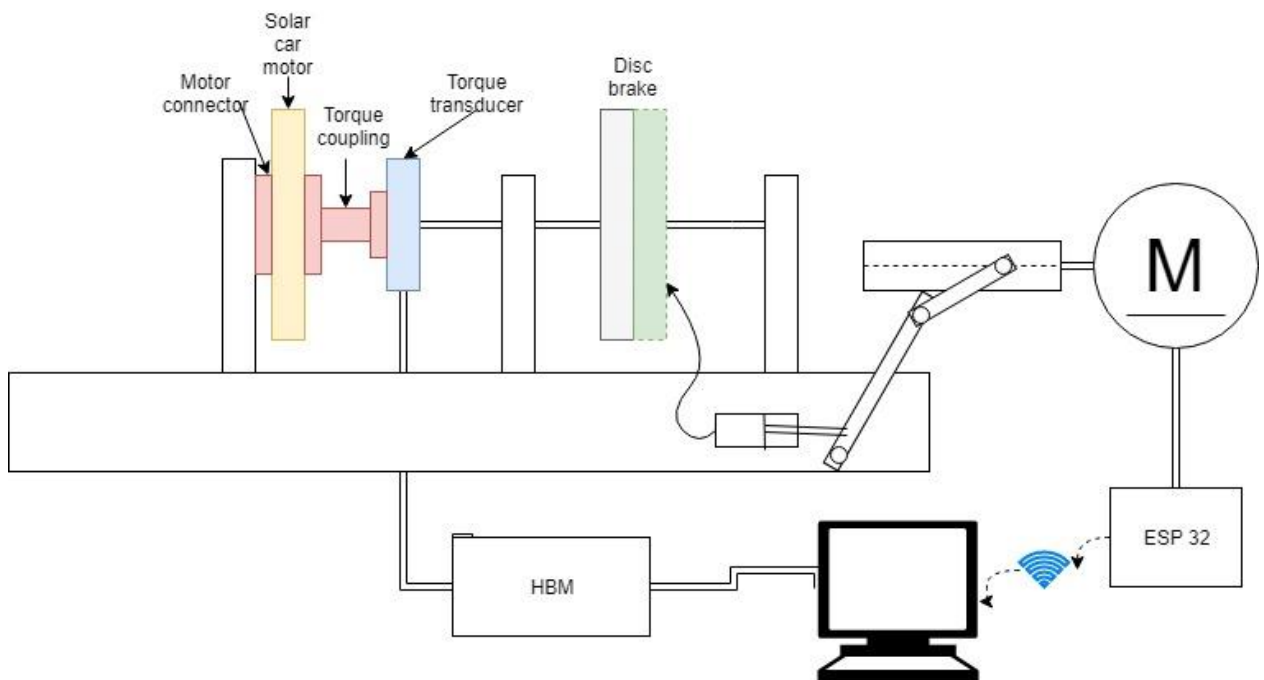


Figure 6-27: Combined concept design 1

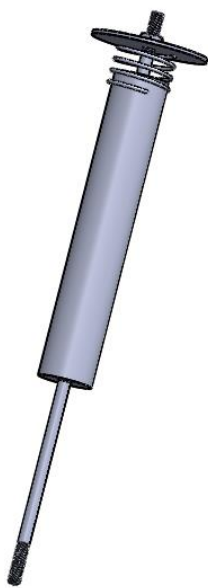


Figure 6-28: Spring return system Solidworks assembly

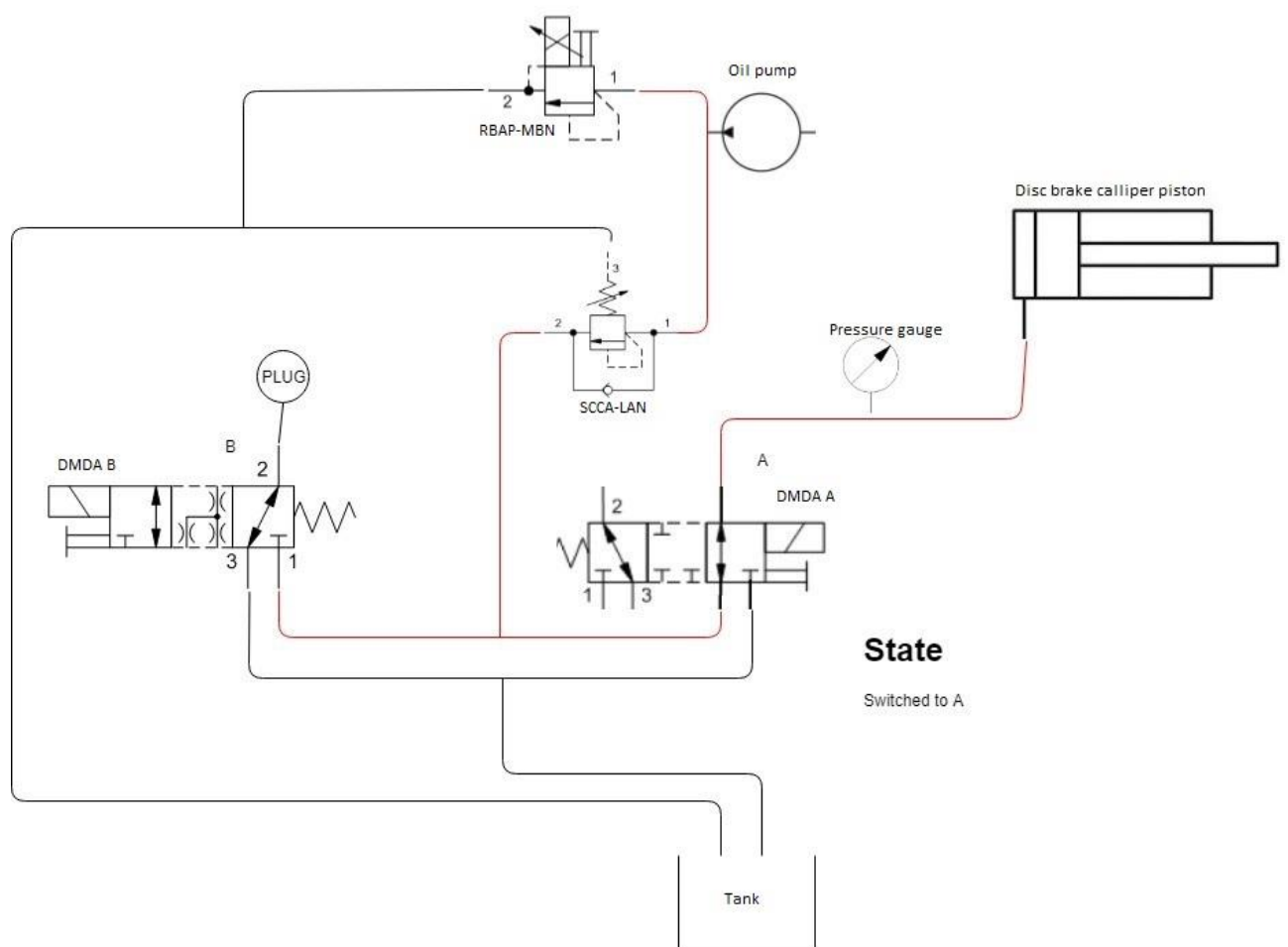


Figure 6-29: Hydraulic system flow diagram DMDA valve A powered

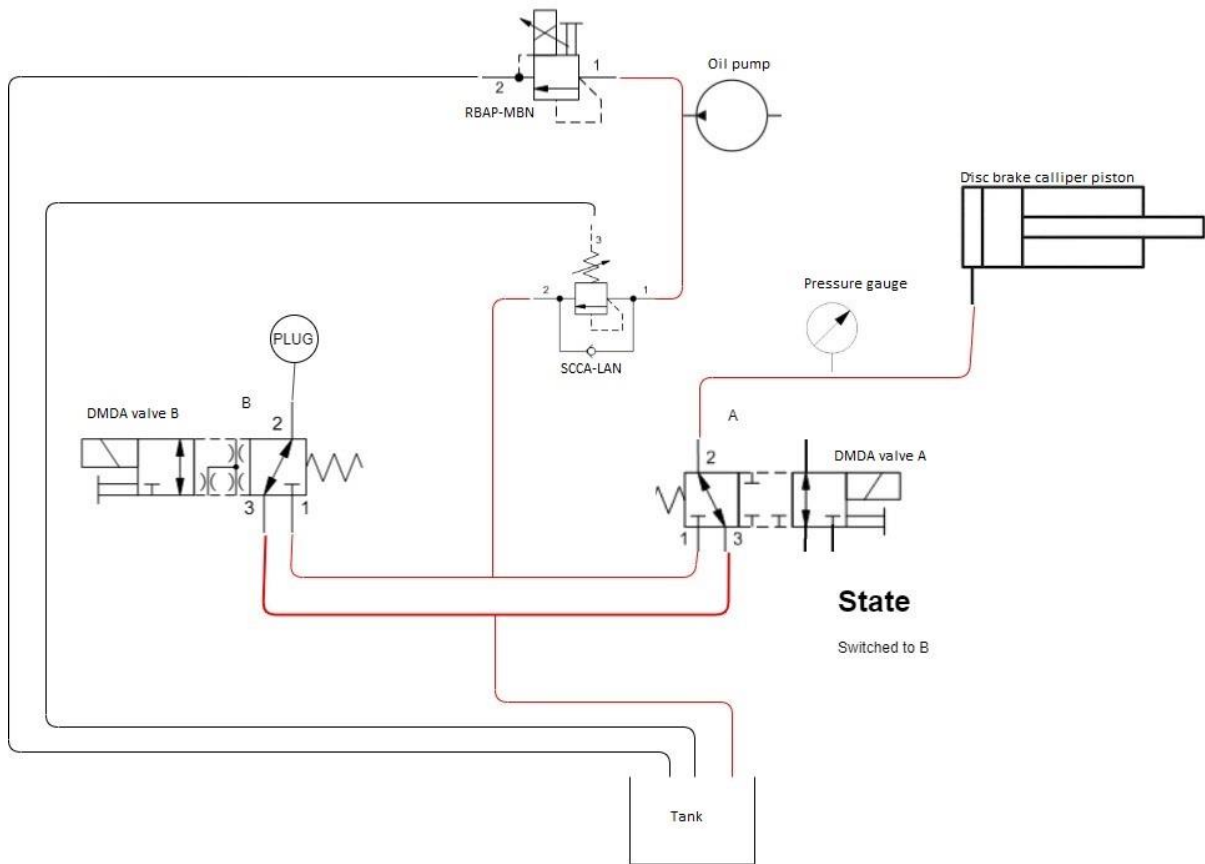


Figure 6-30: Hydraulic system flow diagram DMDA valve B powered

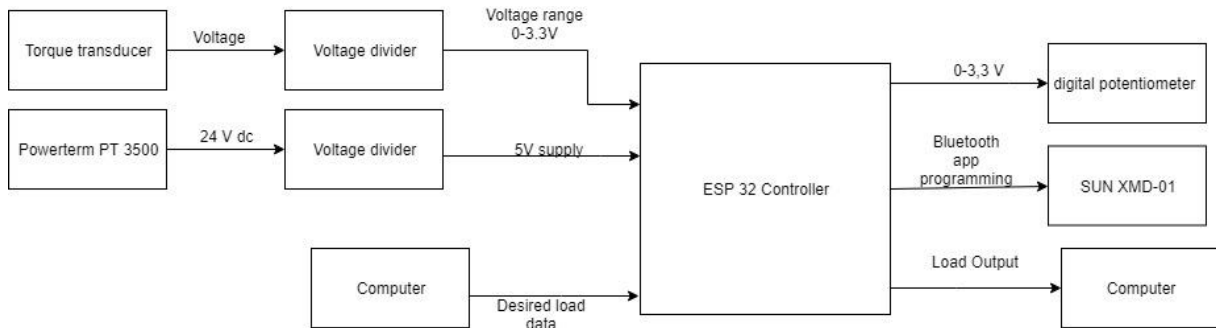


Figure 6-31: ESP 32 connections

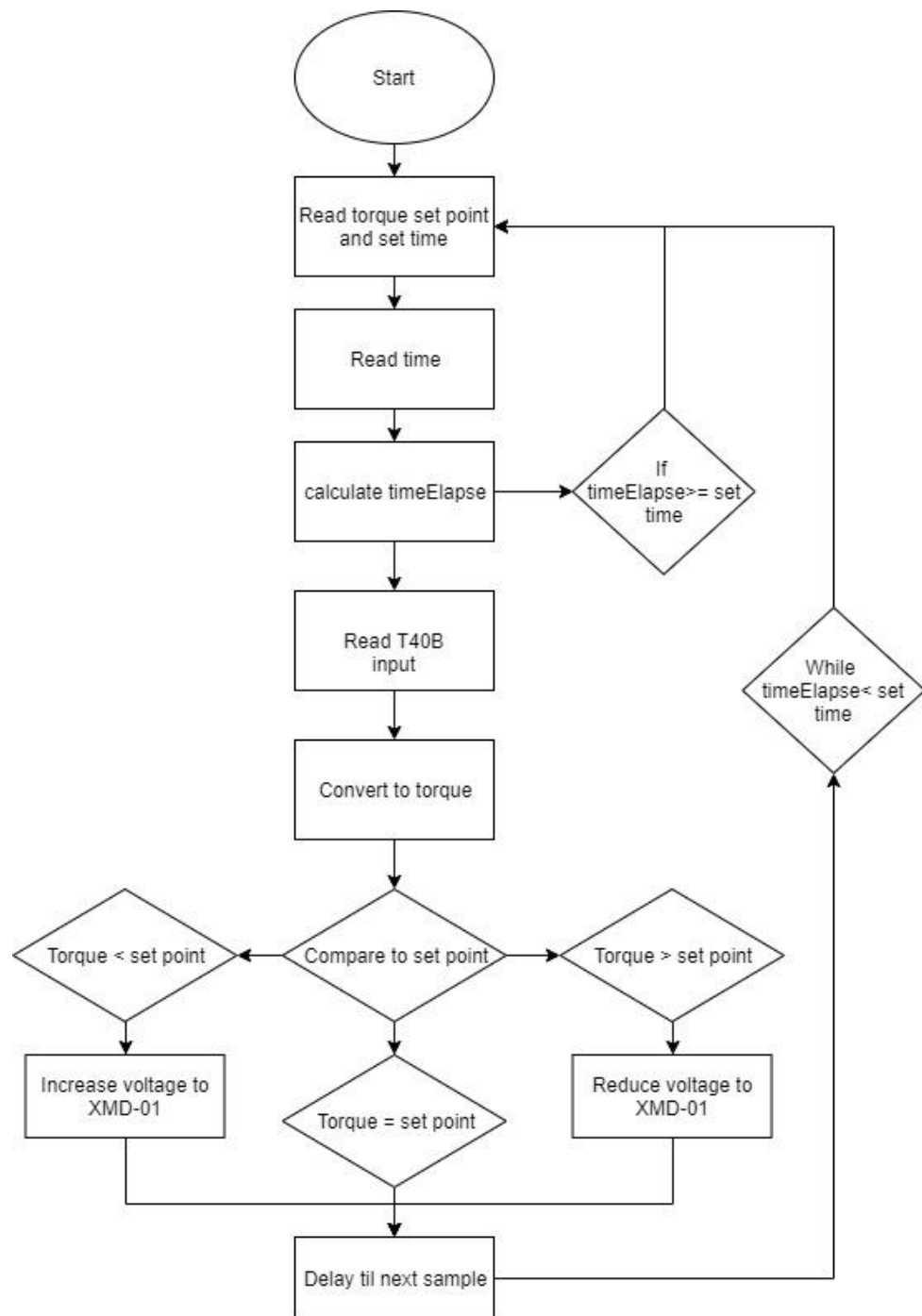


Figure 6-32: Control loop flowchart



Figure 6-33: operating ranges

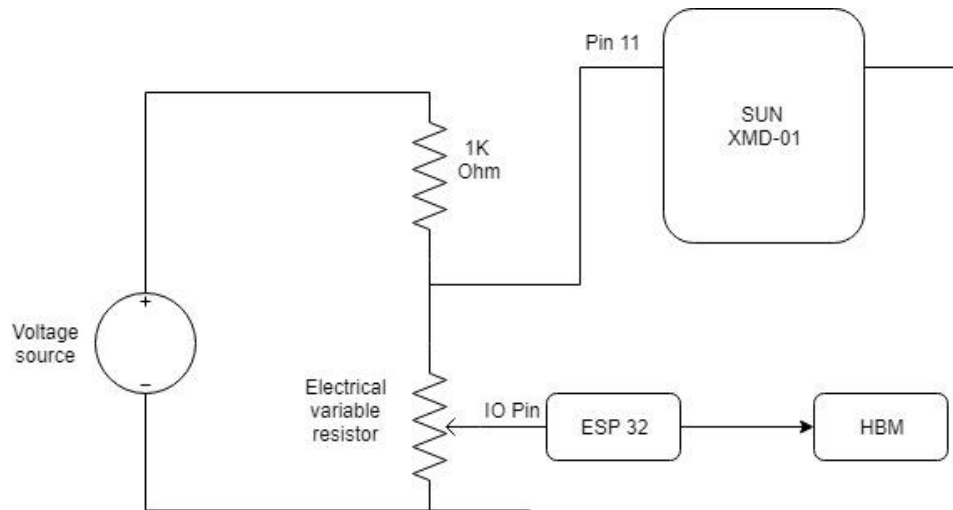


Figure 6-34: combined digital circuitry

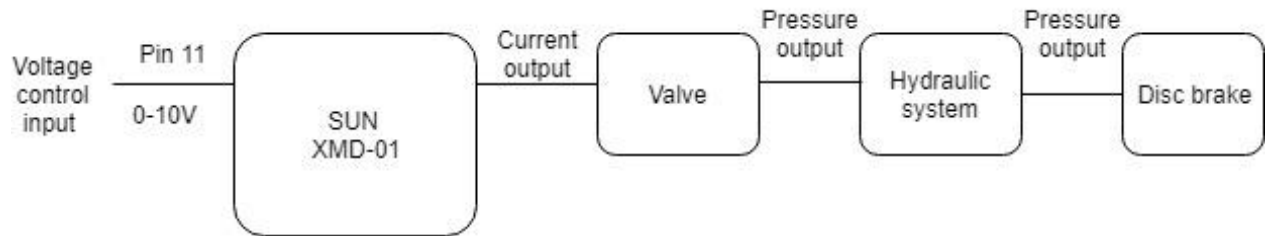


Figure 6-35: process of electrical circuit flow of XMD-01

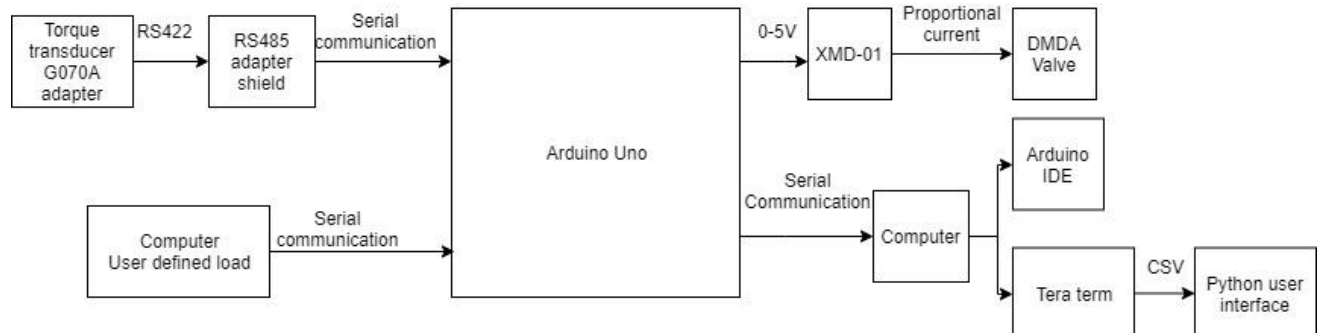


Figure 6-36: Combined electronic system V2.1

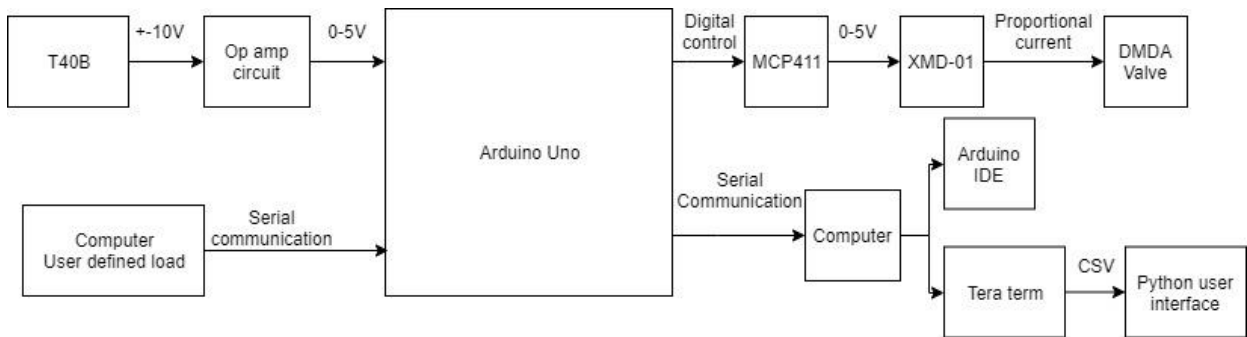


Figure 6-37: Combined electronic system V2.2

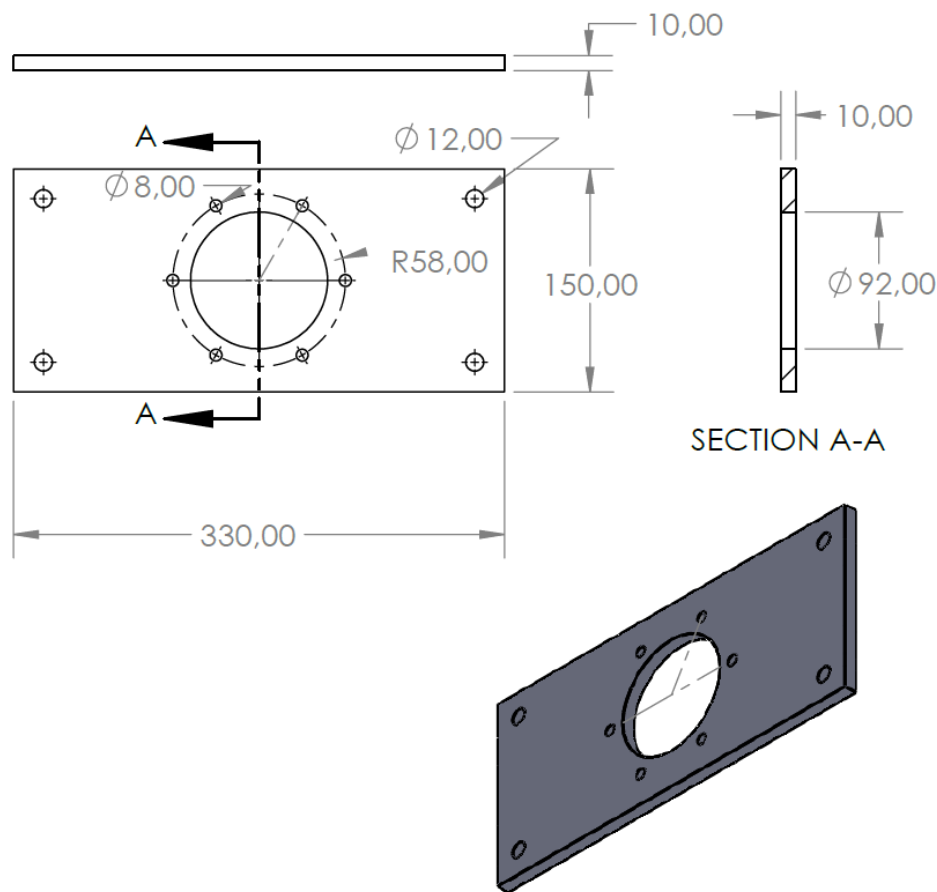


Figure 6-38: motor mounting

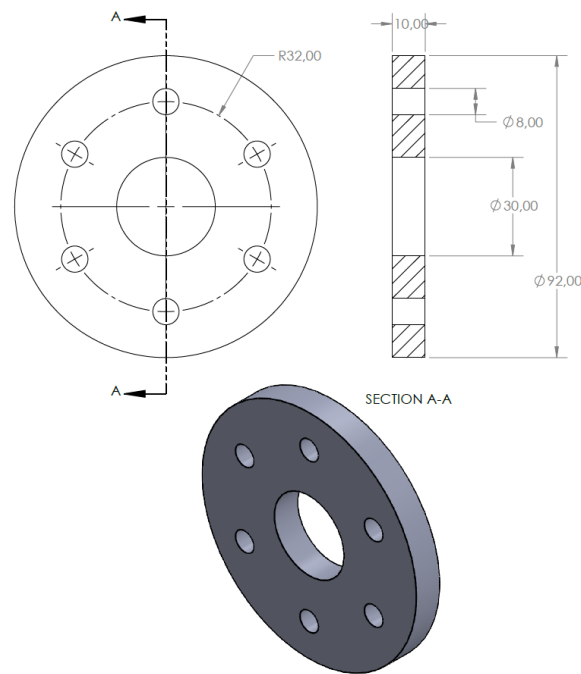


Figure 6-39: Torque flange adapter revision 1

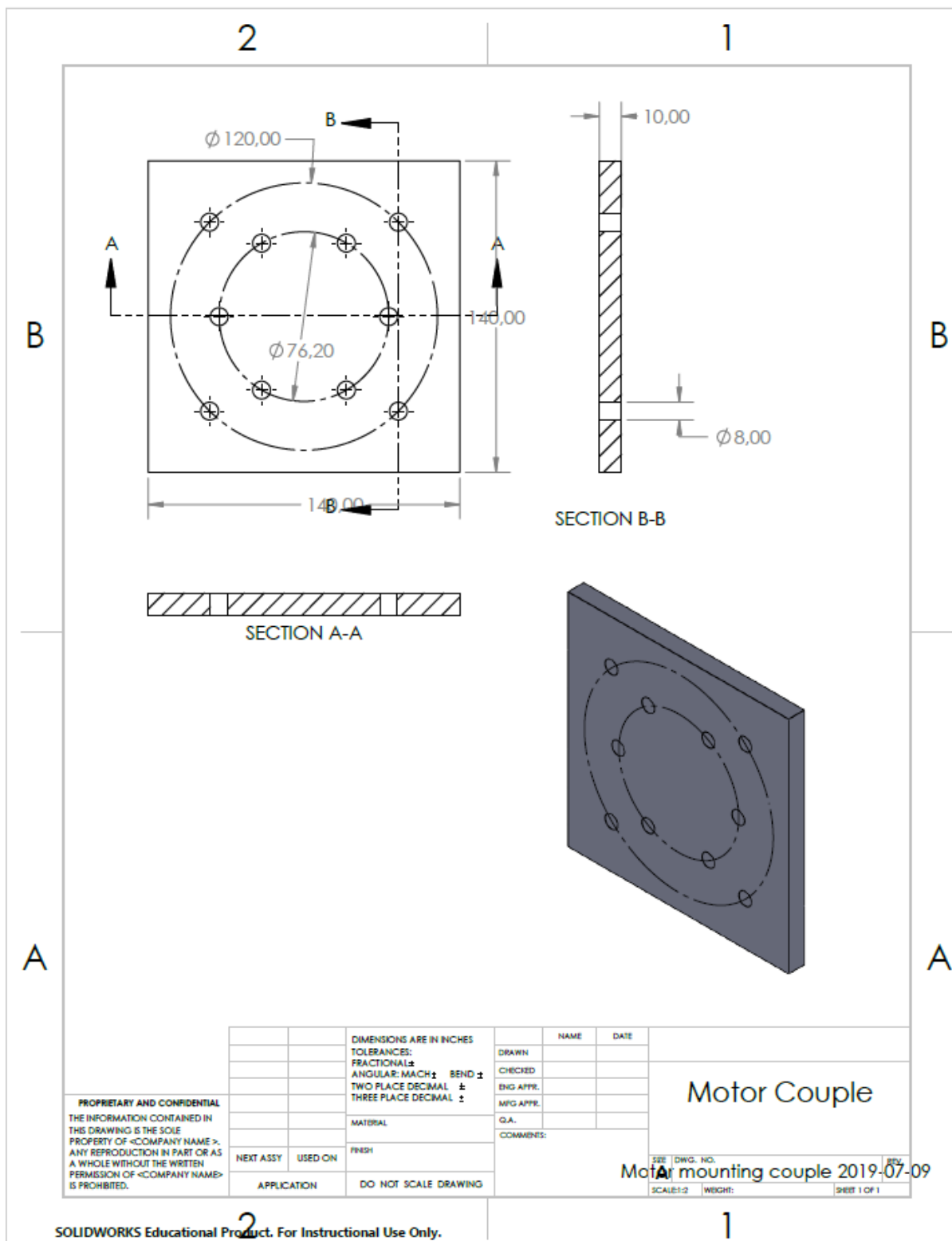


Figure 6-40: Motor coupling diagram

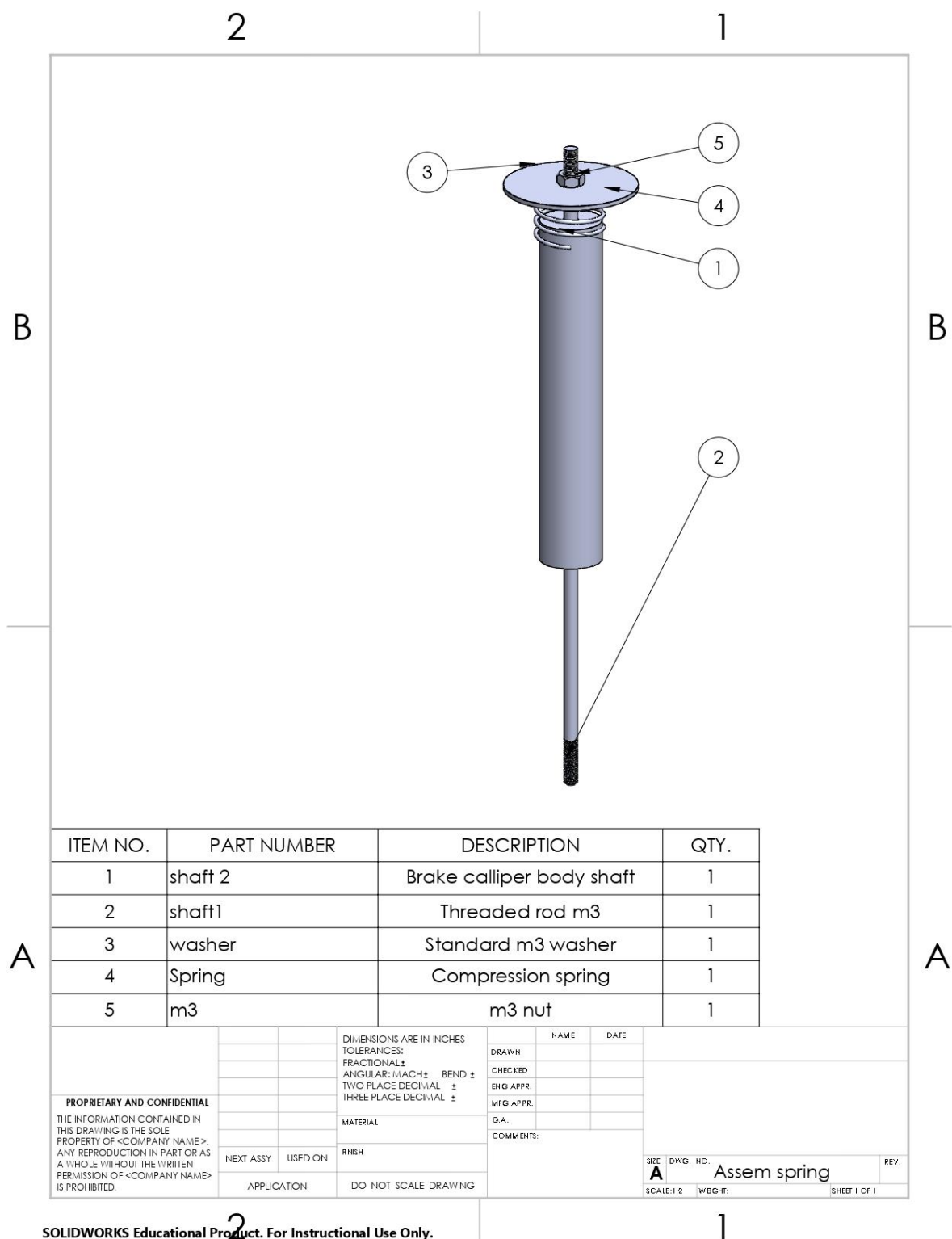


Figure 6-41: Spring assembly drawing

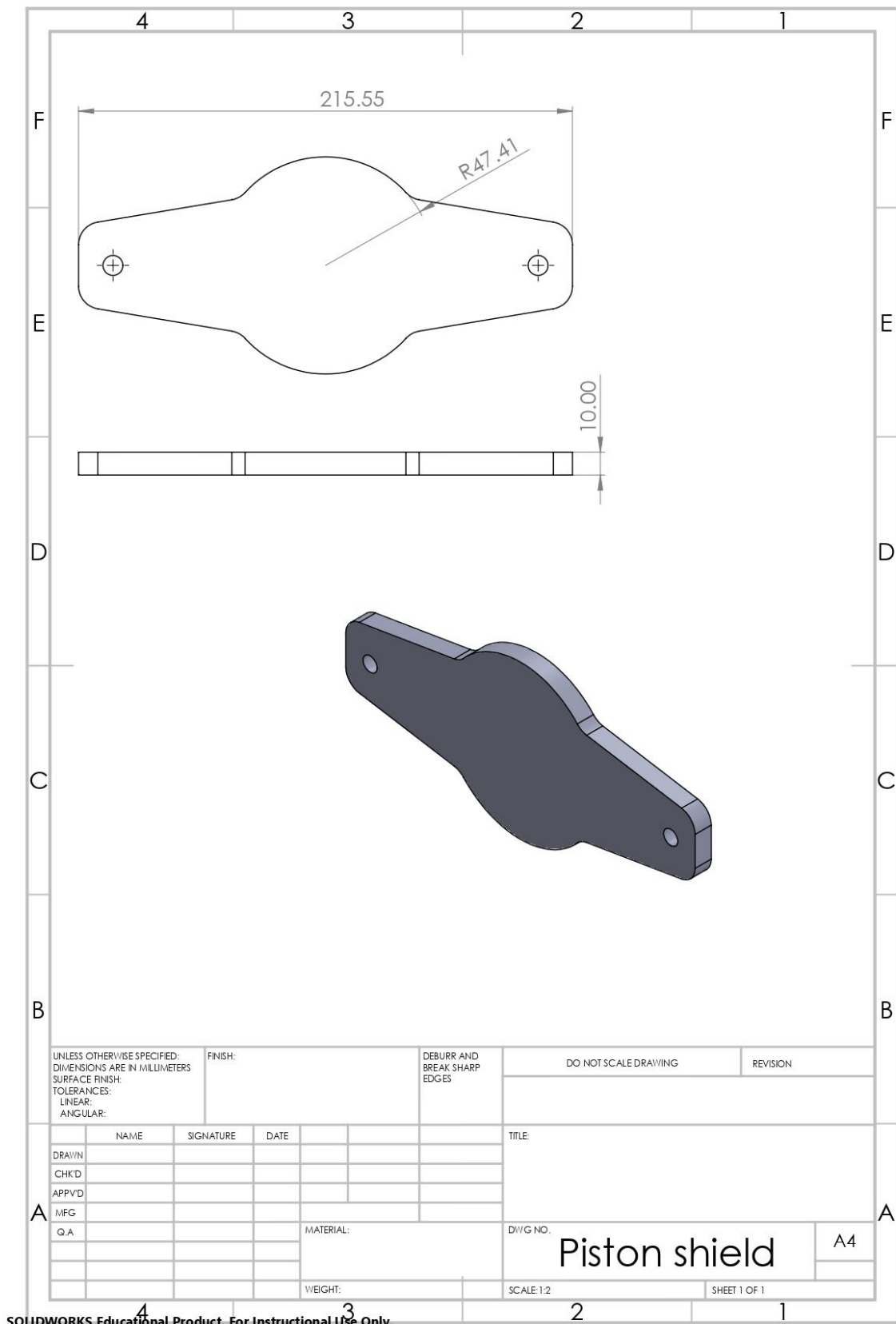


Figure 6-42: piston shield drawing

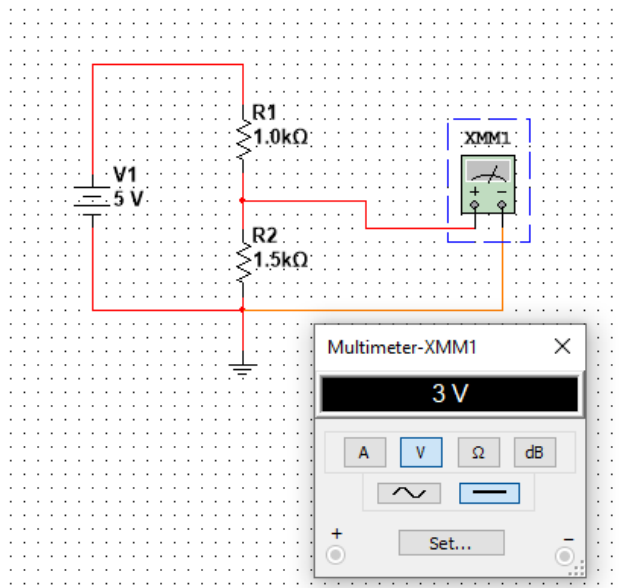


Figure 6-43: Torque Transducer Signal Measurement V1.0 simulation circuit

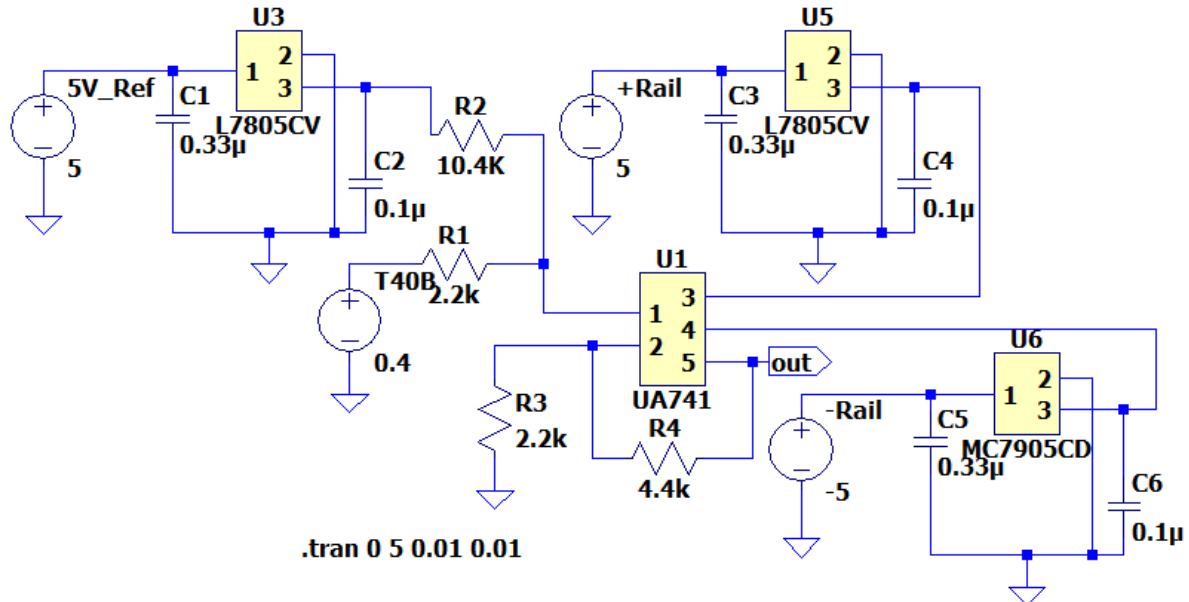


Figure 6-44: Summing amplifier circuit with voltage regulators

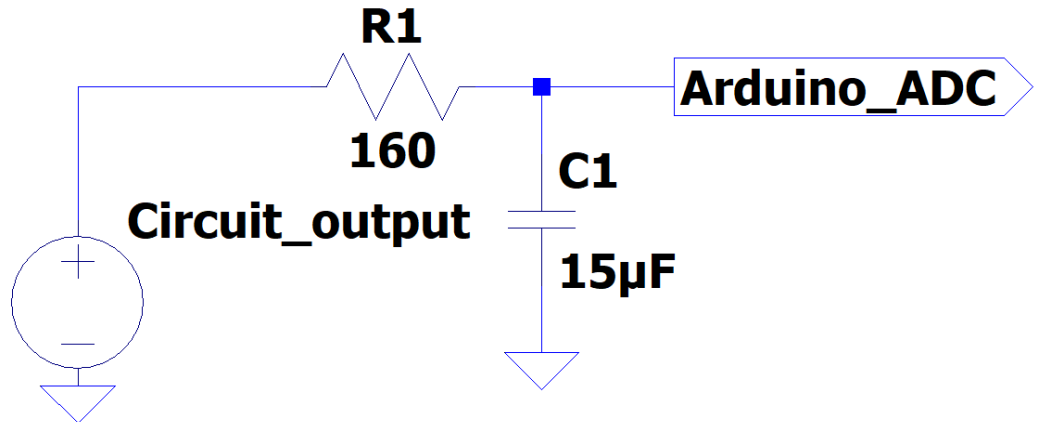


Figure 6-45: RC 66Hz filter

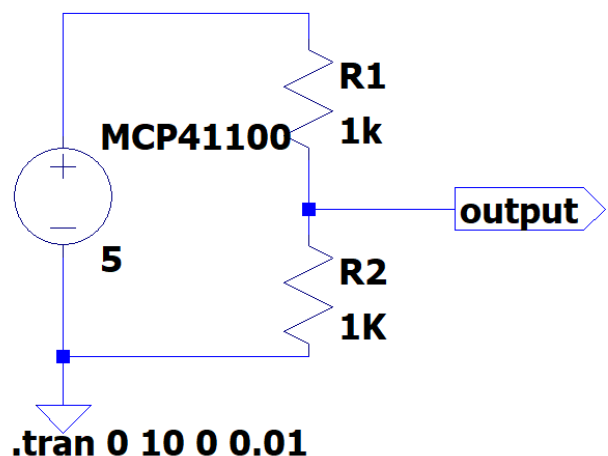


Figure 6-46: MCP41100 voltage divider

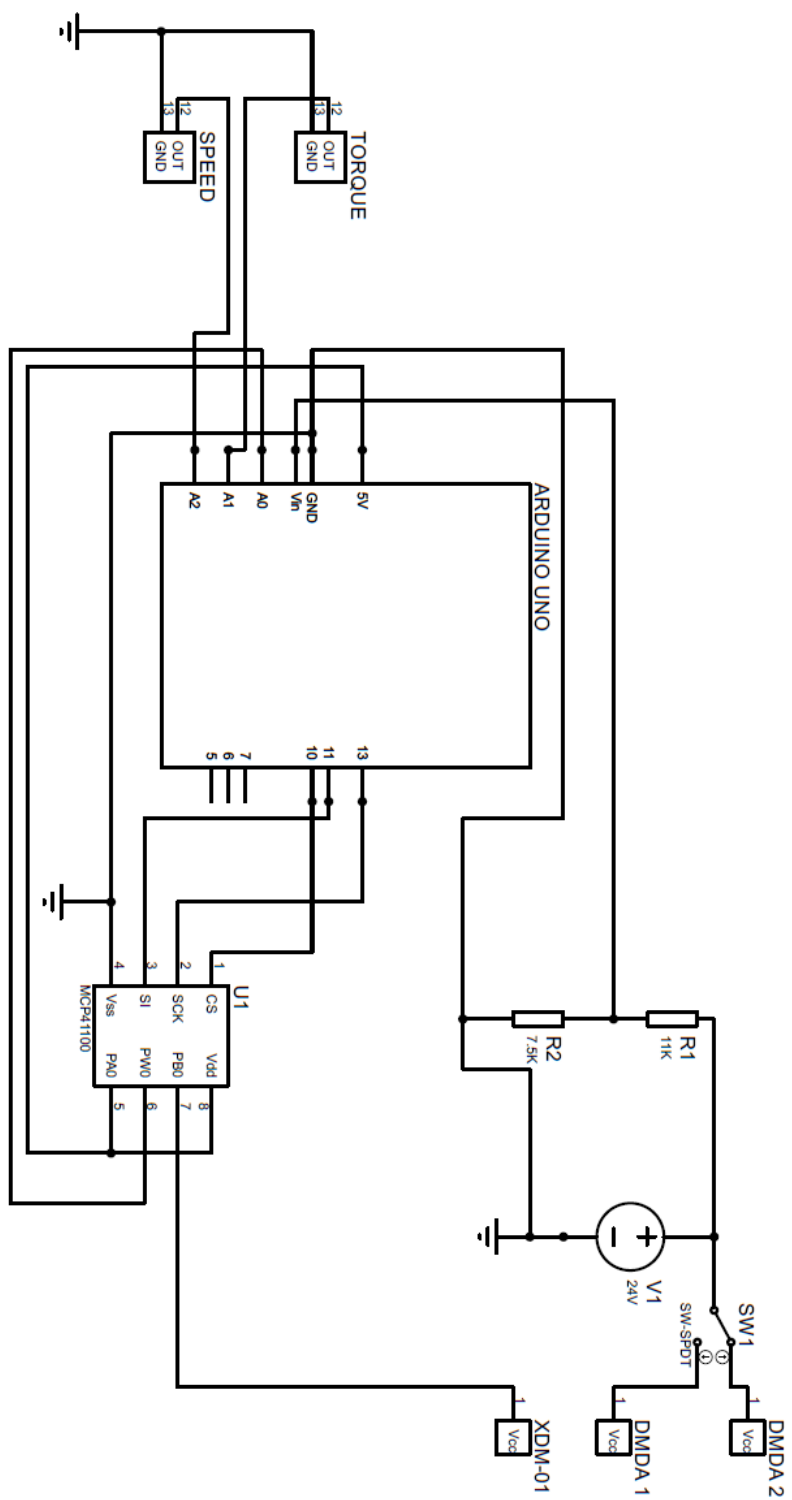


Figure 6-47:Arduino Uno® circuit

APPENDIX B.1: FABRICATION DATA

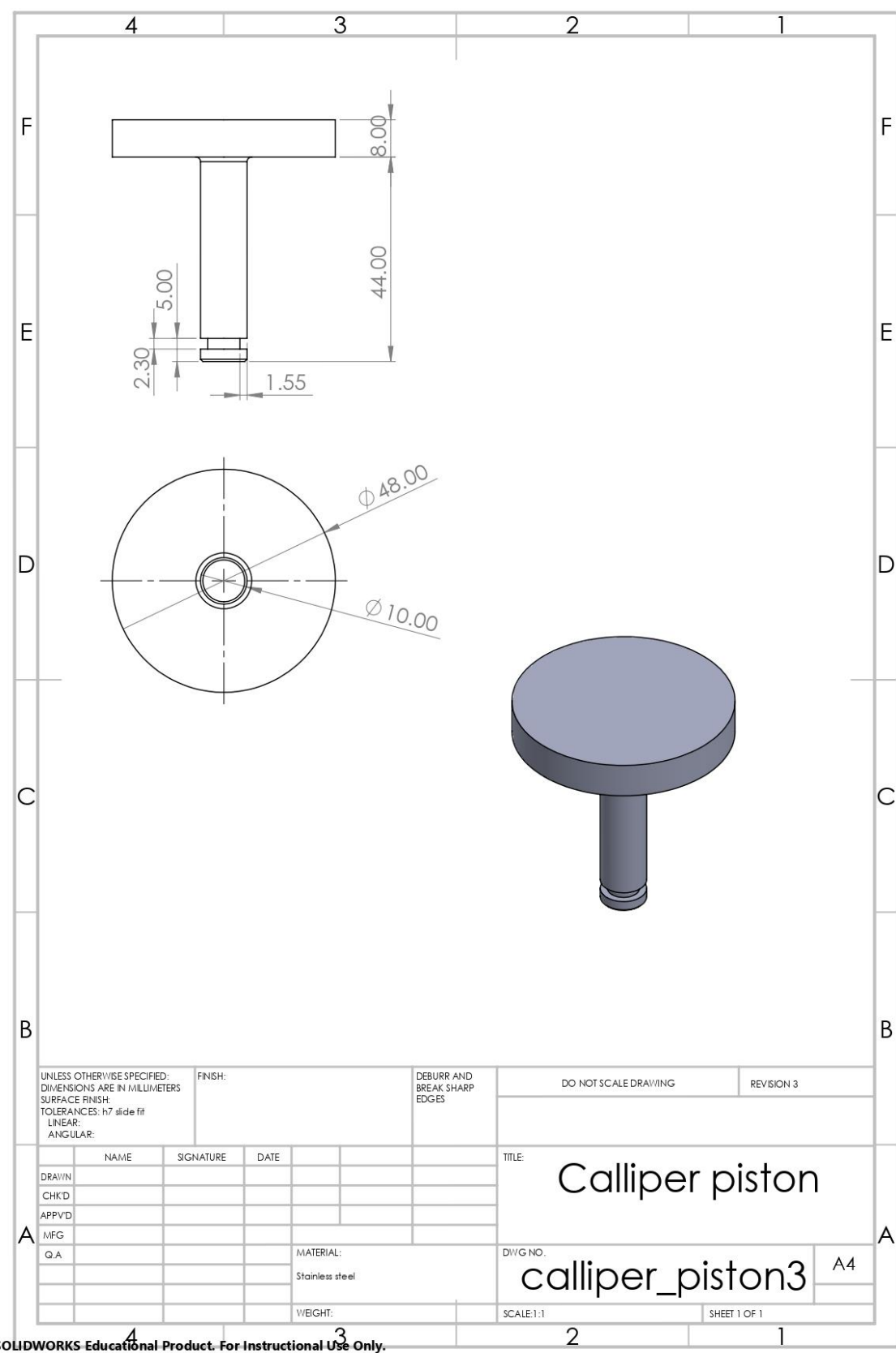


Figure 6-48: Piston calliper

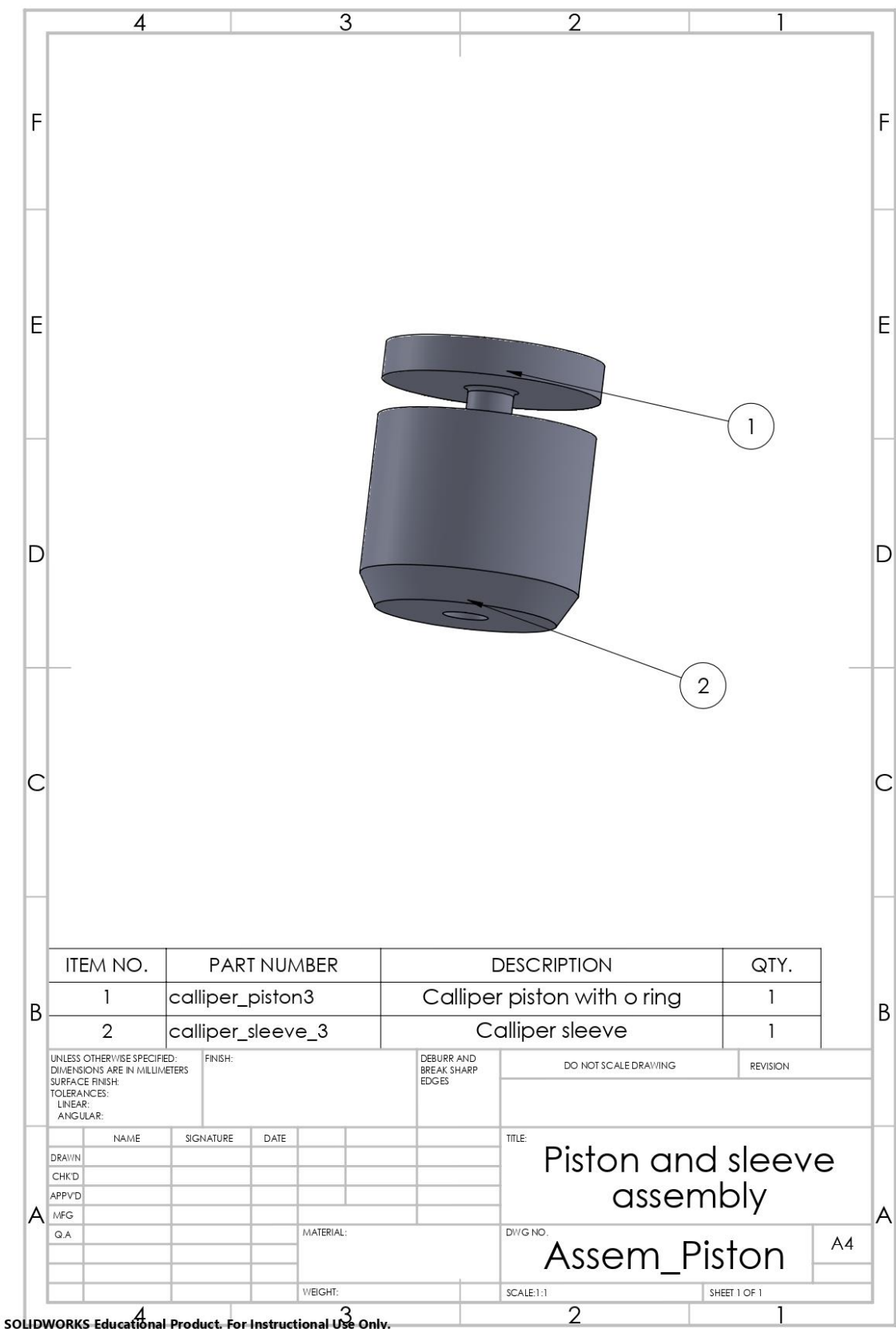


Figure 6-49: Piston and sleeve assembly drawing

APPENDIX B.2: SOFTWARE

APPENDIX B.3: TEST REPORTS

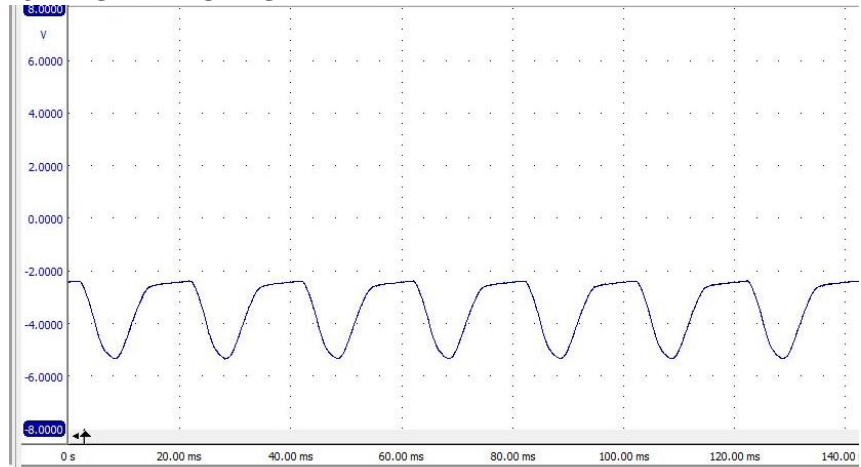


Figure 6-50: Torque adapter RS422 output signal

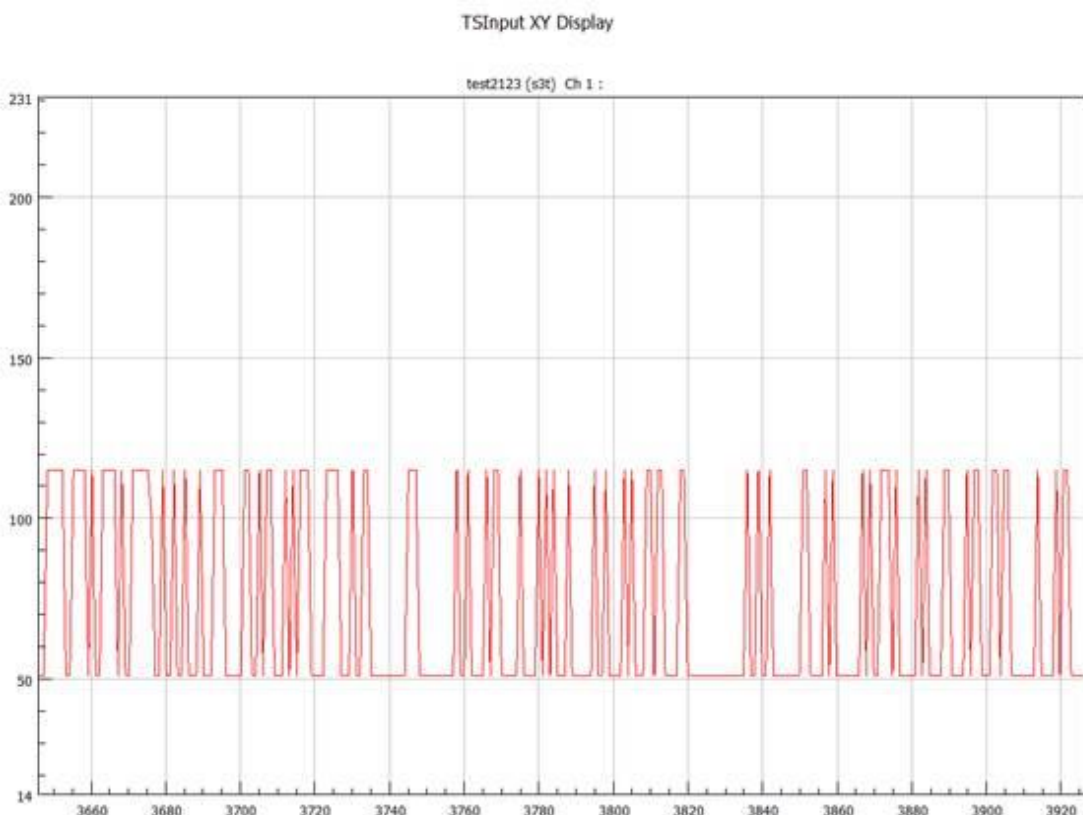


Figure 6-51: Expected frequency output

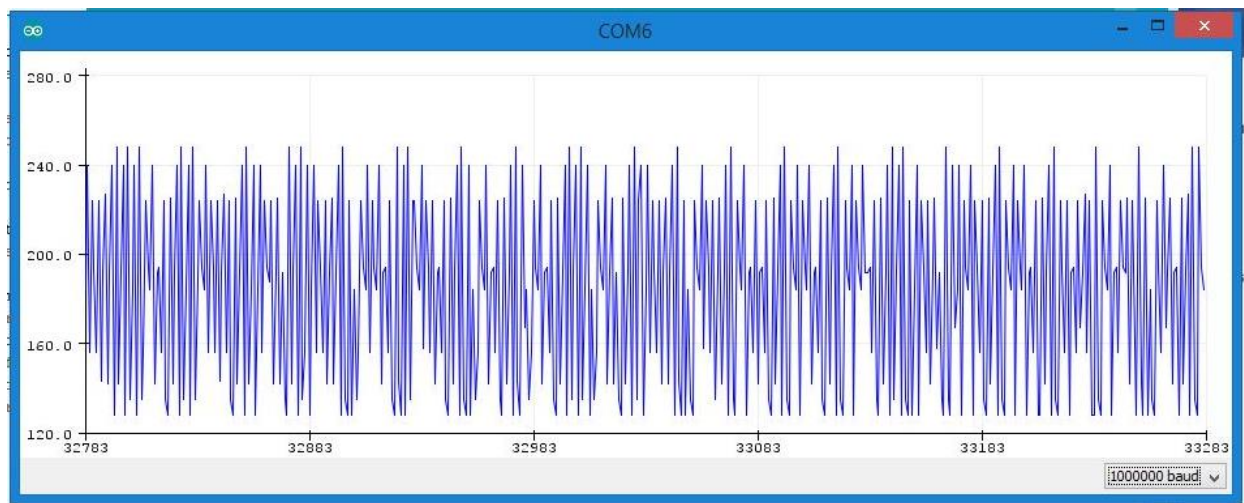


Figure 6-52: Serial plotter 1000 000 Baud rate no load test

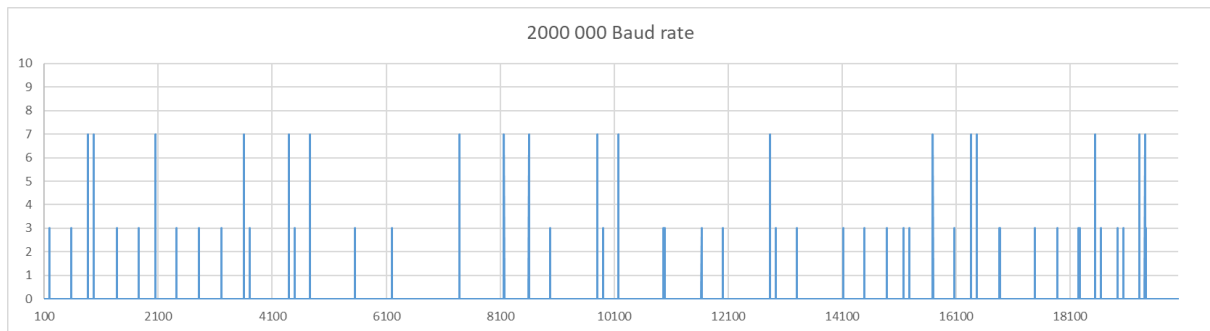


Figure 6-53: 2000 000 Baud rate serial monitor output

Table 6-1: XMD-01 voltage relation to pressure data

XMD-01 Voltage input [V]	Pressure [Bar]
0	10
0.871	15
1.016	18
1.278	20
1.539	25
1.728	30
1.923	35
2.081	40
2.277	45
2.466	50
2.88	60

Table 6-2: Relation between voltage and torque at plug 3 of the T40B

Voltage [mV]	Torque [Nm]
+15	+0.192
0	0
-21	-0.392
-62	-0.812
-90	-1.095
-107	-1.253
-122	-1.361
-133	-1.512
-166.5	-1.814
-182	-2.023
-200	-2.212
-223	-2.421
-241	-2.612

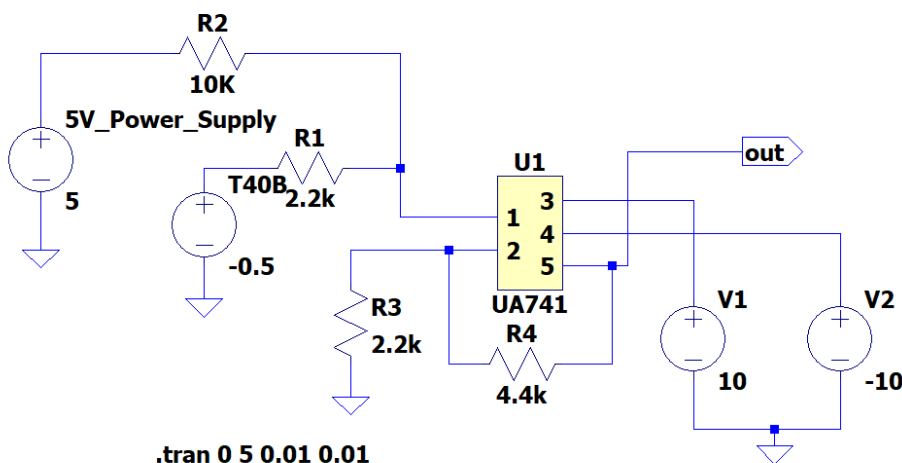


Figure 6-54: Operational amplifier test circuit

Table 6-3: Op amp test results

Input voltage from T40B [V]	+- 10 V rail supply			Simulated output [V]
	Measured out output [V]	Simulated output [V]	Difference between simulated and measured output [V]	
-1	0.259	0.143	0.116	0.245
-0.9	0.633	0.39	0.243	0.491
-0.8	0.886	0.638	0.248	0.737

-0.6	1.349	1.133	0.216	1.229
-0.4	1.8	1.628	0.172	1.721
-0.3	1.94	1.876	0.064	1.967
-0.2	2.41	2.138	0.272	2.213
-0.1	2.58	2.371	0.209	2.459
0.3	3.92	3.361	0.559	3.005
0.6	4.68	4.105	0.575	3.005
0.7	4.89	4.353	0.537	3.005
0.8	5.14	4.599	0.541	3.005

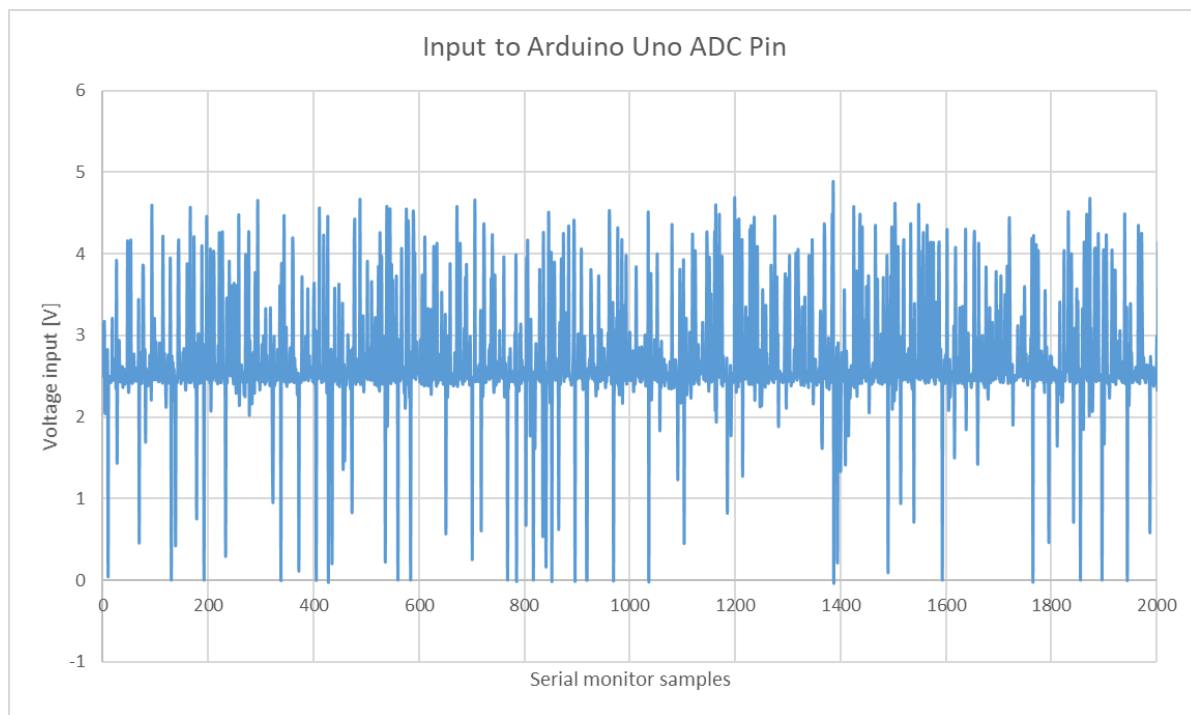


Figure 6-55: Noise input to Arduino ADC Pin

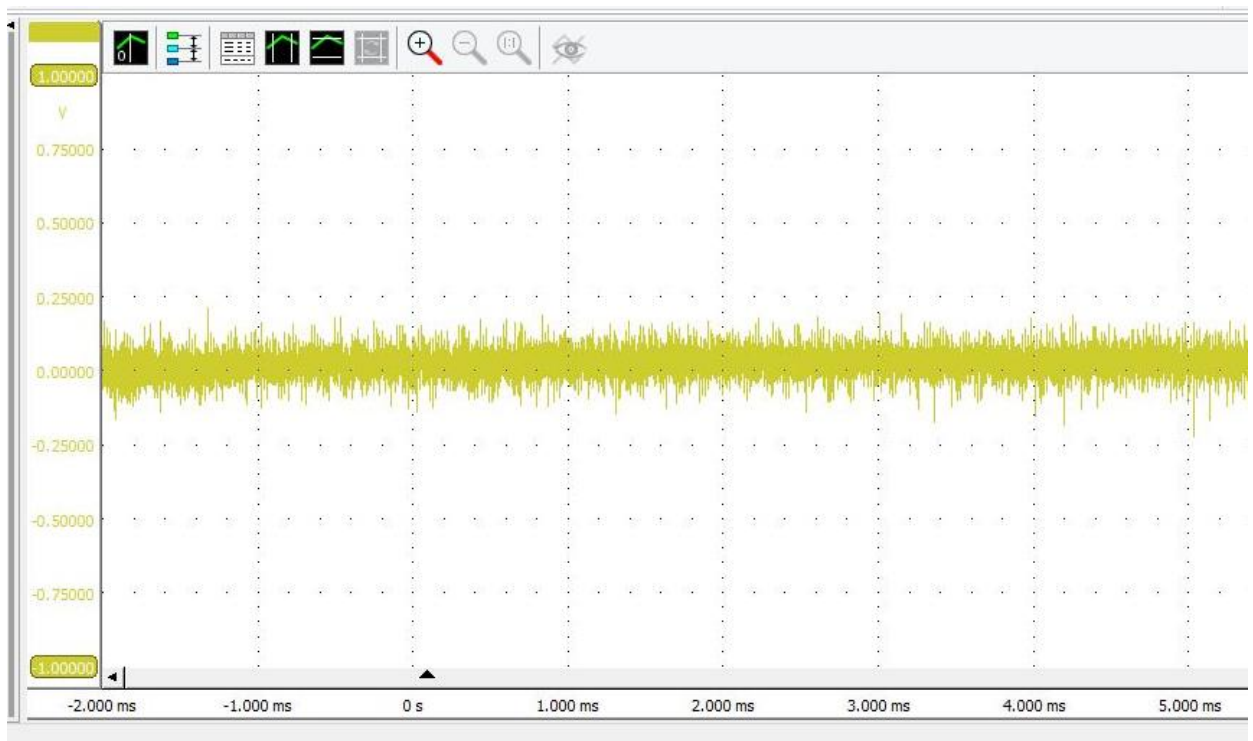


Figure 6-56: TiePie measurement of T40B output voltage, IM off and Grundfos motor off

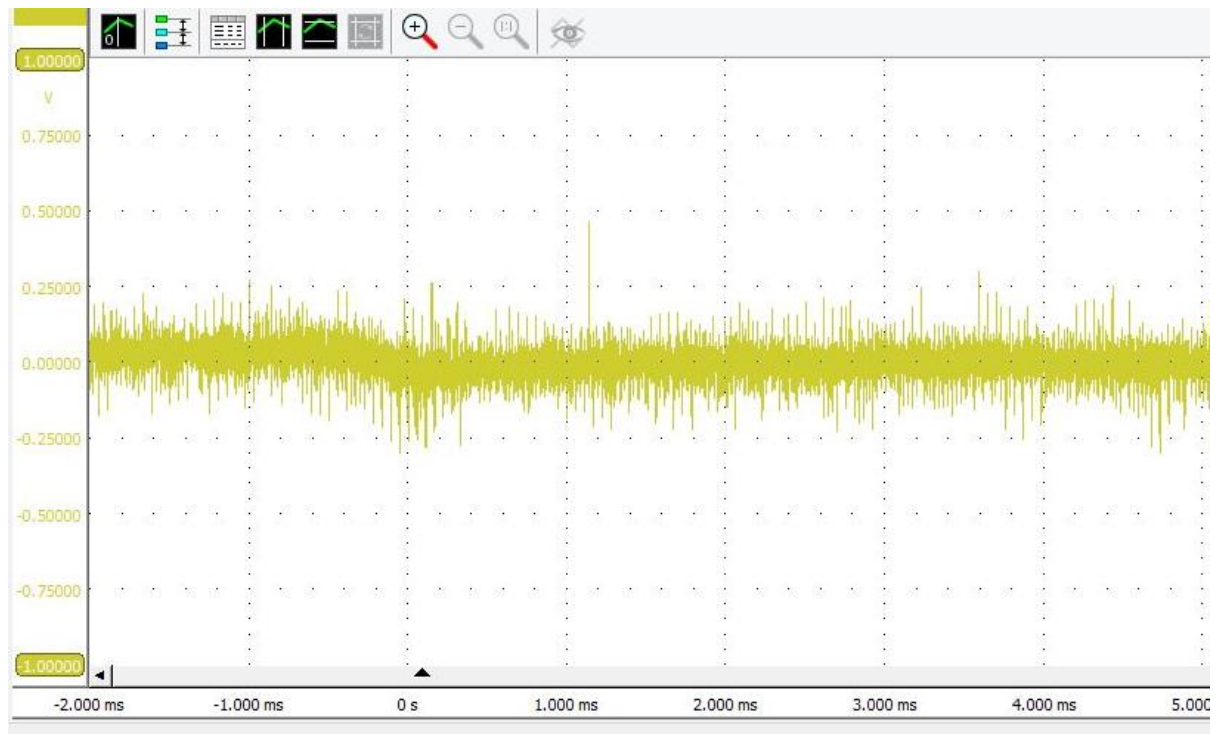


Figure 6-57: TiePie measurement of T40B output voltage, Grundfos motor switched on

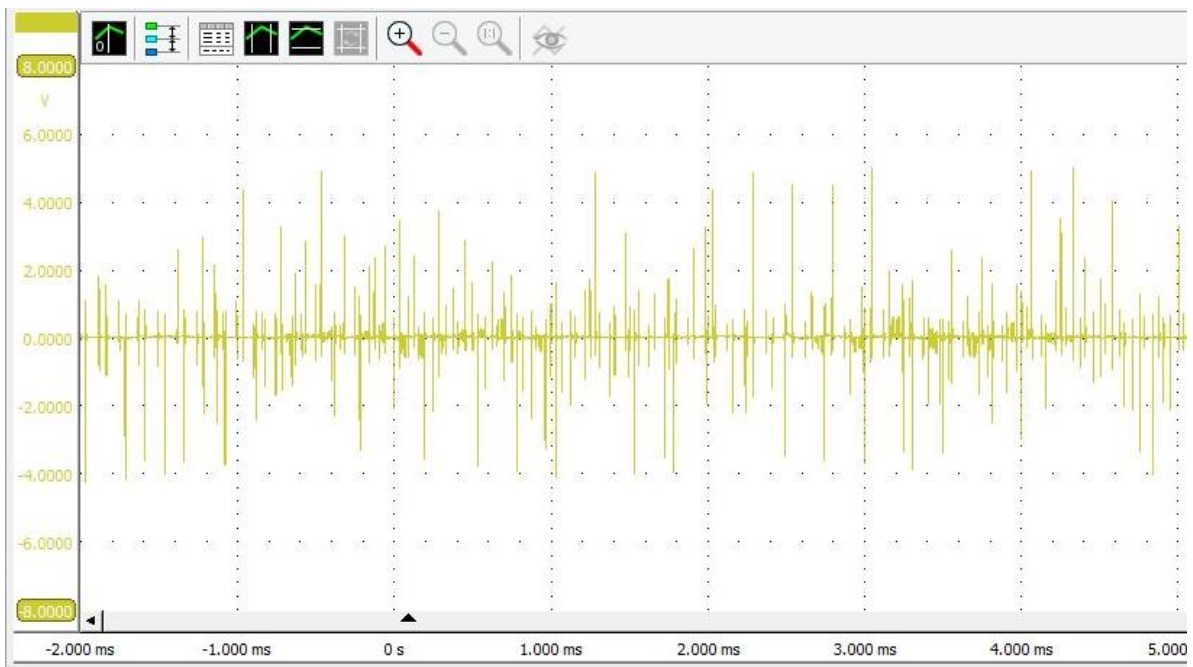


Figure 6-58: TiePie measurement of T40B voltage output, induction motor controlled by VSD

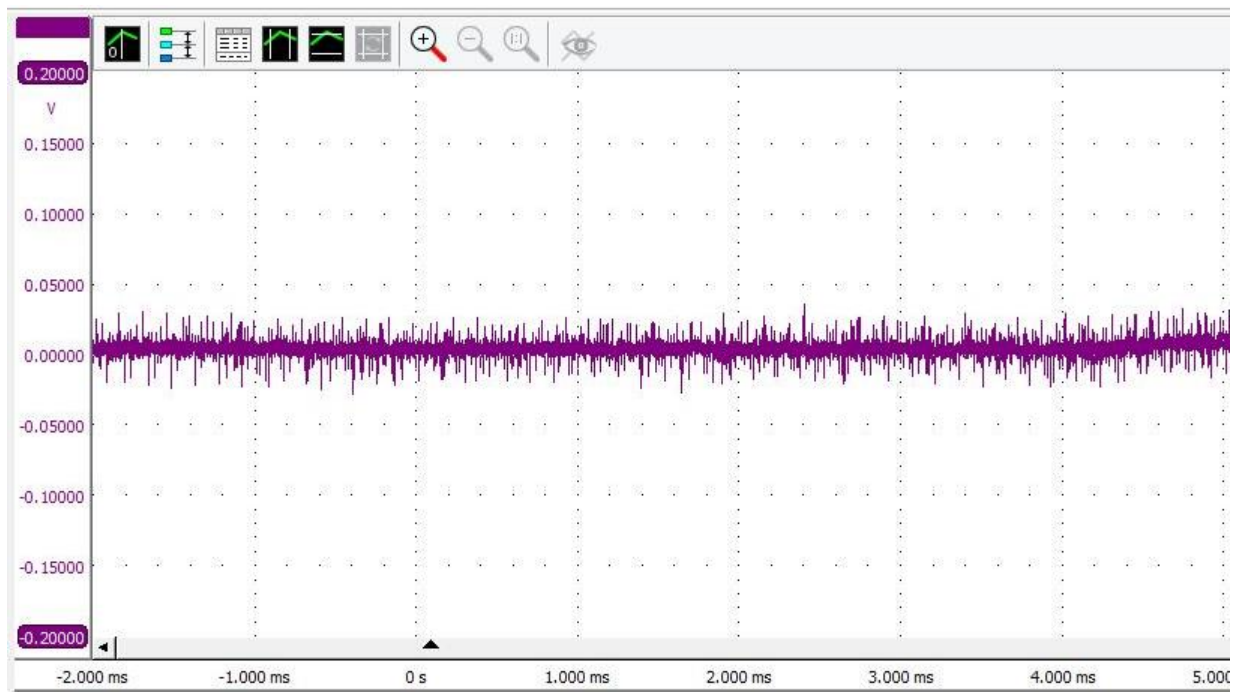


Figure 6-59: TiePie measurement of T40B output voltage, induction motor powered by variac

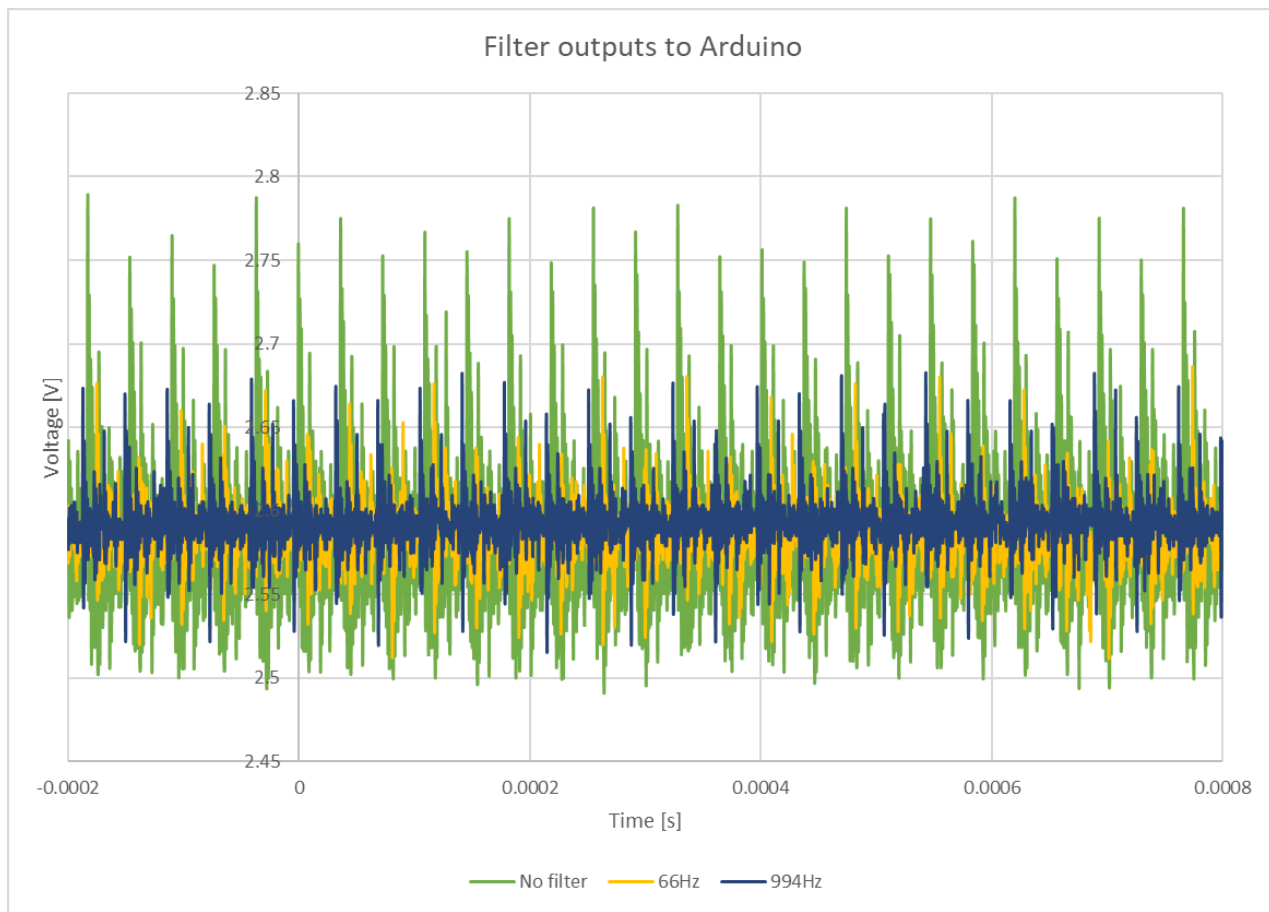


Figure 6-60: Filtered output to the Arduino vs unfiltered output

Table 6-4: Combined system measurements

Test no	Motor Voltage (Phase to phase) [V]	Current [A]	P_in [W]	S_in [VA]	Torque [Nm]	Speed [RPM]	Power Mech [Nm/s]	Pressure [Bar]
1	152.89	0.1027	39.7	69.1	0.344	759	25.56	10
2	153.46	0.2153	82.4	147	1.328	755	104.69	15
3	152.16	0.246	94.61	165.5	1.649	757	132.79	20
4	150.64	0.286	122.6	194.4	2.467	761	195.51	23
5	174.27	0.114	46.1	87.6	0.245	758	20.76	10
6	174.51	0.1631	66.5	126.2	0.735	759	56.96	14
7	174.51	0.1704	74.65	137.4	0.954	754	75.65	16
8	174.8	0.2336	112.3	181.3	1.881	757.6	146.13	21
9	174.51	0.1327	53.69	104.09	0.318	995.9	33.12	10
10	174.85	0.1961	87.54	154.2	1.012	991.9	105.14	15
11	174.96	0.1763	75.22	138.71	0.748	1006	78.78	18
12	174.38	0.2238	106.63	175.5	1.344	1005.5	141.56	16
13	174.39	0.2397	117.51	188.04	1.571	1004.4	165.26	20

14	174.67	0.2546	126.4	200	1.801	1003.9	198.29	21
15	174.36	0.2878	150.45	225.65	2.307	1001.3	241.91	22
16	174.54	0.2918	153.26	229.09	2.389	998.5	249.79	23
17	174.36	0.304	162.08	238.39	2.572	1002.4	270	24
18	173.62	0.3586	212.02	280.07	3.8	996.9	396.71	25
19	173.68	0.3587	212.75	280.23	3.841	996.7	400.88	25
20	174.81	0.1401	58.34	109.71	0.311	1252.7	40.85	10
21	174.03	0.1485	61.48	116.16	0.366	1251.4	47.94	13
22	174.09	0.2012	91.6	157.56	0.856	1248.9	111.9	14
23	173.96	0.2144	100.43	167.78	0.993	1253	130.34	15
24	174.29	0.2411	117.04	189.03	1.278	1248.7	167.06	18
25	174.25	0.2284	108.46	179.03	1.134	1248.9	148.28	16
26	174.33	0.2555	127.86	200.35	1.472	1252.4	193	20
27	173.8	0.3073	165.7	240.27	2.205	1245.8	287.67	23
28	174.12	0.3516	204.37	275.43	3.011	1246.3	392.98	24
29	174.2	0.3572	211.77	279.9	3.211	1244.3	418.4	25
30	174.06	0.3942	251.54	308.63	4.259	1240.1	553.13	27
31	174.24	0.1729	73.73	135.46	0.402	1614.9	68	10
32	174.52	0.175	74.49	137.37	0.43	1618.8	72.9	13
33	174.29	0.2241	105.99	175.7	0.825	1614.9	139.54	14
34	174.16	0.2487	123.59	194.82	1.075	1616.3	182	15
35	174.31	0.2475	122.13	194.04	1.06	1612.2	179	16
36	174.65	0.2573	129.15	202.15	1.157	1610.9	195.1	18
37	174.45	0.2712	139.27	212.84	1.311	1609.9	221.01	20
38	174.3	0.308	165.93	241.46	1.715	1615.8	290.18	21
39	174.09	0.3504	202.84	274.4	2.342	1606.5	393.93	25
40	173.7	0.4	256.67	312.8	3.505	1610.2	591.08	27